The role of sensory nervous system in the regulation of bone formation, remodeling, and repair

Diana Silva

université de BORDEAUX

THÈSE PRÉSENTÉE

POUR OBTENIR LE GRADE DE

DOCTEUR DE

L'UNIVERSITÉ DE BORDEAUX

ÉCOLE DOCTORALE SCIENCES DE LA VIE ET DE LA SANTÉ
BIOLOGIE CELLULAIRE ET PHYSIOPATHOLOGIE

Par Diana Isabel SILVA

Le rôle du système nerveux sensoriel dans l'orchestration de la formation osseuse, le remodelage et la régénération tissulaire

Sous la direction de Joëlle AMÉDÉE

Soutenue le 21 décembre 2017

Membres du jury :

Mme. LAMGHARI, Meriem, PhD, University of Porto	Président
Mme. LAMGHARI, Meriem, PhD, University of Porto	Rapporteur
Mme. CHENU, Chantal, PhD, University of London	Rapporteur
M. CARLE, Georges, PhD, University of Nice	Examinateur
M. HOLY, Xavier, PhD, IRBA, Brétigny-sur-Orge	Examinateur
M. OLIVEIRA, Hugo, PhD, INSERM, Bordeaux	Invité

Le rôle du système nerveux sensoriel dans l'orchestration de la formation osseuse, le remodelage et la régénération tissulaire

Les progrès dans la compréhension de la biologie osseuse ont permis d'identifier le rôle du système nerveux sensoriel dans la formation osseuse, le remodelage et la régénération tissulaire. Cependant, le rôle précis du système nerveux sensoriel sur la l'ostéogénèse reste encore méconnu. La première partie de ce travail a été d'analyser le rôle des neurones du ganglion de la racine dorsale (DRG) sur la différenciation ostéoblastique des cellules souches mésenchymateuse (MSCs). Pour répondre à cette question, nous avons utilisé une plate-forme microfluidique, qui tente de mimer l'innervation sensorielle du tissu osseux. Dans la seconde partie de cette étude, nous avons cherché à mieux caractériser la sous-population de neurones DRG impliqués dans la régulation directe de la différenciation des MSCs vers le lignage ostéoblastique. En conclusion, l'ensemble des résultats permettent de montrer que: i) les neurones sensoriels ont un effet positif et direct sur la différenciation ostéoblastique des cellules ostéoprogénitrices, ii) la voie de signalisation Wnt/β-caténine est impliquée dans cette transduction du signal; iii) cet effet est principalement régulé par des neurones sensorimoteur, iv) qui peuvent induire la libération locale de facteurs neuroactifs.

Mots clés : neurones sensoriels, cellules mésenchymateuses, différenciation des ostéoblastes

---

The role of sensory nervous system in the regulation of bone formation, remodeling, and repair

Advances in the understanding of bone biology have identified the sensory nervous system as a critical regulator in the orchestration of bone formation, remodeling, and repair. However, the precise role of the sensory nervous system on bone tissue, particularly on osteoprogenitor cells, remains unknown. Firstly, we were interested in clarifying whether dorsal root ganglion (DRG) neurons would be able to induce the osteoblast differentiation by acting directly on mesenchymal stem cells (MSCs). Afterwards, we attempted to understand whether the canonical Wnt signaling pathway could be implicated in the DRG neurons-induced osteoblastogenesis. In the second part of this study, we aimed at better characterizing the subset of DRG neurons involved in the direct regulation of osteoblast differentiation from MSCs. In this work we provide several novel insights: i) we show that sensory neurons have a positive and direct effect on osteoblast differentiation of osteoprogenitor cells, ii) by activating the Wnt/β-catenin signaling pathway; and iii) we suggest that this effect is mainly regulated by sensorimotor neurons, iv) which possibly mediate the local release of neuroactive factors.

Keywords : DRG neurons, mesenchymal stem cells, osteoblast differentiation

---

Unité de recherche

Laboratoire BioTis, INSERM U1026, 146 rue Léo Saignat, 33076 Bordeaux, France

Diana Isabel Silva

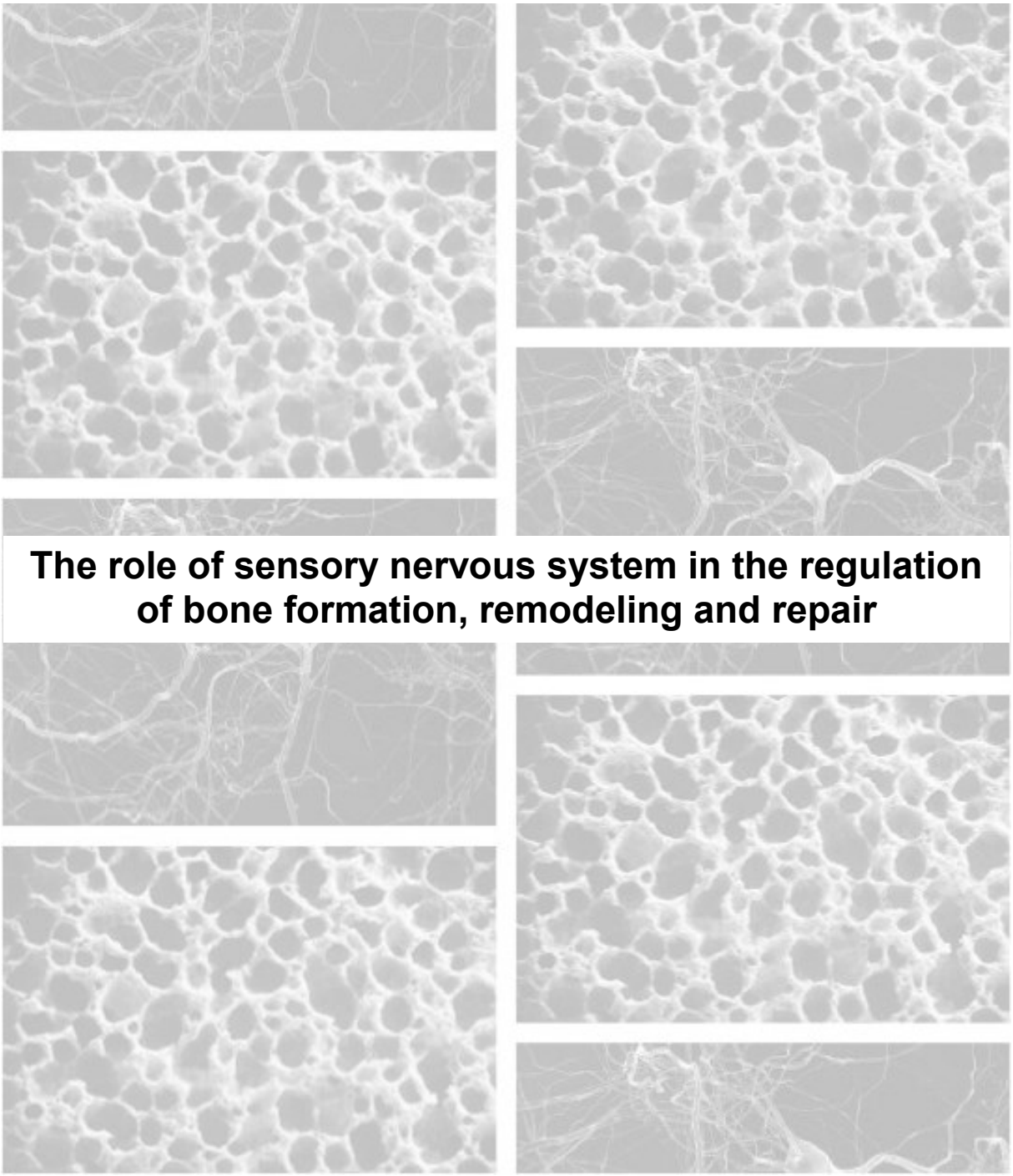

The role of sensory nervous system in the regulation of bone formation, remodeling and repair

Doctor of Cell Biology and Pathophysiology

University of Bordeaux

2017

This dissertation was submitted to the *École Doctorale Sciences de la Vie et de la Santé* of University of Bordeaux in fulfillment of the requirements for the degree of Doctor of Cell Biology and Pathophysiology.

The work presented in this dissertation was developed in *The Laboratory for the Bioengineering of Tissues - Institut national de la santé et de la recherche médicale* (INSERM U1026 – “BioTis”) under the supervision of Doctor Joëlle Amédée, and supported by funds from *Direction générale de l'armement* (DGA).

The results presented in this dissertation are submitted or in preparation for future submission to international peer-review scientific journals:

Diana Isabel Silva, Bruno Paiva dos Santos, Jacques Leng, Hugo Oliveira, Joëlle Amédée. Dorsal root ganglion neurons regulate the transcriptional and translational programs of osteoblast differentiation in a microfluidic platform. *Cell Death and Disease*.

Diana Isabel Silva, Bruno Paiva dos Santos, Hugo Oliveira, Joëlle Amédée. Activation of capsaicin-sensitive dorsal root ganglion neurons induces the osteoblast differentiation of mesenchymal stem cells *in vitro.* (Manuscript under preparation)

Note: the data presented in this dissertation is partially formatted according to the style of the journals of publication with minor modifications.

TABLE OF CONTENTS

NDEX OF FIGURES AND TABLES

ACRONYMS AND ABBREVIATIONS LIST

A

Alp – alkaline phosphatase

APC – adenomatous polyposis coli

B

Bglap – bone gamma-carboxyglutamic acid-containing protein (also known as osteocalcin)

BMP – bone morphogenetic protein

BMU – basic multicellular unit (also known as BRU)

BRU – bone remodeling unit (also known as BMU)

BSA – bovine serum albumin

C

CART – cocaine- and amphetamine-regulated transcript

Cbfa1 – core-binding factor subunit alpha-1 (also known as Runx2)

Ccn1 – CCN family member 1 (also known as Cyr61)

Cdh2 – cadherin-2 (also known as N-cadherin)

CGRP – calcitonin gene-related peptide

CM – conditioned medium

Col1a1 – collagen type I alpha 1 chain

Ctnnb1 – catenin beta 1 (also known as β-catenin)

Cx43 – connexin 43 (also known as Gja1)

Cyr61 – cysteine-rich angiogenic inducer 61 (also known as Ccn1)

D

DAPI – 4',6-diamidino-2-phenylindole

Dkk – Dickkopf

DMEM – dulbecco's modified eagle's medium

DRG – dorsal root ganglion

Dsh – disheveled

E

ECM – extracellular matrix

EGF – epidermal growth factor

ELPs – elastin-like polypeptides

F

FBS – fetal bovine serum

FGF – fibroblast growth factor

Fzd – Frizzled

G

GAGs – glycosaminoglycans

Gapdh – glyceraldehyde 3-phosphate dehydrogenase

Gja1 – gap junction alpha-1 protein (also known as Cx43)

GM-CSF – granulocyte-macrophage colony-stimulating factor

GSK – glycogen synthase kinase

H

Hprt1 – hypoxanthine phosphoribosyl transferase 1

HRP – horseradish peroxidase

HSCs – hematopoietic stem cells

I

IF – immunofluorescence

IFNγ – Interferon gamma

IGF – insulin-like growth factor

Ihh – Indian hedgehog

IL – interleukin

L

Lef – lymphoid enhancer factor

LPR – low-density lipoprotein receptor-related protein

M

M-CSF – macrophage- colony stimulating factor

miRNAs – microRNAs

MMPs – matrix metalloproteinases

MSCs – mesenchymal stem/stromal cells

N

N-cadherin – neural cadherin (also known as Cdh2)

NGF – nerve growth factor

nHA – nanohydroxyapatite

NKA – neurokinin A

NRP1 – neuropilin 1

O

OPG – osteoprotegerin (also known as Tnfrsf11b)

OPGL – osteoprotegerin ligand (also known as RANKL, TRANCE, or Tnfrsf11)

P

PBS – phosphate-buffered saline

PDGF – platelet-derived growth factor

PDL – poly-D-lysine

PDMS – dimethylsiloxane

PEG – polyethylene glycol

Pen/Strep – penicillin/streptomycin

PFA – paraformaldehyde

PG – prostaglandin

PTH – parathyroid hormone

PTHrP – parathyroid hormone-related protein

R

RANKL – receptor activator of nuclear factor kappa-B ligand (also known as TNFSF11, TRANCE or OPGL)

Rplp0 – rat ribosomal protein lateral stalk subunit P0

RT – room temperature

Runx2 – runt-related transcription factor 2 (also known as Cbfa1)

S

SD – standard deviation

SDS-PAGE – sodium dodecyl sulphate-polyacrylamide gel electrophoresis

sFRPs – secreted Fzd-related peptides

Sema – semaphorin

Sp7 – specificity protein transcription factor 7 (also known as osterix)

T

Tcf – T-cell factor

TGF-β – tumor growth factor-beta

TNF – tumor necrosis factor

Tnfrsf11b – tumor necrosis factor ligand superfamily member 11 (also known as OPG)

TRANCE – TNF-related activation-inducing cytokine (also known as RANKL, TNFSF11, or OPGL)

TRAP – tartrate-resistant acid phosphatase

TrkA – tropomyosin receptor kinase A

TRPV1 – transient receptor potential vanilloid subfamily member 1

TSH – thyroid-stimulating hormone

V

VEGF – vascular endothelial cell growth factor

W

WB – western blot

Wif – Wnt inhibitory factor

Wnt – wingless

RELATED LITERATURE.01

Bone is a specialized, living, and constantly changing connective tissue that forms, along with multiple tissue types, the structural elements of the skeleton (*i.e.* the bones). The mechanical functions of the skeletal system depend on the characteristic hardness of bone tissue [1–3].

Old or microdamaged bone is replaced by newly formed bone in a dynamic process termed bone remodeling or bone metabolism. This process requires a tightly regulated interplay among the different types of bone cells. A proper balance between bone resorption and bone formation maintains bone homeostasis [1–3].

1.1.1. Bone Functions

The most evident functions of bones and skeletal system are the gross functions. These functions include mechanical functions, namely structural support for the body, leverage/movement, and protection of vital organs. Moreover, bone tissue performs several critical functions. It serves as a site for blood cells production (*i.e.* hematopoiesis); depository for certain cytokines and growth factors; and reservoir for lipids and minerals, especially calcium and phosphorous. For instance, calcium cations are crucial for muscle contractions and controlling the flow of other ions involved in the transmission of nerve impulses [1,2].

1.1.2. Bone Structure

1.1.2.1. Gross structure of bone – compact bone and spongy bone

Bone is a mineralized tissue classified into the compact (cortical) bone and the spongy (cancellous or trabecular) bone. Compact bone is a very dense and hard tissue that forms the outer shell around the bones (Figure 1). This tissue provides resistance to pressure and shocks and protects the spongy bone. On the other hand, spongy bone has a relatively porous structure and lies beneath the compact bone (Figure 1). It creates the lightweight nature of bones, supports bone marrow, and shifts in weight distribution. Most bones contain the two types of tissue.

However, the distribution and relative amounts of compact and spongy bones are related to the type of bone and its overall functions [2,3].

A long bone (as an example) is usually divided into the diaphysis (consisting mostly of compact bone) and the epiphysis (consisting mostly of spongy bone) (Figure 1).

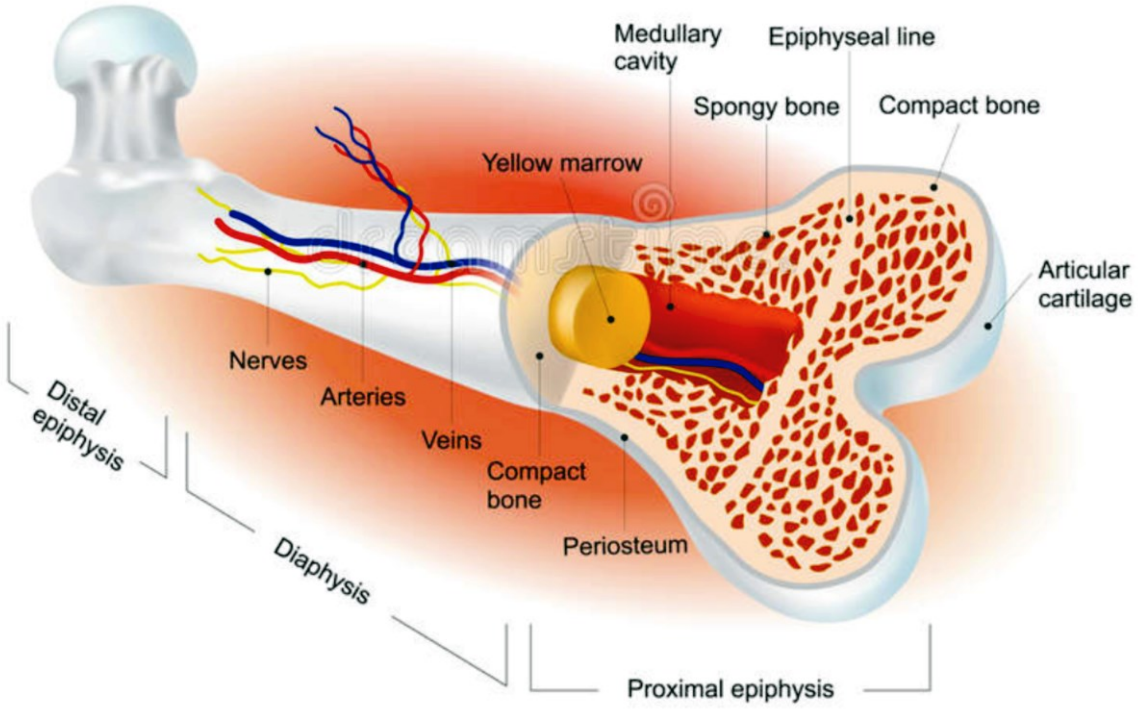

Figure 1. Schematic representation of a typical adult long bone gross structure. The diaphysis flares outward near the end to form the epiphysis. The outer shell is formed of compact bone covered with the periosteum. Beneath the compact bone is the spongy bone. Inside the diaphysis is the medullary cavity, which has an inner core of yellow marrow (adapted from http://www.istockphoto.com).

The diaphysis is the tubular shaft that links the proximal and distal extremities of bone (Figure 1). The hollow region in the diaphysis is called the medullary cavity, which is filled with red marrow in children or yellow marrow in adults, blood vessels, nerves, and lymphatic vessels, and is lined by a delicate connective tissue membrane known as endosteum (Figure 1). The outer shell of long bones is covered with a dense membrane of connective tissue termed periosteum, except at the articular surfaces (*i.e.* joints). In long bones, the joints are coated by hyaline cartilage in order to reduce the friction between adjacent and connected bones (Figure 1; see section 1.1.6.2). The periosteum is composed of two distinct layers: an outer fibrous layer and an inner osteogenic (cellular or cambium) layer (Figure

2). The outer layer is formed by fibroblasts, collagen and elastin fibers, along with a distinctive nerve and microvascular network. The inner layer of the periosteum is highly cellular, containing fibroblasts, mesenchymal stem cells (MSCs), osteoprogenitor cells, and osteoblasts, as well as blood vessels, nerves, and lymphatic vessels [2,3].

The epiphysis is the swollen part at each end of the long bones (Figure 1). It is filled with red marrow between the spaces (cavities) of the spongy bone and contains the epiphyseal line (Figure 1). In a growing long bone between the epiphysis and the diaphysis lies the metaphysis, a narrow portion of bone that contains the epiphyseal (grow) plate. The epiphyseal plate is formed by a layer of hyaline cartilage, which is replaced by compact bone in the early of adulthood, giving rise to the epiphyseal line (see section 1.1.6.2) [2,3].

1.1.2.2. Microstructure of bone – osteon and trabecula

Compact bone and spongy bone are biologically identical, but its microarchitecture is different. The basic structural/functional unit of the compact bone is the osteon or Haversian system (Figure 2). Each osteon is composed of a single central (Haversian) canal surrounded by concentric layers of mineralized matrix, called lamellae (Figure 2). These cylindrical structural units are arranged parallel to one another along the long axis of the compact bone. The central canals connect with each other, with the medullary cavity, and with the periosteum, *via* transverse branches, known as perforating (Volkmann's) canals (Figure 2). Central and perforating canals are lined by endosteum and contain blood vessels, nerves, and lymphatic vessels. Besides the structural function of these canals, they are responsible for the exchange of oxygen/nutrients and removal of metabolic waste products (see section 1.1.5). Between the osteons, the lamellae are called interstitial lamellae, and circumferential lamellae are arranged parallel to the periosteum (Figure 2) [2,3].

In the spongy bone, the microscopic unit is the trabecula. The trabeculae are composed of lamellae arranged in a honeycomb-like structure (Figure 2). This arrangement creates a considerable amount of open space within the bone filled with marrow, blood vessels, nerves, and lymphatic vessels [2,3].

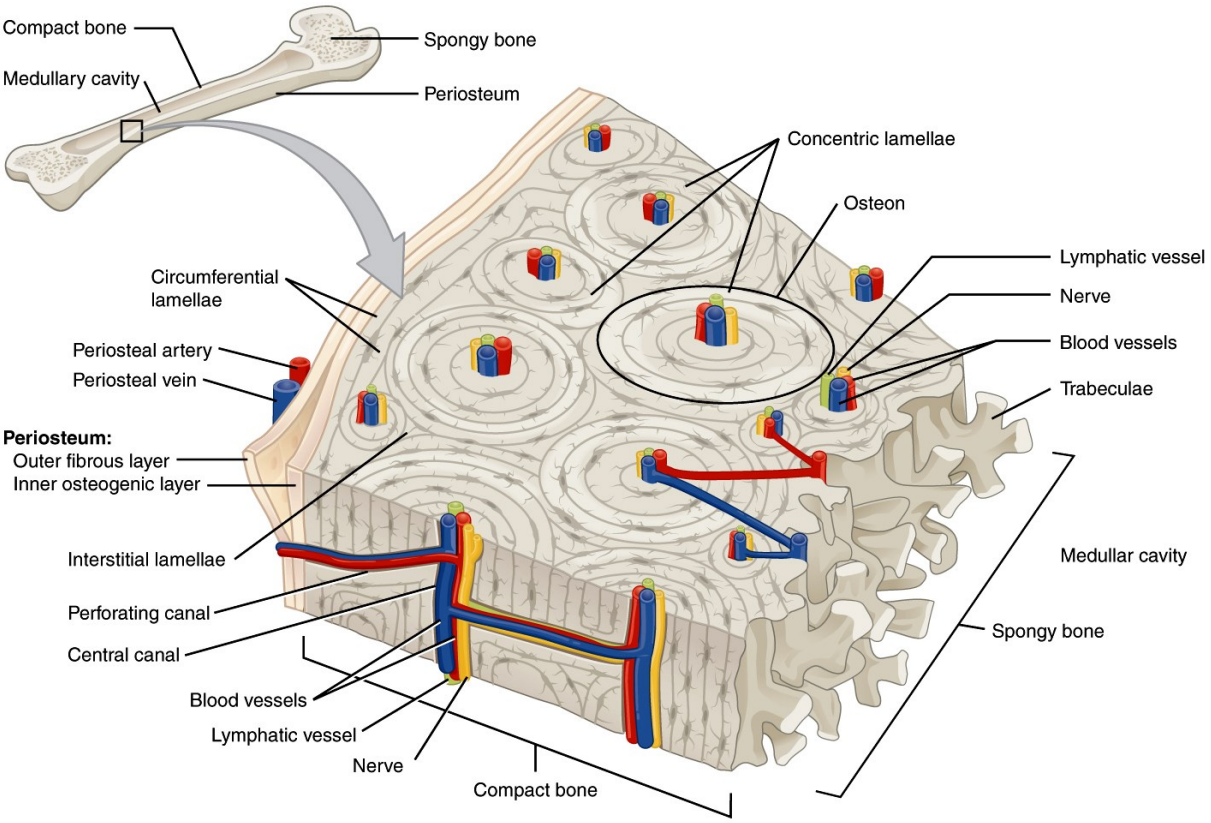

Figure 2. Schematic representation of the distinct microarchitectures of bone tissue. Compact bone is arranged in concentric lamellae around a central canal (osteons). The central canals connect with each other, with the medullary cavity, and with the periosteum, *via* perforating canals. Spongy bone is arranged in irregularly lamellae (trabeculae) (adapted from https://cnx.org/).

1.1.3. Bone Cells – The O‘ Cells

The bone volume is composed by a small amount of bone cells. Nevertheless, these cells play an essential role in bone functions. There are four special types of bone cells, known as the O´cells: osteoprogenitor cells, osteoblasts, osteocytes, and osteoclasts (Figure 3) [1–3].

1.1.3.1. Osteoprogenitor cells

Osteoprogenitor cells are MSCs with the capacity for extensive self-renewal and osteoblast differentiation. These cells are found in the bone marrow and in the inner layer of the periosteum (Figure 3) [1–3].

1.1.3.2. Osteoblasts

Osteoblasts or bone-forming cells are mononuclear cells with a limited lifespan (Figure 3). Their shape varies from flat to plump, reflecting their level of maturation and cellular activity. Osteoblasts develop from multipotent MSCs in a process called osteoblastogenesis. During this process, MSCs undergo successive stages of differentiation with a decreasing proliferation potential, giving rise to pre-osteoblasts and subsequently, osteoblasts. As osteoblasts differentiate, they acquire the ability to form bone tissue. Osteoblasts are then responsible for the synthesis/deposition of the organic components of bone matrix and orchestration of its mineralization (Figure 3; see section 1.1.4). The organic matrix that has not yet been mineralized is known as osteoid. Once the osteoid is mineralized, osteoblasts can be buried within the bone matrix as an osteocyte, become a bone-lining cell (quiescent flat-shaped osteoblasts that cover the bone surfaces), or undergo programmed cell death (*i.e.* apoptosis). Osteoblasts are located on the periosteal and endosteal bone surfaces (Figure 3) [1–3].

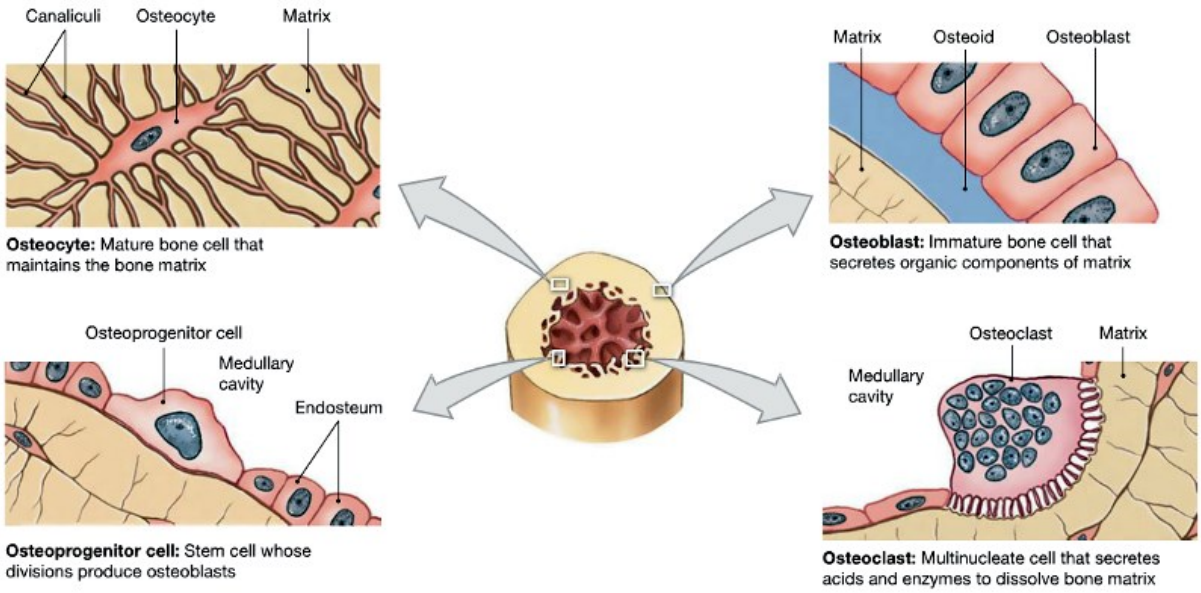

Figure 3. Bone type of cells: osteoprogenitor cells, osteoblasts, osteocytes, and osteoclasts. Each cell type has a specialized function and is found in different locations in bones (adapted from http://www.istockphoto.com).

1.1.3.3. Osteocytes

Osteocytes or star-shaped cells are the most common type of bone cell. These terminally differentiated cells result from the trapping of osteoblasts within the bone

matrix during the mineralization process. Each osteocyte is located inside a space, termed lacuna, surrounded by lamellae (Figure 4). Osteocytes form long and multiple cytoplasmic processes, known as filopodia, within a network of small channels called canaliculi (Figures 3 and 4). The lacunocanalicular system facilitates the communication of osteocytes with each other and with osteoblasts/bone-lining cells *via* gap junctions, which are mainly composed of connexin 43 (Cx43). Osteocytes play an important role in triggering bone remodeling (see section 1.1.7). Like osteoblasts, osteocytes lack mitotic activity [1–3].

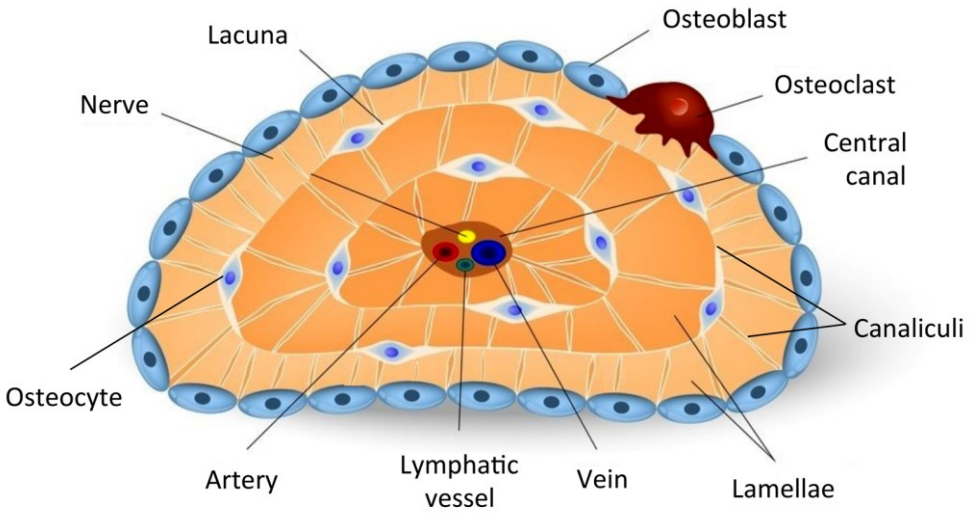

Figure 4. Schematic representation of the osteocytic lacunocanalicular system. Osteocytes are present in lacunae between lamellae. They are connected with each other *via* numerous cellular filopodial processes extended inside the canaliculi (adapted from http://www.istockphoto.com).

1.1.3.4. Osteoclasts

Osteoclasts or bone-resorbing cells are multinucleated giant cells with a “foamy” cytoplasm (Figure 3). These terminally differentiated cells derive from the fusion of myeloid progenitor cells (*i.e.* hematopoietic lineage cells (HSCs)) in a process called osteoclastogenesis. Their differentiation pathway is common to that of macrophages and dendritic cells and is under the influence of several factors. Among these factors, the macrophage colony-stimulating factor (M-CSF), secreted by osteoprogenitor cells and osteoblasts, and receptor for activation of nuclear factor kappa B ligand (RANKL), secreted by MSCs, osteoprogenitor cells, osteoblasts, and osteocytes, are the two main cytokines involved in osteoclast differentiation. The signaling between

M-CSF and its receptor CSF-1R is essential for proliferation of osteoclast precursors. The interaction of RANKL/RANK in the presence of M-CSF directly stimulates fusion of osteoclast precursors and activation of mature osteoclasts. Osteoblasts also express a secreted factor called osteoprotegerin (OPG), which acts as a decoy receptor for RANKL to inhibit osteoclastogenesis. Osteoclasts are specialized cells that dissolve the mineralized matrix through the synthesis of acids and specific enzymes (Figure 3). During this process, termed osteolysis, they release stored minerals and soluble factors, which regulate calcium homeostasis and bone remodeling (see section 1.1.7). Osteoclasts are found in the periosteum and the endosteum (Figure 3) [1–4].

1.1.4. Bone Matrix

Bone matrix is composed of ~60% inorganic (mineral) phase, ~25% organic (protein) phase, and ~15% water. The inorganic phase serves as a reservoir for minerals, containing ~99% calcium, ~88% phosphate, and ~50% sodium and magnesium of the human body. This phase is formed by ~95% hydroxyapatite crystals (resulting from the interaction between calcium phosphate and calcium hydroxide - $Ca_{10}(PO_4)_6(OH)_2$), and ~5% other inorganic compounds, such as calcium carbonate, calcium fluoride and magnesium fluoride. These minerals give to the bone its characteristic hardness and the ability to resist compression. The organic phase serves as a depository for cytokines and growth factors and reservoir for lipids. This phase consists of ~90% type I collagen triple helices organised in fibrils, ~8% noncollagenous proteins (glycoproteins, proteoglycans, cytokines, and growth factors), and ~2% lipids. Glycoproteins are the most abundant noncollagenous proteins in bone and include osteocalcin, alkaline phosphatase (Alp), osteonectin, RGD (Arg-Gly-Asp) peptide - containing proteins (thrombospondin, fibronectin, vitronectin, osteopontin, and bone sialoprotein), fibrillin, and tetranectin. Proteoglycans are macromolecules characterized by the covalent attachment of long-chain polysaccharides (glycosaminoglycans, GAGs) to core protein molecules composed of the leucine-rich repeat sequences (decorin, biglycan, fibromodulin, and osteoadherin). Proteoglycans form a highly hydrated swelled gel-like matrix, which provides the bone with the ability to resist stretching and twisting. Cytokines and growth factors are important modulators of the bone remodeling process (see section 1.1.7) [1–3].

1.1.5. *Neurovascular Supply of Bone*

Blood supplies oxygen, nutrients and regulatory factors to bone tissue, and also removes metabolic waste products [5,6].

In long bones (as an example), small arteries of the periosteum (*i.e.* periosteal arteries) enter the diaphysis through many perforating canals to supply the outer part (1/3) of compact bone (Figure 2). The inner part (2/3) of compact bone and the medullary cavity (including the walls composed of spongy bone) receive nourishment from a large nutrient artery that penetrates the diaphysis through a small opening, called nutrient foramen (Figure 5). The nutrient artery runs transversely through the compact bone and on entering the endosteal cavity divides into proximal and distal branches, which course towards each end of the long bone (Figure 5). Each one of these two branches divides into several radial branches (Figure 5). The ends of long bones are supplied by the metaphyseal/epiphyseal arteries, which arise from arteries that supply the associated joint (Figure 5). At the region of metaphysis, metaphyseal/epiphyseal arteries anastomose with terminal branches of the nutrient artery. As the blood passes through the different parts of the bone, it is collected by respective vein (nutrient vein, metaphyseal/epiphyseal veins, and periosteal veins) and carried out of the bone (Figure 5) [5,6].

Nerve fibers accompany the same paths that blood vessels into the bone, where they tend to concentrate in the more metabolically active regions. Innervation is involved in the regulation of blood supply and bone formation. The periosteum is rich in sensory nerve fibers, some of which carry severe pain sensations resulting from a trauma, fractures, or bone tumors [7–9].

1.1.6. *Bone Formation*

There are two processes of bone formation in the fetus and young children, intramembranous ossification and endochondral ossification [10,11].

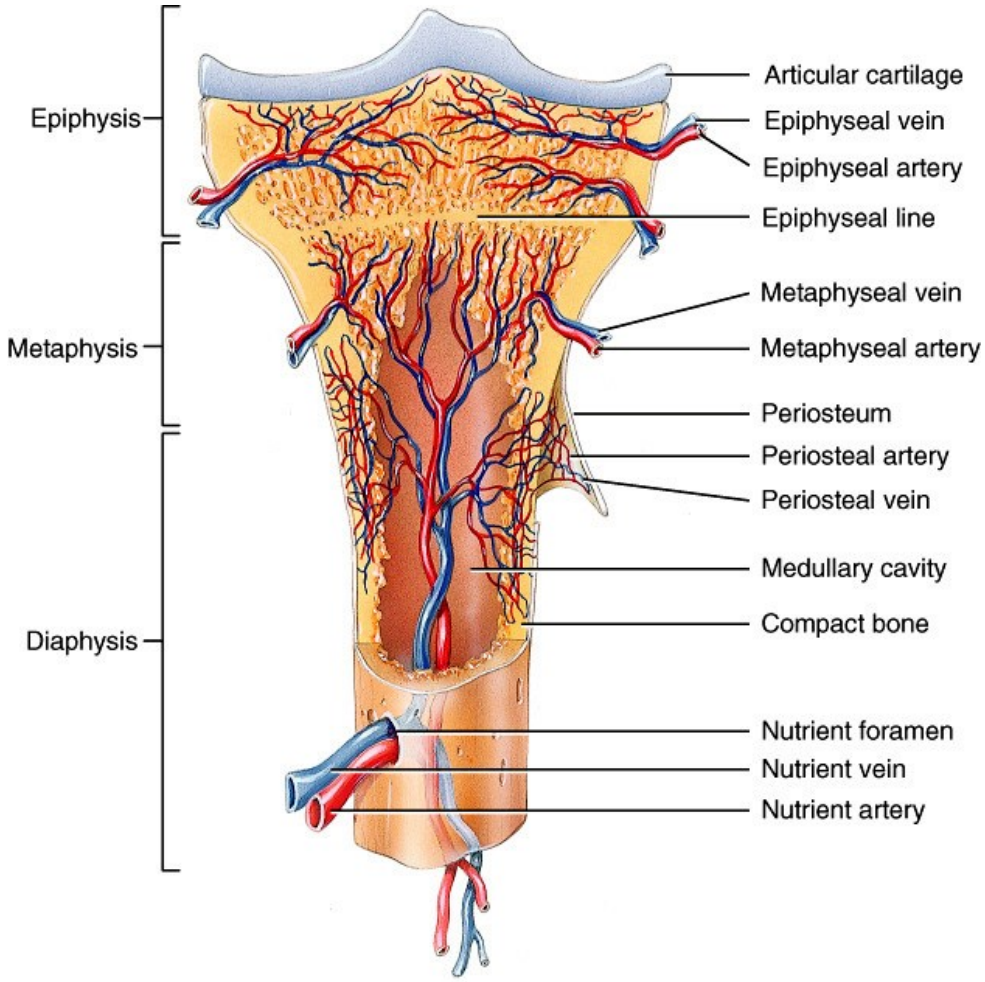

Figure 5. Schematic representation of blood supply of a typical long bone. Blood supply to long bone comes from three sources: periosteal system, nutrient system, and metaphyseal-epiphyseal system (Copyright 2009, John Wiley & Sons, Inc.)

1.1.6.1. Intramembranous ossification

Intramembranous ossification is the source of compact and spongy tissues of flat bones of the skull, the mandible, and the clavicle. This process occurs from sheets of a relatively undifferentiated connective tissue, called embryonic connective tissue or mesenchyme, containing MSCs. Intramembranous ossification occurs about the same time as blood vessels begin to develop (see section 1.1.9). It begins as MSCs proliferate and condense within the mesenchyme, forming small and dense/compact clusters of cells, called ossification centers (Figure 6a). Some of the MSCs support capillary formation, while others differentiate into osteoprogenitor cells and then osteoblasts to form bone tissue. Blood components help osteoblasts to produce and mineralize the osteoid (Figure 6a). As ossification proceeds, some osteoblasts are trapped within the matrix, where they become osteocytes (Figure 6b). The

mineralized matrix grows outwards from the ossification centers in small struts termed bony spicules. These spicules eventually fuse with each other giving rise to the trabeculae of the woven bone. As the spicules interconnect they trap blood vessels within the bone (Figure 6c). Periosteum is formed from compact layers of MSCs lining the periphery of the ossification center (Figure 6c). Osteoblasts of the inner surface of the periosteum, deposit layers of bone matrix and fill spaces between trabeculae, creating a zone of compact bone parallel to the remaining spongy bone (Figure 6d). Once the rudimentary spongy and compact bones are formed, the endosteum begins to develop. Crowds of blood vessels near the spongy bone, condensate and form the red marrow [11,12].

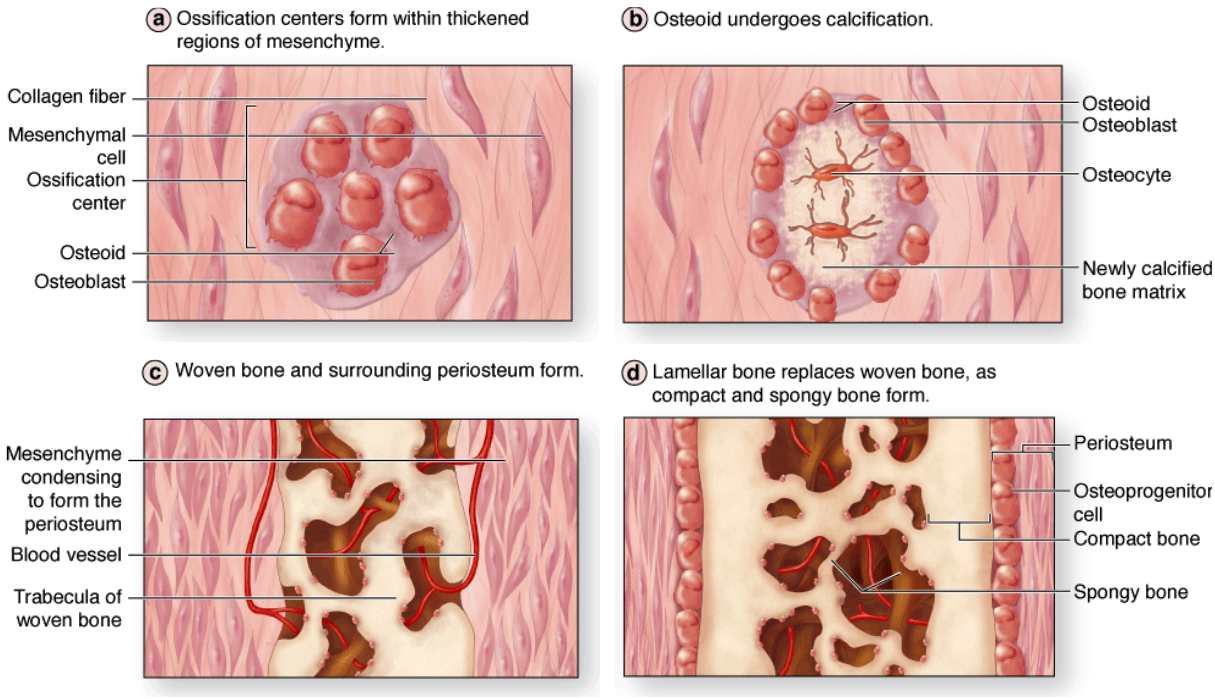

Figure 6. Schematic representation of the intramembranous ossification process. a) MSCs proliferate and condense into centers of ossification, where they differentiate into osteoblasts that secrete osteoid. b) Osteoblasts trapped inside the calcified matrix become osteocytes. c) Bone matrix develops into trabeculae of woven bone. Blood vessels grow into spaces between trabeculae. Mesenchyme at the periphery of the bone matrix condenses and develops into the periosteum. d) Osteoprogenitor cells of the inner layer of the periosteum differentiate into osteoblasts, which produce the compact bone parallel to the existing spongy bone (adapted from www.accessmedicine.com).

1.1.6.2. Endochondral (intracartilaginous) ossification

In endochondral ossification, the MSCs first differentiate into hyaline cartilage (avascular tissue), which is later replaced by bone tissue (highly vascular tissue).

This type of ossification is responsible for the formation of most of the bones of the skeleton, particularly short and long bones. Endochondral ossification begins as clusters of MSCs differentiate into chondrocytes (*i.e.* cartilage cells). Chondrocytes then form a cartilaginous skeletal precursor, whose shape resembles a small version of the bone to be formed. This hyaline cartilage template is covered with a membrane, called perichondrium, which later become the periosteum (Figure 7-1). Some MSCs of the perichondrium differentiate into osteoprogenitor cells and then osteoblasts to form a bone collar around the diaphysis (Figure 7-2). This periosteal bone collar supports the growing bone. In the center of the cartilage template, chondrocytes undergo a degenerative process. This process is characterized by chondrocyte proliferation and differentiation into hypertrophic chondrocytes (Figure 7-2), and ultimately their apoptosis (Figure 7-3). The terminally differentiated chondrocytes stop to produce collagen and other proteoglycans and begin to secrete Alp, which promote the calcification of the surrounding cartilage matrix (Figure 7-2). In addition, these chondrocytes secrete vascular endothelial cell growth factor (VEGF), which induces the sprouting of blood vessels from the perichondrium (Figure 7-2; see section 1.1.9). As hypertrophic chondrocytes die, they leave cavities within the calcified cartilage matrix (Figure 7-3). A periosteal bud penetrates the diaphysis, previously perforated by osteoclasts, invades these cavities and branch in opposite directions (Figure 7-3). The periosteal bud contains blood vessels, nerves, and lymphatic vessels. The blood vessels carry HSCs, osteoprogenitor cells, and other cells into the cavities. The HSCs will later form the bone marrow. Osteoblasts derived from osteoprogenitor cells use the calcified cartilage as a scaffold to create spongy bone in the primary ossification center (Figure 7-3). Osteoblasts of the newly formed periosteum deposit compact bone around the spongy bone. Osteoclasts break down some spongy bone and form the medullary cavity (Figure 7-4). The development of secondary ossification centers continues somewhat later (after birth) in the epiphyses by a similar process (Figure 7-4). Bone replaces hyaline cartilage, except the articular cartilage and epiphyseal plate of long bones. Articular cartilage persists throughout adult life while the epiphyseal plates remain until early adulthood, *i.e.* until the bone stops growing (Figure 7-5). The epiphyseal line replaces the epiphyseal plate and the diaphysis and epiphysis regions fuse together to form a single adult bone in a process known as the epiphyseal closure (Figure 7-5) [10–12].

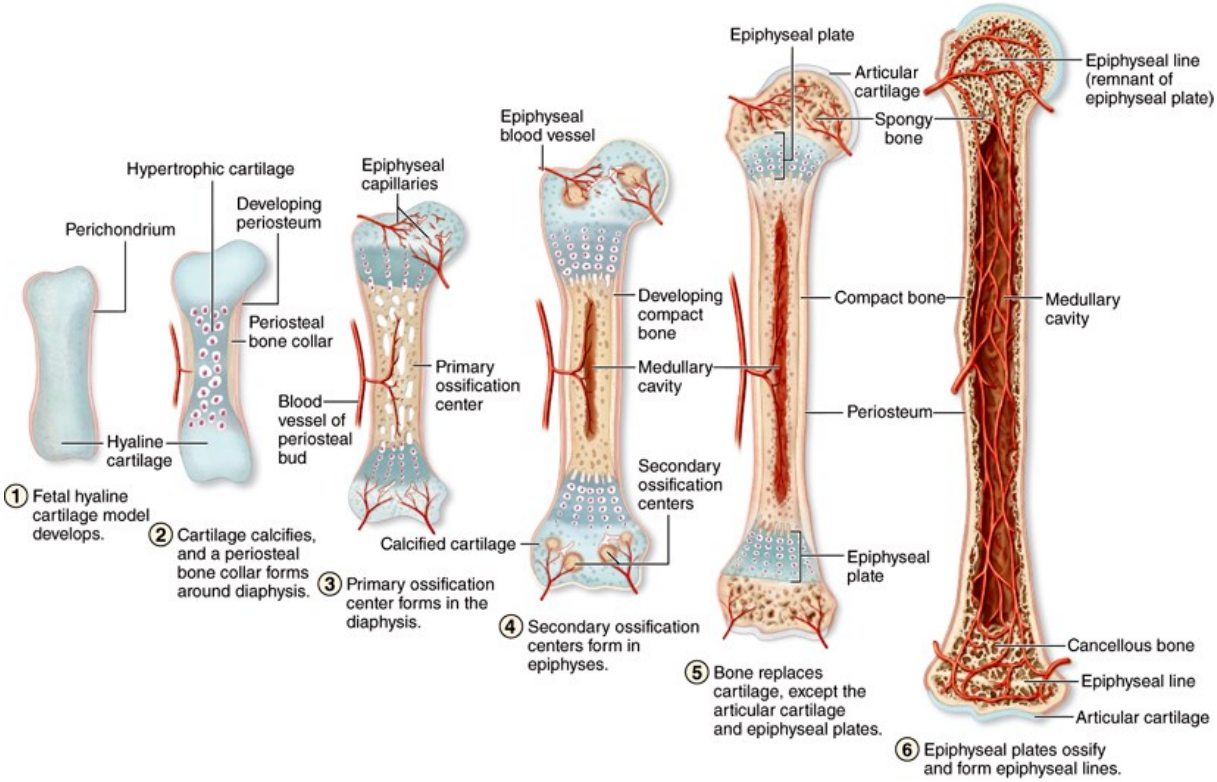

Figure 7. Schematic representation of the endochondral ossification process. 1) A hyaline cartilage model of the respective bone is formed. 2) Around the diaphysis of the cartilage model, a periosteal bone collar is produced by perichondrium. In the center region, the chondrocytes undergo a degenerative process with cell enlargement (hypertrophy) and matrix calcification 3) Chondrocytes die and leave cavities within the calcified cartilage matrix. Blood vessels penetrate the bone collar and invade the cavities in the diaphysis bringing osteoprogenitor cells to this region. These cells become osteoblasts, which form the spongy bone around the cavities. In this way, the primary ossification center is established in the diaphysis. 4) Osteoclasts dissolve some spongy bone to develop the medullary cavity and osteoblasts produce the compact bone beneath the periosteum. Secondary ossification centers appear at the epiphyses. 5) Bone replaces cartilage except the articular cartilage, which persists throughout adult life, and the epiphyseal plate, 6) which is replaced by epiphyseal line in the early of adulthood (adapted from www.accessmedicine.com).

1.1.7. Bone Remodeling

Bone remodeling (metabolism) is a dynamic process by which old/microdamaged bone is replaced by new bone. This process plays an essential role in calcium homeostasis and ensures the mechanical integrity of the skeleton. An imbalance in the regulation of bone resorption and bone formation results in metabolic bone diseases, such as osteoporosis (bone resorption>bone formation) and osteopetrosis (bone formation>bone resorption). Most of the metabolism occurs at the bone surfaces. Due to the higher surface area of spongy bone compared to cortical bone, most of the turnover takes place at the endosteal surface of spongy bone. Bone

remodeling occurs due to coordinated actions of osteoclasts, osteoblasts, osteocytes, and bone lining cells, associated with blood vessels and nerves. Together, they form a temporary anatomical structure, called basic multicellular unit (BMU) or bone remodeling unit (BRU) [13–17].

1.1.7.1. Bone remodeling cycle

Bone remodeling cycle involves a series of highly regulated phases: resting (activation), resorption, reversal (transition), formation, and mineralization (termination) (Figure 8) [13–16].

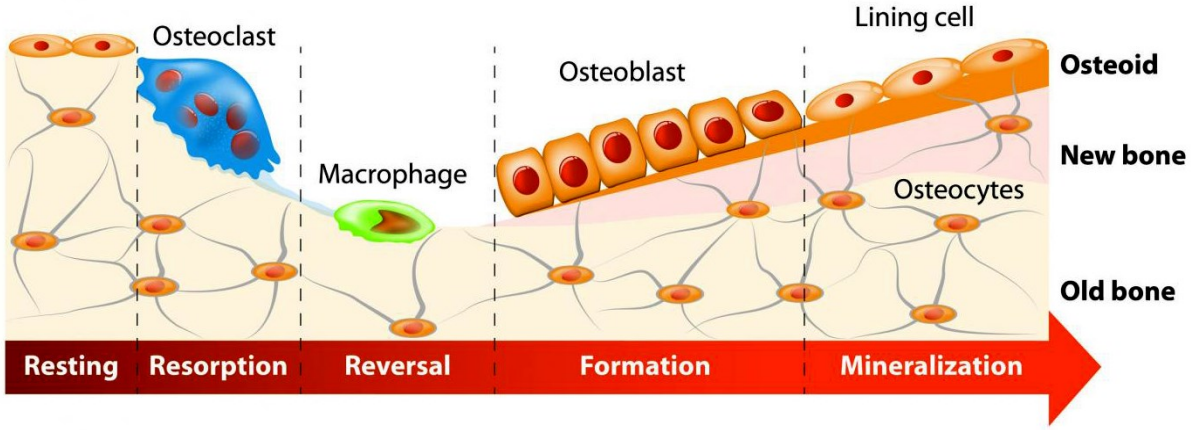

Figure 8. Schematic representation of the bone remodeling cycle. Bone remodeling consists of a series of sequential phases that are highly regulated. Bone resorption by osteoclasts is followed by the recruitment of osteoblasts and formation of new bone matrix. The newly synthesized matrix is then slowly mineralized (adapted from http://www.istockphoto.com).

The activation of the quiescent bone surface results in the retraction of bone-lining cells by matrix metalloproteinases (MMPs). This activation process is partly regulated by osteocytes, which act as sensors of mechanical loading and biochemical stimuli. Osteoclast precursor cells are then recruited by chemotaxis to the activated surface and fuse to form mature osteoclasts (Figure 8). These osteoclasts attach to the bone surface through a contiguous adhesion belt, known as sealing (clear) zone, which creates an isolated microenvironment beneath the cell. Within the sealing zone, the osteoclast plasma membrane develops into the ruffled border, which acts as the resorptive organelle of these cells (Figure 9). As a consequence, osteoclasts dissolve the inorganic matrix by creating an acidic microenvironment through the secretion of several acids and a large amount of protons (H^+), and digest the organic matrix by

releasing specific enzymes, such as lysosomal enzymes, tartrate-resistant acid phosphatase (TRAP), cathepsin K, and MMP-9 (Figure 9). Bone degradation products are then removed from the functional secretory domain *via* transcytotic vesicles (Figure 9). Osteoclast activity results in the formation of resorption pits on bone surface, called as Howship's lacunae (Figure 9). Once the osteoclasts have completed their work, mononuclear cells with an unclear phenotype prepare the surface of Howship's lacunae for bone formation and provide matrix-derived signals, such as transforming growth factor-β (TGF- β) and insulin-like growth factor I and II (IGF-I/II), for osteoblast differentiation and migration (Figure 8) [13–17].

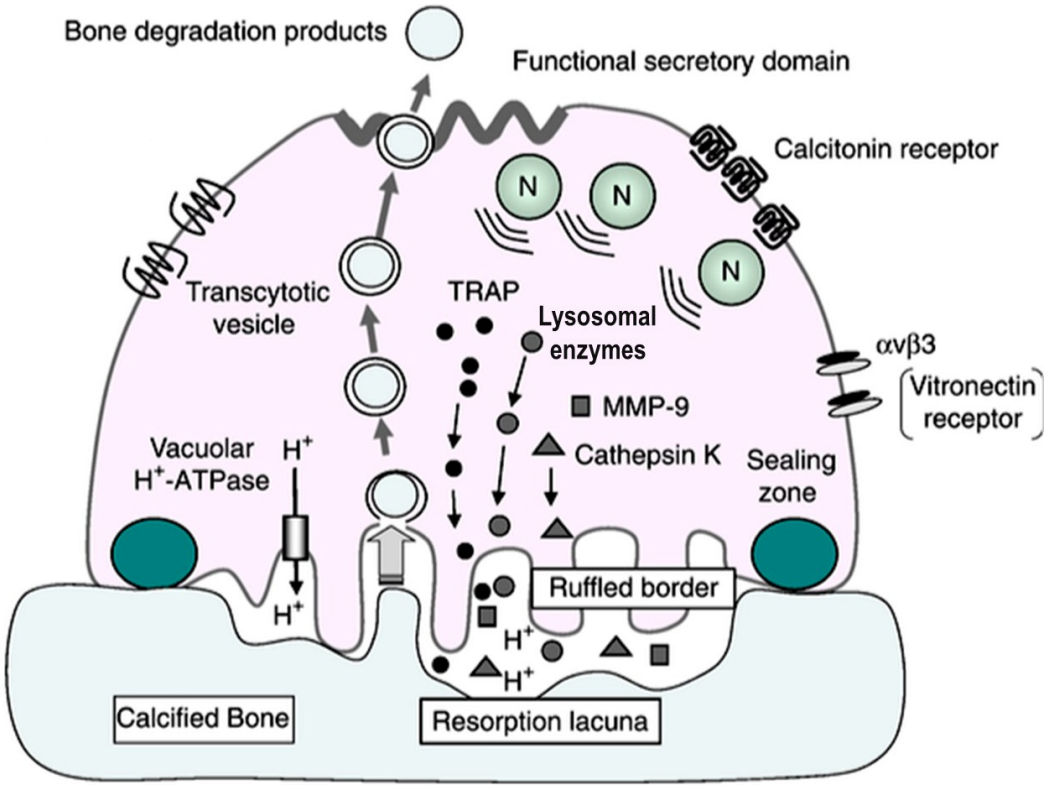

Figure 9. Schematic representation of the osteoclast activity. Osteoclasts form sealing and ruffled borders. Bone resorption is achieved by transport of protons into the resorption lacunae through vacuolar H^+-ATPase and secretion of specific enzymes (cathepsin K, MMP-9 and TRAP). Matrix degradation products are removed from the functional secretory domain *via* transcytotic vesicles (adapted from Takahashi *et al*., BoneKEy Reports, 2014).

The bone remodeling cycle is finished with the synthesis/deposition of organic components of bone matrix by osteoblasts, and its subsequent mineralization (Figure 8). The collagen network is synthesized first followed by incorporation of non-

collagenous proteins. The production of type I collagen and formation of the collagenous matrix is followed by an increased expression of ALP. This gradually decreases when matrix mineralization is progressed. Osteocalcin appears at the latest stages of differentiation pathway, approximately at the onset of mineralization. The newly formed bone surface is completely covered with bone-lining cells and maintained until the next remodeling cycle is initiated (Figure 8). The resorption activity in adult human bone takes approximately 3 weeks and the formation response 3 to 4 months [13–17].

1.1.7.2. Regulatory factors in bone remodeling

The regulation of bone remodeling is both systemic and local. The main interrelated systemic factors include: genetics; age; nutrition; exercise (mechanical loading); and hormones, particularly thyroid hormones, thyroid-stimulating hormone (TSH), parathyroid hormone (PTH) / parathyroid hormone-related protein (or PTHrP), calcitonin, calcitriol (1,25-dihydroxyvitamin D, $1,25(OH)_2D$ or Vitamin D), growth hormone, gonadal hormones, insulin, and glucocorticoids. Table 1 summarises the role of the "classic" hormones in bone metabolism [18,19].

As far as local regulation of bone remodeling is concerned, it has been identified a large number of autocrine/paracrine molecules produced by bone cells and soluble factors released from the bone matrix during osteolysis. Important growth factors, cytokines, and prostaglandins acting on bone turnover are tabulated in Table 2, according to its function [18–21].

Another category of molecules called semaphorins (Sema) has been recognized as a modulator of bone remodeling. Sema are a class of secreted and membrane-associated proteins that were originally identified as axonal growth cone guidance molecules. It was found that Sema4D, expressed in osteoclasts, and Sema3A, abundantly expressed in osteoblasts, are important regulators of bone metabolism. During bone resorption, Sem4D inhibits bone formation by binding to its receptor (Plexin-B1) present in osteoblasts [22]. On the other hand, Sema3A, secreted by sensory neurons, promotes bone formation indirectly by modulating the local nerve ingrowth and not by acting directly on osteoblasts (see chapter 1.3) [23].

More recently, microRNAs (miR) have been regarded as one of the most important modulators in bone turnover. miR are short single strand non-coding molecules of RNA (between 18 and 25 nucleotides long) that negatively regulate gene expression either by mRNA degradation or translational silencing. In this context, miR can act as

both negative and positive regulators of differentiation of osteoblasts and osteoclasts (Table 3) [24].

Table 1. Hormones involved in bone remodeling.

Decrease Bone Resortion	Increase Bone Resorption	Increase Bone Formation	Decrease Bone Formation
Calcitonin	PTH/PTHrP	Growth hormone	Glucocorticoids
Estrogens	Glucocorticoids	Vitamin D metabolites	Thyroid hormones
TSH	Thyroid hormones	Androgens	
	High-dose vitamin D	Estrogens	
		Progesterone	
		Insulin	
		Low-dose PTH/PTHrP	
		TSH	
		Thyroid hormones	

PTH, parathyroid hormone; PTHrP, parathyroid hormone-related protein; TSH, thyroid-stimulating hormone

Table 2. Growth factors, cytokines, and prostaglandins involved in bone remodeling.

	Stimulate bone formation	Stimulate bone resorption	Inhibit bone resorption	Inhibit bone formation
Growth factors	BMP-2, BMP-4, BMP-5, BMP-6, BMP-7, BMP-9, TGF-β, IGF-I, IGF-II, PDGF, VEGF, FGF	EGF, PDGF, FGF, GM-CSF, M-CSF	TGF-β	BMP-3
Cytokines and Prostaglandins	IL-3, IL-13, IL-17 IFN, CT-1	TNF, RANKL, IL-1, IL-6, IL-8, IL-11, PGE_1, PGE_2, PGG_2, PGH_2, PGI_2	OPG, IFNγ, IL-4, Il-10, IL-12, IL-18, IL-23	

BMP, bone morphogenetic protein; CT1- cardiotrophin-1; EGF, epidermal growth factor; FGF, fibroblast growth factor; GM-CSF, granulocyte-macrophage colony-stimulating factor; IFNγ, interferon gamma; IGF, insulin-like growth factor; IL, interleukine; M-CSF, macrophage-colony stimulating factor; OPG, osteoprotegerin; PDGF, platelet-derived growth factor; PG, prostaglandin; RANKL, receptor activator of nuclear factor kappa-B ligand; TGF- β, tumor growth factor-beta; TNF, tumor necrosis factor

Table 3. Key miR regulators of bone remodeling

	Activate Differentiation	Inhibit Differentiation
Osteoblasts	MiR-15b; MiR-17~92; MiR-20a; MiR-29a; MiR-181a; MiR-322; MiR-335-5p	MiR-17-5p; MiR-30c; MiR-34c; MiR-93; MiR-100; MiR-125b; MiR-133a; MiR-135a; MiR-137; MiR-138; MiR-141; MiR-200a; MiR-143; MiR-182; MiR-204/211; MiR-205; MiR-206; MiR-208; MiR-217; MiR-218; MiR-338; MiR-542-3p; MiR-637; MiR-764-5p
Osteoclasts	MiR-21; MiR-29b; MiR-31; MiR-34a; MiR-148a; MiR-223	MiR-29b; MiR-125a; MiR-146a; MiR-155; MiR-223; MiR-503

Adapted from Alečković M and Kang Y, BoneKEy Reports, 2015.

1.1.8. Canonical Wnt Signaling Pathway in bone formation and remodeling

The canonical Wnt pathway (Wnt/β-catenin pathway) regulates many cellular activities, such as proliferation, differentiation, maturation, migration, survival, and apoptosis. It is widely demonstrated that this pathway is critical for osteoblast differentiation and function and consequently, for bone formation and metabolism. Wnt/β-catenin pathway is also important in adipogenesis, chondrogenesis and hematopoiesis and may be stimulatory or inhibitory at different stages of osteoblastogenesis [25–28].

The central function of the canonical Wnt pathway is the regulation of β-catenin (encoded by *Ctnnb1*) stabilization. β-catenin is a dual-function protein that coordinates cell-cell adhesion and acts as an intracellular signal transducer in the Wnt/β-catenin pathway. β-catenin binds to cadherin and α-catenin at the plasma membrane, and this cadherin-catenin complex links to the actin filaments and several actin-binding proteins to promote cell-cell adhesion (Figure 10) [25–28].

When Wnt/β-catenin signaling is not activated, β-catenin is degraded after being recruited to a complex composed of axin, adenomatous polyposis coli (APC), glycogen synthase kinase (GSK) 3β, and other proteins (Figure 10). Axin and APC act as scaffold proteins promoting the interaction of β-catenin with GSK-3β. The phosphorylation of β-catenin by GSK-3β targets it for ubiquitination and subsequently, recognition and constitutive degradation by the ubiquitin-proteasome system (Figure 10) [25–28].

When a Wnt secreted glycoprotein (*e.g.* Wnt3a and Wnt10b) binds to its Frizzled (Fzd) receptor and co-receptor low-density lipoprotein receptor-related protein (LRP) - 5/6, axin and the cytoplasmic protein disheveled (Dsh) are recruited and tethered to the ligand-receptor complex (Figure 10). Axin binds to the phosphorylated LRP5/6 and disables the degradation complex. Phosphorylated Dsh binds to the Fzd receptor and transduces a signal for inhibition of the GSK3β activity, which leads to accumulation of nonphosphorylated β-catenin in the cytosol (Figure 10). The stabilized β-catenin is then translocated into the nucleus to activate the transcriptional expression of Wnt-related genes *via* lymphoid enhancer binding factor (Lef) and T cell factors (Tcf) (Figure 10). Runt-related transcription factor 2 (*Runx2*) is a direct target gene of β-catenin/Tcf/Lef. Wnt/β-catenin signaling activates expression of *Runx2* in MSCs for the control of osteoblast differentiation and bone formation. It determines the osteoblastogenesis at the early stage and inhibits it at the late stage. Runx2 interacts with other transcription factors, especially osterix, to regulate the transcriptional expression of important bone phenotyping genes, such as collagen type I alpha 1 chain (*Col1a1)*, *Alp*, and bone gamma-carboxyglutamic acid-containing protein (*Bglap*, encoding osteocalcin). Tumor necrosis factor ligand superfamily member 11 (*Tnfrsf11b*), encoding the anti-osteoclastogenic factor OPG, is known to be another Wnt-related gene. The canonical Wnt signaling suppresses indirectly osteoclast differentiation and bone resorption through upregulation of OPG in osteoblasts [25–28].

The amplitude of the Wnt/β-catenin signaling is fine-tuned in part *via* negative feedback by secreted extracellular antagonists, such as secreted Fzd-related peptides (sFRPs), Wnt inhibitory factor (Wif) - 1, dickkopf (Dkk) 1/2, and sclerostin. While sFRPs and Wif-1 interact directly with Wnt proteins, Dkk 1/2 and sclerostin bind to the extracellular domains of LRP5/6, thus preventing signaling activation and leading to decreased bone formation [25–28].

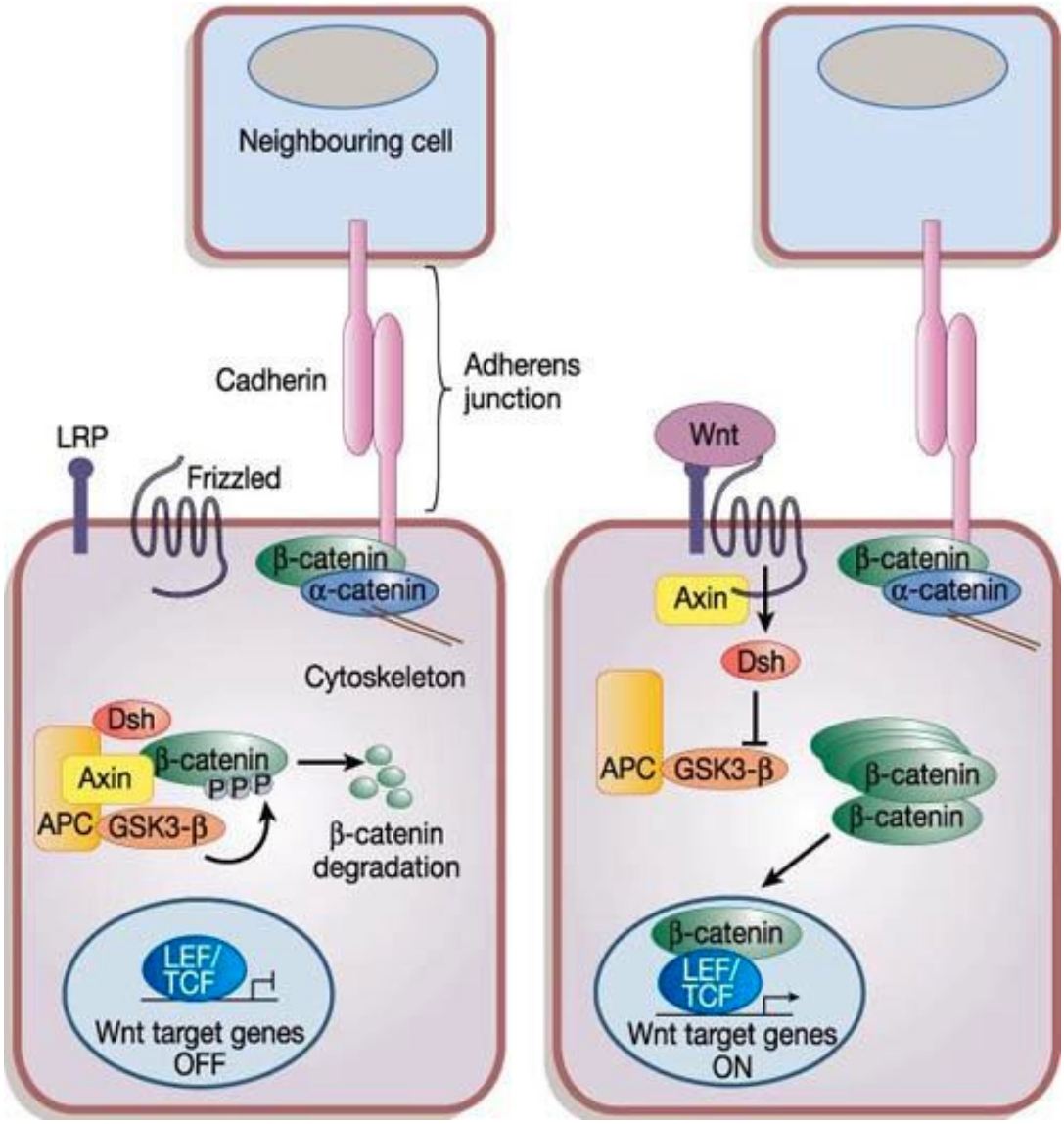

Figure 10. Schematic representation of the canonical Wnt signaling pathway. β-catenin forms a cadherin-catenin complex at the plasma membrane that regulates cell-cell adhesion. (Left panel) In the absence of Wnt signaling, β-catenin is prone to degradation, by forming a complex with axin, APC and GSK3-β. β-catenin is phosphorylated by GSK3-β that marks it for ubiquitination and subsequent degradation by the proteasome. (Right panel) In the presence of Wnt signaling, β-catenin is uncoupled from the degradation complex, accumulates and translocates into the nucleus, where it acts as a co-activator of Lef/Tcf transcription factors (adapted from Reya T and Clevers H, Nature, 2005).

The canonical Wnt signaling cooperates with a number of other bone formation signaling pathways, such as PTH/PTHrP, bone morphogenetic proteins (BMPs)/TGF-β, and Indian hedgehog.

1.1.9. *Angiogenesis/Vascularization in bone formation and remodeling*

Bone formation and remodeling processes require the action of both intrinsic and extrinsic inductive factors produced from multiple cell types, which function in a hierarchical and temporal fashion to control angiogenesis and osteogenesis. Endothelium (*i.e.* the inner lining of blood vessels) is an integral part of bone tissue, and its interaction with bone cells is crucial for skeletal development, homeostasis, and healing [30]. The interplay between endothelial and bone cells has been extensively investigated, and numerous modes of cell communication have been proposed, specifically *via* secretion of humoral factors, growth factors, chemokines, and direct cell-cell contact through gap junctional proteins [31]. Among the growth factors, VEGF expressed in endothelial cells plays a critical role in the orchestration of bone formation and remodeling, by increasing the production of BMPs [32]. In addition, other factors secreted by endothelium, such as endothelin-1 and angiotensin-II, are also able to induce bone formation [33–35].

Previous studies have shown that angiogenesis is preceded by peripheral innervation during bone formation and regeneration [31], suggesting that peripheral nervous system controls these processes through the local release of neuronal mediators. A recent study indicates that sonic hedgehog, a traditional neurogenic morphogen, inversely regulates the vascular morphogens angiopoietin-1 and angiopoietin-2, thus contributing to blood vessel growth, maturation and stabilization in a neurovascular network [36].

These and other studies provide a robust body of evidence that bone is regulated by different tissues/systems, evidencing its complexity and dynamic nature [29]. In this dissertation we focused on the regulation of osteoblast and bone formation by the sensory nervous system.

The sensory nervous system is the part of the peripheral nervous system responsible for processing sensory information. Sensory neurons carry this information as a nerve impulse from the viscera, sense organs, muscles, bones and joints towards the central nervous system (CNS), where the information is perceived and interpreted. Despite this classic function, a specific subgroup of sensory neurons also has the ability to release neuropeptides from their peripheral endings to regulate organ/tissue activities [37–39].

1.2.1. Functional Organization of the PNS

The peripheral nervous system (PNS) consists of the nervous tissue that lies outside the brain and spinal cord (*i.e.* outside the CNS). It forms the communication network between the CNS and rest of the body. The CNS interacts with the PNS through 12 of cranial nerves, which connect the brain to areas of the head and neck, and 31 pairs of spinal nerves, which connect the spinal cord to the rest of the body. The spinal nerve emerges from the spinal cord between adjacent vertebrae through an opening called intervertebral foramen. Each spinal nerve is formed by dorsal root housing afferent (sensory) neurons and ventral root carrying efferent (motor) neurons. These two roots are actually parts of the two major divisions of the PNS: sensory, or afferent, and motor, or efferent, divisions (Figure 11). The sensory division consists of afferent neurons that carry sensory information from receptors in the periphery of the body to the CNS (Figure 11). The motor division contains efferent neurons that carry motor information from the brain to the rest of the body. This division is subdivided into somatic nervous system and autonomic nervous system (Figure 11). The somatic nervous system includes the voluntary motor neurons and transmits signals from the CNS to skeletal (striated) muscles (Figure 11). It is responsible for stimulating muscle contraction (conscious activities). The autonomic nervous system includes the involuntary motor neurons and transmits signals from the CNS to cardiac muscle, smooth muscles, and glands (Figure 11). It is responsible for secretion of chemical signals from the glands and maintains the proper function of the visceral organs, such as the heart, stomach, and intestines

(subconscious activities). There are two subdivisions of the autonomic nervous system, the sympathetic and parasympathetic (Figure 11). The sympathetic nervous system is responsible for mobilization of energy and resources during times of stress and arousal, while the parasympathetic nervous system acts as an antagonist that returns the body to its normal resting state (Figure 11). This antagonistic functional relationship serves as a balance to help maintain homeostasis [37–39].

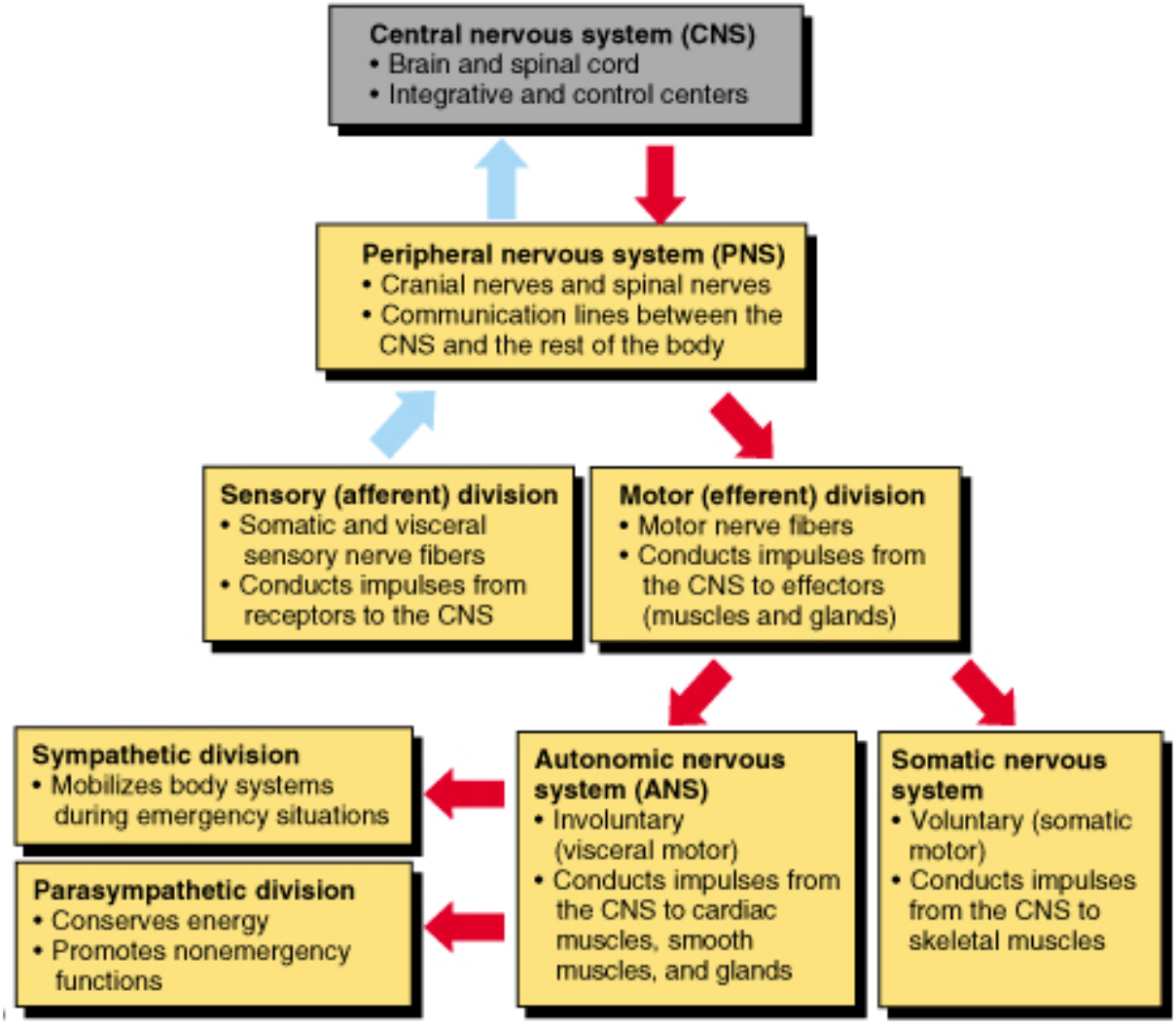

Figure 11. Functional organization of the peripheral nervous system. The PNS is divided into sensory (afferent) and motor (efferent) divisions. The afferent division sends sensory signals to the CNS and the efferent division receives motor signals from the CNS. The efferent division can be subdivided into two groups: autonomic and somatic nervous systems. The autonomic nervous system itself can be divided into the sympathetic and parasympathetic nervous systems (adapted from www.apsubiology.org)

1.2.2. Basic Function and Structure of a Neuron

The nervous system contains two types of cells: glial cells and neurons. The glial cells protect and nourish the neurons and are the key element to support their function. Neurons are considered to be the basic working unit of the nervous tissue. These specialized cells receive and transmit signals to other cells. They have a main part called cell body or soma and extensions of their membranes, generally referred to as processes. The cell body contains the nucleus and cytoplasm with most of the major organelles (Figure 12) [37–39].

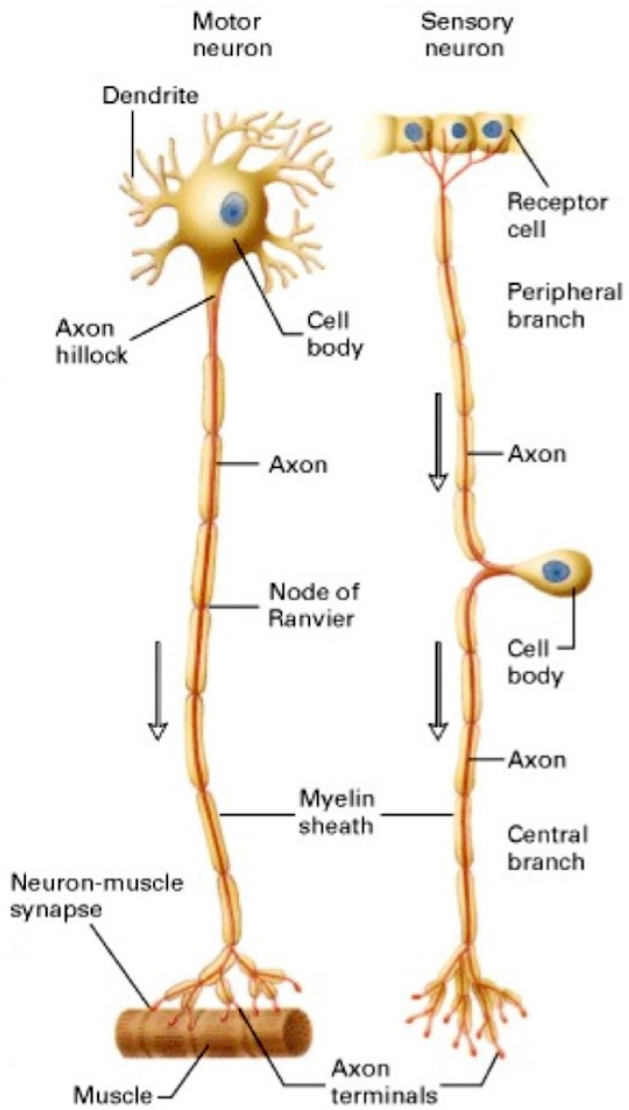

Figure 12. Schematic representation of neuron structure. (Left) A motor neuron with a single axon projected from the cell body, which is located in the ventral root ganglion, to the effector cell. (Right) A sensory neuron with an axon that divides into a central and peripheral branch just after it leaves the cell body, which is located in the dorsal root, trigeminal root, and nodose ganglia. The peripheral branch carries the electrical impulse from the receptor cell to the cell body; the central branch and axon terminals carry the impulse from the cell body to the CNS (adapted from Lodish H, *et al.* New York: W. H. Freeman; 2000).

There is one important process called an axon, which is the fiber that emerges from the cell body and projects to target cells (Figure 12). The single axon can branch repeatedly into axon terminals to communicate with multiple target cells *via* synapses (Figure 12). The neuron transmitting the signal is termed the presynaptic neuron, and the neuron receiving the signal is called the postsynaptic neuron. There are two different types of synapses, electrical and chemical. At electrical synapses, current flows directly and passively from pre- to postsynaptic cells through specialized membrane channels (gap junctions) (Figure 13A). At chemical synapses, the vesicular release of chemical messengers (neurotransmitters) by a presynaptic cell into the synaptic cleft, produces secondary current flow in a postsynaptic cell by activating specific receptors on the plasma membrane (Figure 13B). The current flow switches the postsynaptic membrane from an internal negative charge to a positive charge state. This change is known as depolarization, which generates an action potential or nerve impulse. This depolarization of the membrane is followed by a rapid repolarization, returning the membrane potential to the resting state [37–39].

Another type of process extended from the cell body is the dendrite (Figure 12). Dendrites are usually highly branched and are responsible for receiving most of the information from axon terminals of other neurons (Figure 12) [37–39].

The specialized structure where the axon emerges from the cell body is known as the axon hillock or initial segment (Figure 12). This structure integrates signals from multiple synapses [37–39].

Many axons are wrapped with a layered myelin sheath, which acts as an insulator and speeds the transmission of the nerve impulse along the axon (Figure 12). In the PNS, this sheath is made of specialized cells known as Schwann cells. Each gap uncovered by myelin is termed a node of Ranvier and is critical for myelin functionalization. The action potential jumps between axonal nodes of Ranvier to increase the speed of its propagation (Figure 12) [40].

In the PNS, a cluster of neuron cell bodies is referred to as a ganglion and a bundle of axons or fibers are called a nerve [39–41].

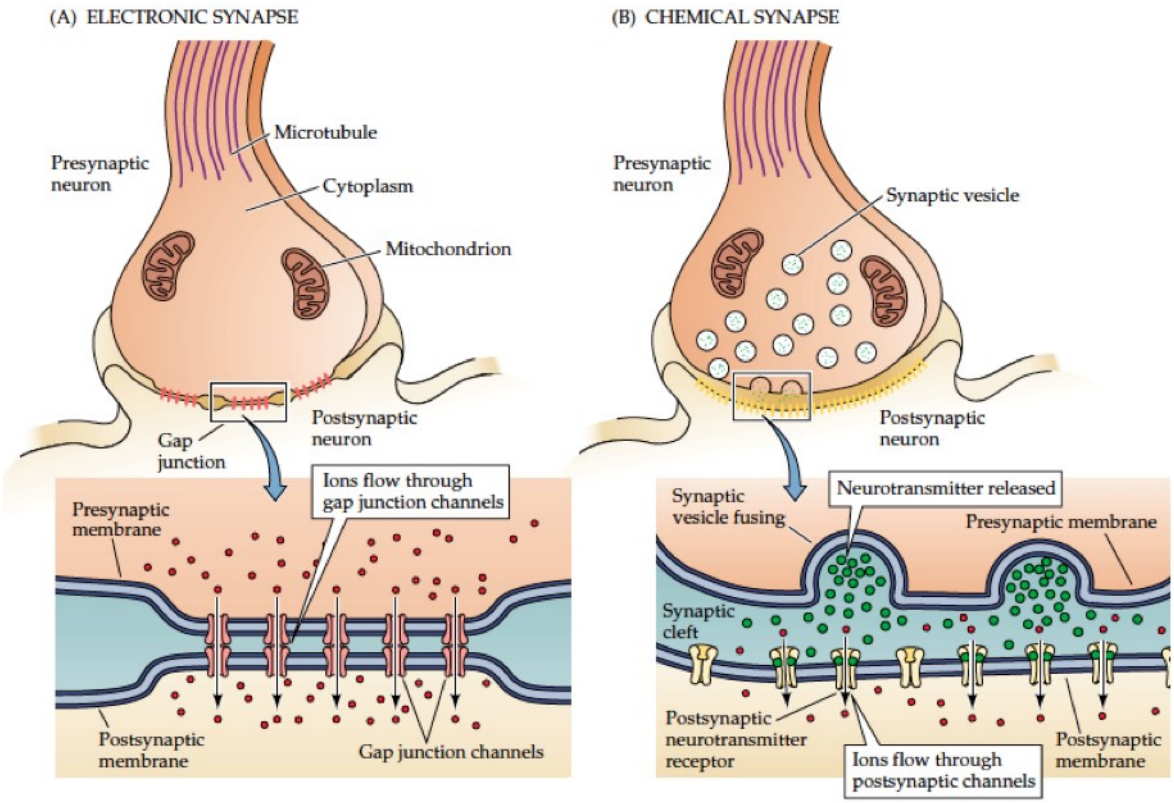

Figure 13. Schematic representation of electric and chemical synapses. (A) At an electrical synapse, ions flow directly and passively through gap junctions resulting in a localized depolarization of the postsynaptic membrane. (B) At a chemical synapse, when the neurotransmitters released by presynaptic cell bind to specific receptors on the postsynaptic membrane, the ligand-gated ion channels open and ions cross the membrane changing its charge (adapted from Purves D, *et al.* Sunderland (MA): Sinauer Associates; 2004).

1.2.3. *Types of Sensory Receptors*

Sensory receptors are either specialized endings of sensory neurons or separate cells that signal to sensory neurons. They are adapted to respond to specific stimuli and to convert them into nerve impulses that are transmitted to the CNS. Different types of sensory neurons have different sensory receptors. Sensory receptors can be classified on the basis of their morphology or function. Morphologically, there are three groups of sensory receptors: free nerve endings, encapsulated nerve endings, and specialized transducing cells. Free nerve endings are simply free dendrites extend into a tissue (Figure 14a). This type of sensory receptor is sensitive to heat, cold, and tissue injury. An encapsulated nerve ending is a nerve ending wrapped in a round capsule of connective tissue (Figure 14b). Mechanical forces stimulate this

type of sensory receptor. Specialized transducing cells detect stimuli from special senses such as vision, hearing, smell, taste, and balance (Figure 14c). Each of the specialized cells is sensitive to a unique special sense. [41]

Functionally, there are three major classes of sensory receptors: mechanoreceptors, nociceptors, and thermoreceptors. Mechanoreceptors are free nerve endings that respond to mechanical stimuli, such as touch, vibration, stretch, pressure, and movement. Nociceptors are unspecialized free nerve endings that respond to noxious stimuli, including extreme temperatures, acidic pH, and tissue damage, by sending pain signals to the CNS. Thermoreceptors monitor changes in temperature inside the body and in its surroundings [37–39].

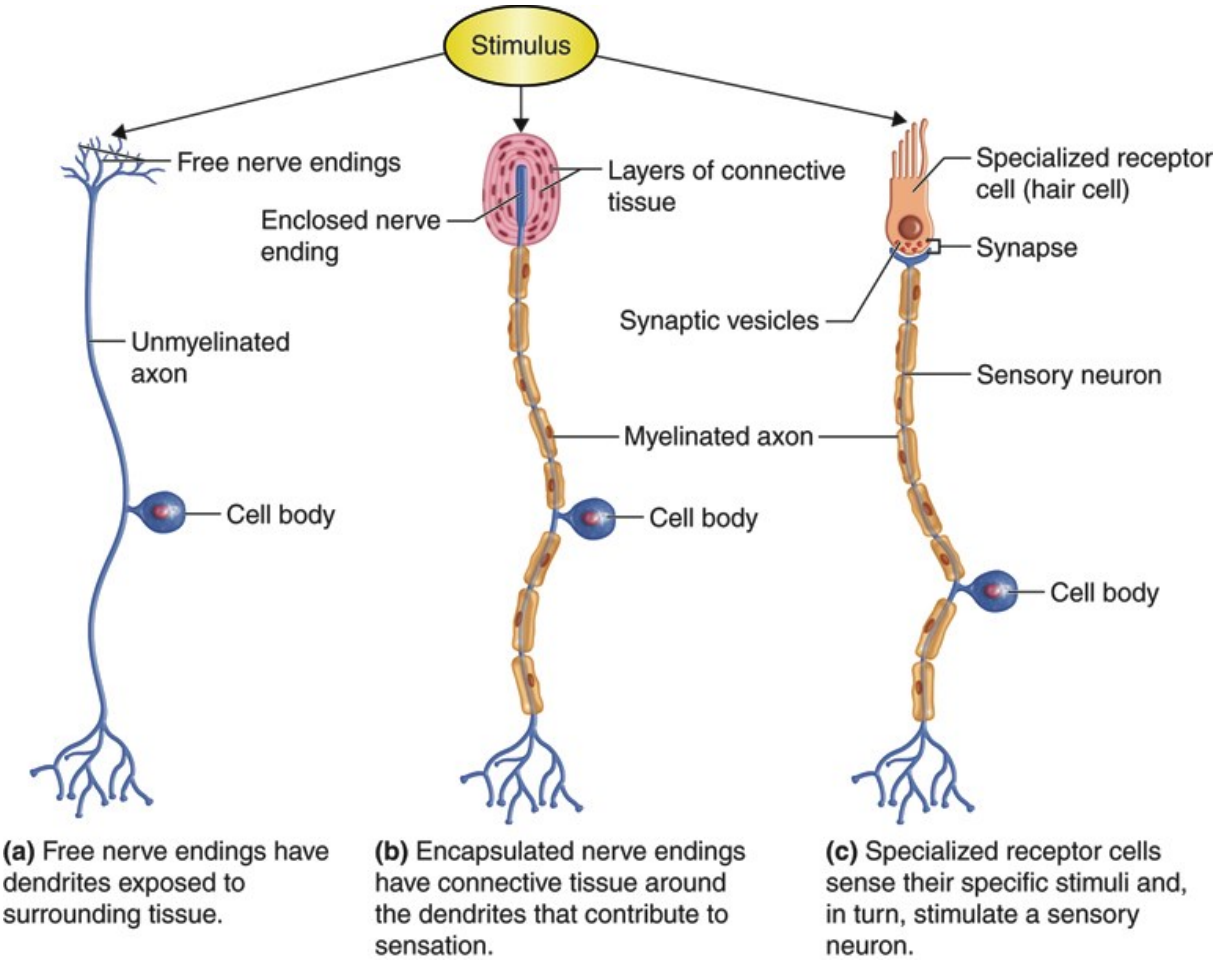

Figure 14. Schematic representation of sensory receptor types. (a) Simply receptors are neurons with free nerve endings. (b) Complex neural receptors have nerve endings enclosed in connective tissue capsules. (c) Most special senses receptors are cells that release neurotransmitter onto sensory neurons, initiating an action potential (adapted from www.pasadena.edu).

1.2.4. *Classification of the Sensory Nerve Fibers*

According to the Lloyd-Hunt classification, the sensory nerve fibers can be classified into type I-fibers, with diameters from 13 to 20 μm (80-120 m/s conduction velocity); type II-fibers, with diameters between 6 and 12 μm (35-75 m/s conduction velocity); type III-fibers, with diameters from 1 to 5 μm (5.0-30 m/s conduction velocity); and type IV-fibers represented by the unmyelinated nerve fibers, with diameters between 0.2 and 1.5 (0.5-2.0 m/s conduction velocity) (Table 4). Type I-fibers are frequently subdivided in type Ia and Ib to differentiate among afferences from muscle spindles and Golgi tendons. The Erlanger-Gasser classification is used to define both afferent and efferent fibers. Thus, type I-fibers represents the Aα-fibers of the Erlanger-Gasser classification; type II-fibers equivalents to the Aβ-fibers; type III-fibers corresponds to the Aδ-fibers; and type IV-fibers represents C fibers (Table 4) [42].

Table 4. Classification of sensory nerve fibers.

Lloyd-Hunt Classification	Erlanger-Gasser Classification	Myelin	Fiber Diameter (μm)	Conduction Velocity (m/s)	Type of Receptor Supplied
Ia and Ib	Aα	Yes	13-20	80-120	Mechanoreceptor
II	Aβ	Yes	6-12	35-75	Mechanoreceptor
III	Aδ	Yes	1-5	5.0-30	Mechanoreceptor Thermoreceptor Nociceptor
IV	C	No	0.2-1.5	0.5-2.0	Mechanoreceptor, Thermoreceptor Nociceptor

Adapted from www.clinicalgate.com

1.2.5. *Dual Afferent and "Efferent" Function of Sensory Neurons*

Sensorimotor neurons are a subpopulation of polymodal nociceptive sensory neurons (*i.e.* respond to painful thermal, mechanical, and chemical stimuli) with a dual afferent and efferent function. They contain predominantly C-fibers and a

smaller population of Aδ-fibers. The cell bodies of the sensorimotor neurons lie in the dorsal root and trigeminal root ganglia. A sensorimotor neuron has a single axon that divides into a central and peripheral branch just after it leaves the cell body. The central branch conveys information about a stimulus to the CNS (afferent function). The peripheral branch communicates with target cells through the release of neurotransmitters from specialized swelling of the axon called varicosities (efferent function) [43]. The main neuropeptides released in the periphery include calcitonin gene-related peptide (CGRP), substance P (SP), and neurokinin A (NKA). CGRP and SP are frequently coexpressed and/or coreleased from sensorimotor neurons. These sensory neuropeptides are implicated in the neurogenic inflammatory response, CGRP mediates vasodilatation and SP mediates plasma extravasation. There is evidence of other cotransmitters in the sensory nerve endings, such as the vasoactive intestinal polypeptide, bombesin, and adenosine triphosphate (ATP) [37].

Histologic and functional studies have shown that these neurons are widely distributed in many organs/tissues, such as the heart, blood vessels, smooth muscle of the bladder and airways, skeletal muscle, and gastrointestinal tract. According to the target organ/tissue, sensory neuropeptides can be differentially expressed in the peripheral terminals of C- and Aδ-fibers [37].

The activation of peripheral endings of sensorimotor neurons by noxious stimuli (*e.g.* tissue damage) leads to the release of pain neurotransmitters at the central ending. Concomitantly, in general neurotransmitters are released from the peripheral terminals to promote neurogenic inflammation and tissue repair. The majority of these stimuli activate a specific receptor. One of the main receptors expressed in sensorimotor neurons is the transient receptor potential vanilloid subfamily member 1 (TRPV1), also known as capsaicin receptor. Only TRPV1 is activated by capsaicin, the pungent compound found in hot peppers that elicits a burning sensation. This receptor is not expressed in most of other neurons, which confers to capsaicin a relative specificity for afferent C- and Aδ-fibers. As other noxious stimuli, the activation of TRPV1 by capsaicin evokes the neurotransmitter release from varicosities of sensorimotor neurons. On the other hand, prolonged activation of TRPV1 by capsaicin inhibits the neurotransmission through a combination of effects, including TRPV1 desensitization [37].

1.3. SENSORY NERVOUS SYSTEM AND BONE

It is clear that bone tissue is richly innervated by afferent nerve fibers. These fibers were found in the periosteum, mineralized bone, medullary cavity, and epiphyseal plate, with distinct densities. Indeed, the periosteum and areas with higher metabolic rate display a more intense network of sensory nerve fibers than that of the other bone parts, suggesting a role of the sensory nervous system on bone metabolism [44–48].

In contrast to the sympathetic nervous system, a positive role of the sensory nervous system has been reported in the regulation of bone development, homeostasis and repair. Animal studies have demonstrated that capsaicin-mediated sensory denervation leads to a significant bone loss [49,50]. More recently, it was shown that mice with conditional knockout of Sema3A in sensory neurons had a significant decrease of bone sensory innervation and consequent decrease of bone mass, similar to general Sema3A knockout mice. Interestingly, mice with specific ablation of Sema3A in osteoblasts had normal bone mass. These findings revealed that Sema3A produced in sensory neurons plays an essential role in bone remodeling by contributing to the local development of sensory nerve fibers in an autocrine manner [23].

Bone tissue is mainly innervated by small diameter myelinated (Aδ) fibers and unmyelinated peptide-rich C-fibers [46,51–53]. The presence of nonpeptidergic C-fibers and large diameter fibers, particularly Aβ, in bone is still unclear [46,52,54,55]. Most sensory nerve fibers that innervate bone tissue respond to noxious stimuli by releasing neuropeptides, especially CGRP and SP [46,52,53]. Importantly, many bone cells express a wide variety of receptors that are activated by sensory neuropeptides, thus modulating bone metabolism and repair [56]. It was demonstrated a direct anabolic and catabolic effect of SP on bone remodeling [57]. On the other hand, CGRP was described to promote bone formation by acting directly on osteoblastogenesis and indirectly on osteoclastogenesis[58,59].

HYPOTHESIS, OBJECTIVES AND EXPERIMENTAL DESIGN.02

HYPOTHESIS, OBJECTIVES AND EXPERIMENTAL DESIGN.02

The role of the sensory nervous system in bone physiology and pathophysiology has been drawing increased interest of the scientific community over the last few years. However, it is unclear how and in which bone cells can sensory neurons orchestrate the regulation of bone formation, remodeling and regeneration. In this context, we raised the following hypothesis:

« Sensory neurons induce the process of osteoblast differentiation by acting directly on MSCs »

To evaluate this hypothesis, the following specific objectives were set:

1. To develop and validate a microfluidic platform for culture of dorsal root ganglion (DRG) neurons and MSCs that more faithfully represents the *in vivo* scenario of bone sensory innervation.
2. To optimize the culture conditions of each cell population in order to preserve their physiological properties.
3. To assess the impact of the DRG neurons on proliferation and differentiation of MSCs.
4. To investigate the effect of DRG neurons on Cx43 and N-cadherin expression in MSCs during the osteoblast differentiation.
5. To identify signaling pathways involved in DRG neurons-induced osteoblastogenesis.
6. To characterize the subset of DRG neurons and the main neuronal factors directly implicated on osteoblast lineage development.

This dissertation can be divided into two main parts (Article 1 and Article 2). The article 1 concerns fundamental discoveries on the direct interaction and communication of DRG neurons with MSCs in a microfluidic platform (Figure 15). The article 2 stands on the role of capsaicin-sensitive DRG neurons and the emerging sensory neuropeptides, particularly Substance P and CGRP, in the regulation of osteoblast differentiation (Figure 16).

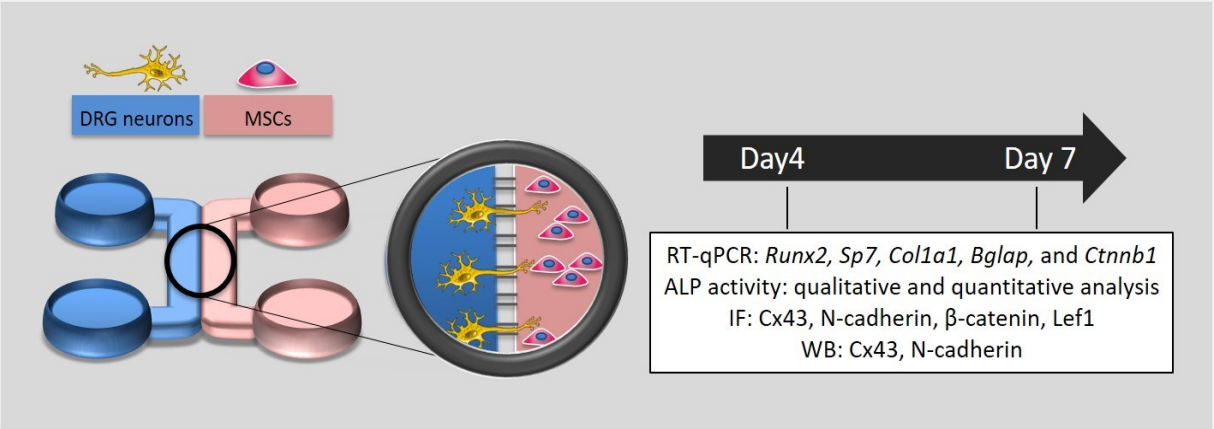

Figure 15: Experimental design of article 1. DRG neurons and MSCs were cocultured in a microfluidic platform. After 4 and 7 days of coculture, cellular and molecular biology techniques were performed to analyse the expression profile of osteoblast-related genes and proteins in MSCs.

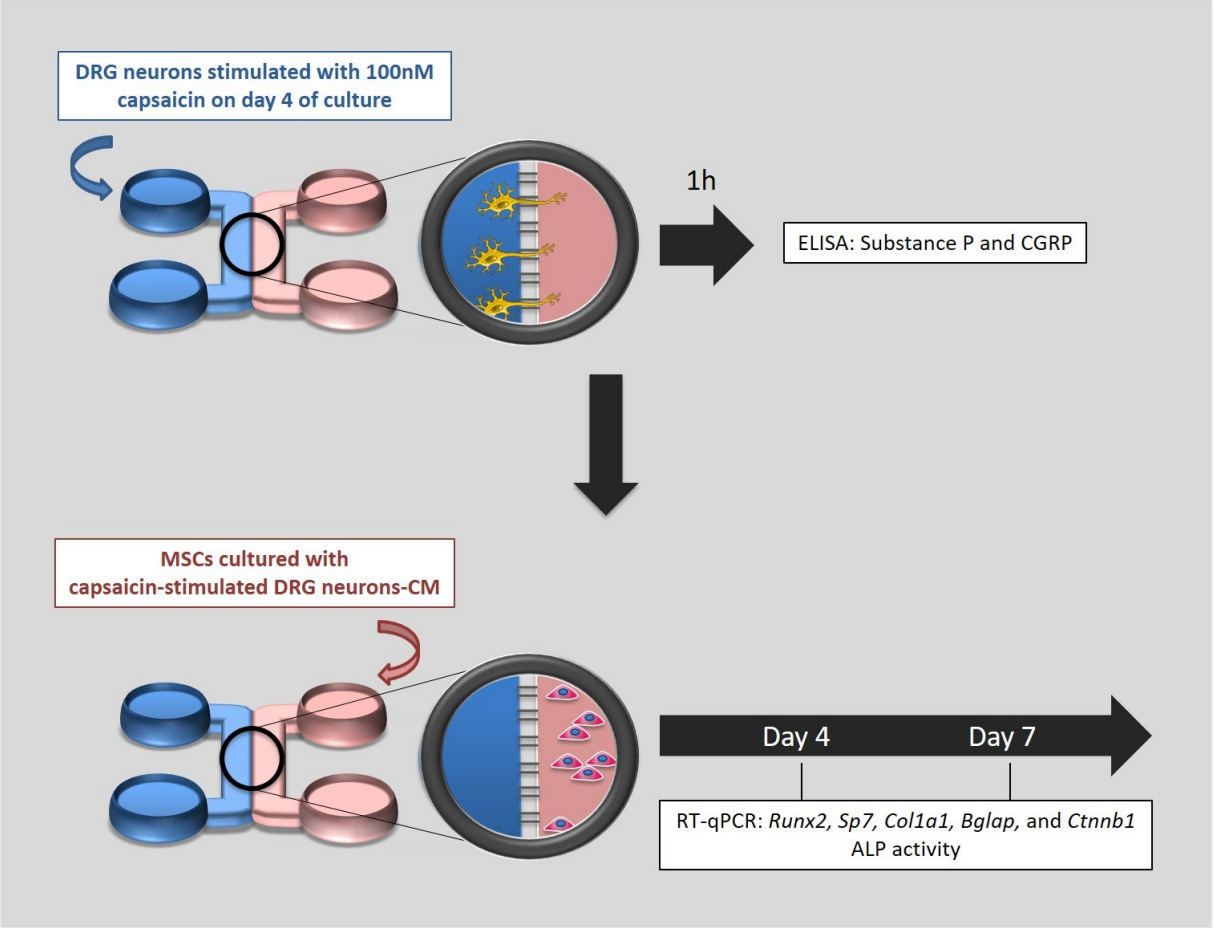

Figure 16: Experimental design of article 2. On day 4 of culture, DRG neurons were stimulated with capsaicin for 1h. Substance P and CGRP levels in the cell culture medium were quantified by ELISA. This medium was also used as conditioned medium (CM) to culture MSCs. After 4 and 7 days of culture, cell and molecular biology techniques were performed to analyse the expression profile of osteoblast-related genes and proteins in MSCs.

ARTICLE 1.03

Dorsal root ganglion neurons regulate the transcriptional and translational programs of osteoblast differentiation in a microfluidic platform

Diana Isabel Silva[1*], Bruno Paiva dos Santos[1], Jacques Leng[2], Hugo Oliveira[1], Joëlle Amédée[1]

[1] Univ. Bordeaux, Tissue Bioengineering, U1026, F-33076 Bordeaux, France; INSERM, Tissue Bioengineering, U1026, F-33076 Bordeaux, France.
[2] Univ. Bordeaux, LOF, UMR5258, F-33600 Pessac, France; CNRS, LOF, UMR5258, F-33600 Pessac, France; Solvay, LOF, UMR5258, F-33600 Pessac, France.
*Correspondence: diana.da-silva@inserm.fr

Running Title : Sensory neurons enhance osteoblastogenesis

Manuscript accepted for publication in *Cell Death & Disease*

ABSTRACT.3.1

Innervation by the sensory nervous system plays a key role in skeletal formation and in orchestration of bone remodeling and repair. However, it is unclear how and in which bone cells can sensory nerves acts to control these processes. Here, we show a microfluidic coculture system comprising dorsal root ganglion (DRG) neurons and mesenchymal stem cells (MSCs) that more faithfully represents the *in vivo* scenario of bone sensory innervation. We report that DRG neurons promote the osteogenic differentiation capacity of MSCs by mediating the increase of alkaline phosphatase activity and the upregulation of osteoblast-specific genes. Furthermore, we show that DRG neurons have a positive impact on Cx43 levels in MSCs during osteoblastogenesis, especially at an early stage of this process. Conversely, we described a negative impact of DRG neurons on MSCs N-cadherin expression at a later stage. Finally, we demonstrate a cytoplasmic accumulation of β-catenin translocation into the nucleus, and subsequently Lymphoid Enhancer Binding Factor 1 - responsive transcriptional activation of downstream genes in cocultured MSCs. Together, our study provides a robust body of evidence that the direct interaction of DRG neurons with MSCs in a bone-like microenvironment leads to an enhancement of osteoblast differentiation potential of MSCs. The osteogenic effect of DRG neurons on MSCs is mediated through the regulation of Cx43 and N-cadherin expression and activation of the canonical/β-catenin Wnt signaling pathway.

Specific bone cell activity, local factors, and systemic hormones regulate the skeletal morphogenesis and homeostasis [1]. However, accumulated evidence has demonstrated that central and peripheral nervous systems play also an essential role in bone formation, remodeling, and regeneration [2]. Histologic studies revealed the presence of sensory and sympathetic nerve fibers, frequently accompany with blood vessels, in the periosteum, trabecular and cortical bone, bone marrow, and epiphyseal plate [3,4]. Interestingly, the distribution pattern of nerve fibers was shown to vary according to the bone region. The periosteum and mineralized bone regions with high osteogenic activity present an intensive network of sensory and sympathetic nerve fibers expressing neurotransmitters and neurotrophins [3–8]. Additionally, bone cells have shown to actively respond to a wide range of neuronal signaling molecules through specific receptors [9]. A large number of animal experiments has reinforced these observations by demonstrating that denervation has a detrimental effect on bone development, homeostasis and repair [10,11]. More recently, a work published by Fukuda and coleagues [12] revealed that sensory nervous system (SNS) is the main regulator of bone formation and remodeling in mice. In this work, the authors identified the Semaphorin 3A (Sema3A) produced in sensory neurons as a crucial protein for proper bone mass accrual. Similarly, it was reported that intravenous administration of Sema3A in Sema3A$^{-/-}$ mice prevented bone loss [13].

Taken together, these *in vivo* findings have proven that SNS plays an extensive and pivotal role in bone physiology and pathophysiology. However, this evidence at molecular/cellular levels is poorly understood. Indeed, the underlying molecular mechanisms and bone cells under direct control of SNS remain unclear and further studies are required. Additionally, the majority of *in vitro* studies comprising sensory neurons and bone cells were performed with conventional cocultures that are far from mimicking the *in vivo* scenario of bone sensory innervation [14–16].

In this study, we used a microfluidic coculture system in order to explore in a more accurate microenvironment the effect of dorsal root ganglion (DRG) neurons on the ability of mesenchymal stem cells (MSCs) to undergo osteoblast differentiation. Our results demonstrate that DRG neurons enhance the osteoblastogenesis by regulating

the canonical/β-catenin Wnt signaling pathway and expression of osteoblast-related genes/proteins in MSCs.

3.3.1. Microfluidic devices allow the neurite outgrowth within the MSCs compartment

The identification of the role of the SNS in the regulation of osteogenesis raises a fundamental question whether DRG neurons operate directly in osteoblast differentiation of MSCs. To explore this hypothesis, we fabricated a microfluidic platform, whose design was adapted from previously validated geometric patterns for neuronal studies [17]. Conventional lithography techniques were used to create the microfluidic device, which consist of a miniaturized two-chamber system (Figure 1a) connected by well-defined microgrooves (Figure 1b). This microdevice enables to separately culture the cell bodies of DRG neurons and target cells, using specific culture media for each cell type, and assess the distinct gene/protein profile of each cell population [18,19].

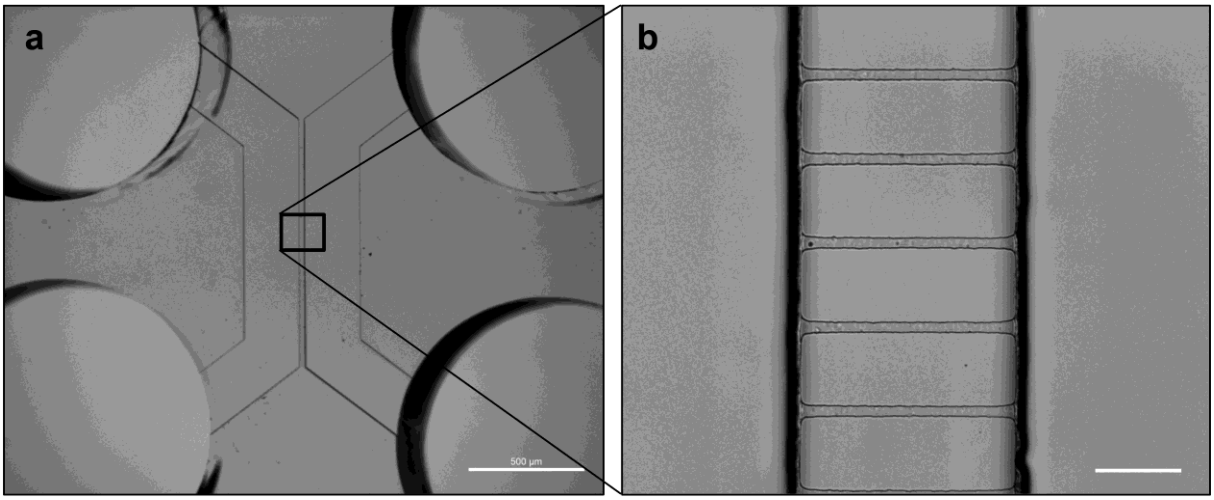

Figure 1. Microfluidic coculture device. Conventional photolithography and soft lithography techniques were used to create the microfluidic device. Phase contrast microphotograph of the (a) device and (b) microgrooves with the following dimensions: 3.6 µm of high, 7 µm wide, and 148 µm long (spaced 48 µm one another). Scale bar = 10 µm.

Primary cultures of DRG neurons and MSCs were obtained from adult male Wistar rats (Supplementary Figure S1). The morphology of DRG neurons was analyzed by immunofluorescence (IF) for calcitonin gene-related peptide (CGRP) (Supplementary

Figure S1A). The spindle-shaped morphology of bone marrow MSCs was verified under an optical microscope (Supplementary Figure S1B), and the expression of positive and negative cell surface markers was confirmed by flow cytometry (Supplementary Figure S1C).

Prior to assembling the coculture system in the microfluidic device (Figure 2), MSCs were cultured alone under standard conditions until they attained confluence. Thereafter, DRG neurons were seeded into the somal side of the microdevice, while MSCs were plated into the axonal side (Figure 2a). DRG neurons were incubated in growing medium and MSCs were cultured with osteogenic induction medium (OIM). IF against β-III Tubulin was performed on day 7 to observe neurite outgrowth within the microfluidic platform. We observed that DRG neurons spread neurites from the neural cell bodies, placed on the somal side, toward the MSCs compartment through microgrooves (Figure 2a, arrows). Notably, neurites could be detected within the axonal side in close proximity with MSCs from day 4 of coculture (Figure 2b, arrow).

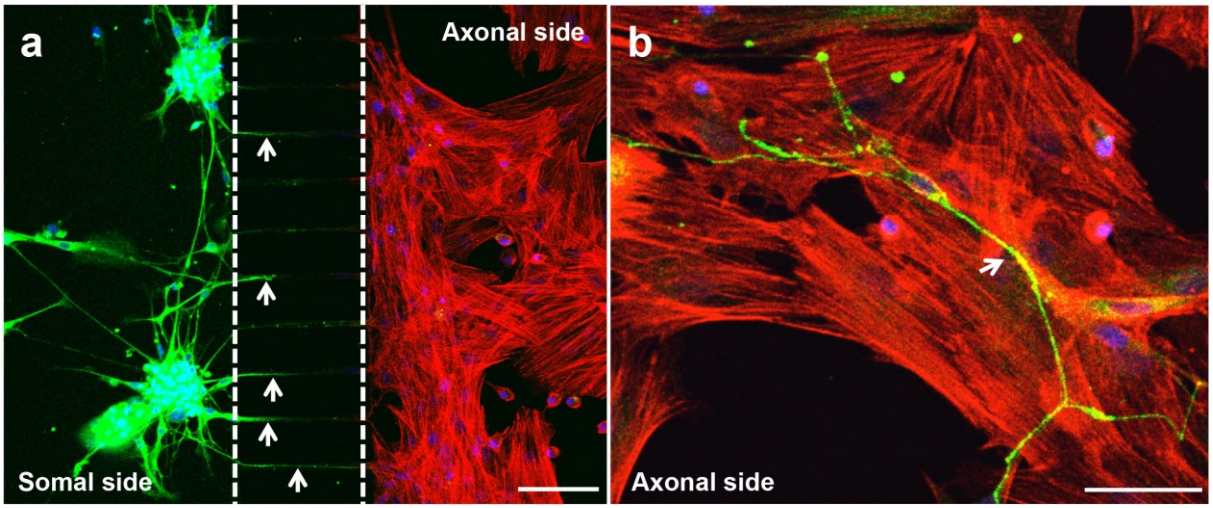

Figure 2. Neurites cross the microgrooves to the axonal side of the microfluidic device. Sensory neurons derived from rat DRG (5 x 10^4 cells/cm^2) and rat bone marrow MSCs (10^4 cells/cm^2) were cocultured in microfluidic devices for 7 days. DRG neurons were maintained in DMEM supplemented with 2 % (v/v) B-27 and 1 µM AraC; MSCs were incubated in OIM composed of DMEM-low glucose with 10 % (v/v) FBS, $1x10^{-9}$ M dexamethasone, 10 mM β-glycerophosphate, and 50 µg/mL ascorbic acid. (a and b) The presence of neurites reaching MSCs was evaluated on day 7 of coculture by IF using an antibody directed against a neuronal specific marker (β-III Tubulin) coupled to Alexa Fluor® 488 (green), and DAPI (nuclei; blue) under a confocal microscope. Actin filaments of MSCs were stained using Alexa Fluor® 568 (red)-conjugated phalloidin. Arrows point to neurites. Scale bar = 100 µm (a), 50 µm (b).

To assess the impact of coculture with DRG neurons on MSCs proliferation in the microfluidic platform, we evaluated DNA content and metabolic activity in MSCs after

4 and 7 days of coculture in the presence of OIM (Figure 3). No differences were found in the DNA concentration between MSCs in mono and coculture (Figure 3a). However, we observed an increase of 40 % on day 4 and more than 55 % on day 7 in the metabolic activity of cocultured MSCs in relation to their respective control MSCs (Figure 3b). These results indicate that coculture with DRG neurons stimulates the metabolic activity of MSCs during osteoblastogenesis.

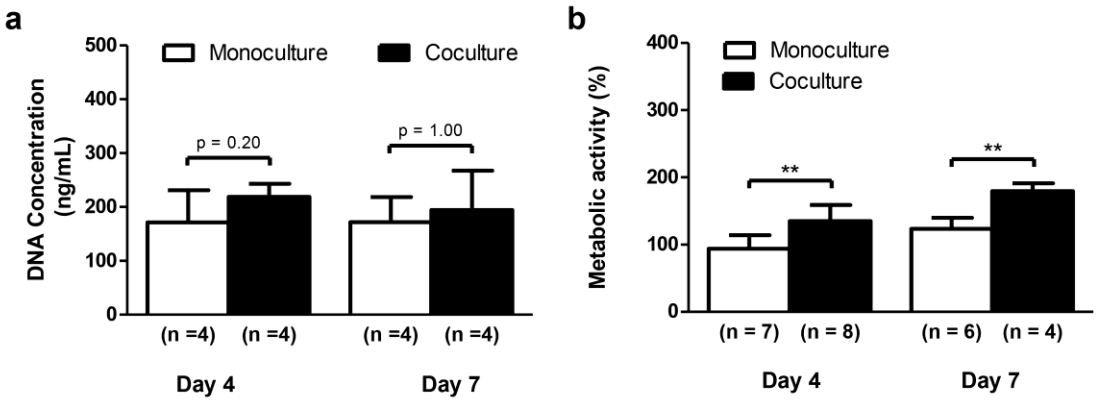

Figure 3. DRG neurons stimulate the metabolic activity in MSCs. Sensory neurons derived from rat DRG (5 x 10^4 cells/cm^2) and rat bone marrow MSCs (10^4 cells/cm^2) were cocultured in microfluidic devices for 7 days. DRG neurons were maintained in DMEM supplemented with 2 % (v/v) B-27 and 1 µM AraC; MSCs were incubated in OIM composed of DMEM-low glucose with 10 % (v/v) FBS, $1x10^{-9}$ M dexamethasone, 10 mM β-glycerophosphate, and 50 µg/mL ascorbic acid. (a) The DNA concentration of MSCs was determined at 4 and 7 days of coculture by CyQUANT™ Cell Proliferation Assay. (b) The relative metabolic activity of MSCs was measured at 4 and 7 days of coculture by resazurin-based assay and normalized to the monoculture levels on day 4. Data expressed as mean ± SD. (n) indicates the total number of samples for each group. **$p < 0.01$ statistically different from monoculture. The results represent three independent experiments.

3.3.2. DRG neurons enhances the differentiation of MSCs towards the osteoblast lineage

The osteoblast formation from MSCs involves several cellular/molecular processes, including the transcriptional regulation of bone phenotyping genes [20]. To investigate whether the coculture with DRG neurons had an influence on the osteoblast differentiation capacity of MSCs in the microdevice, we analyzed the transcriptional expression of osteoblast-marker genes in MSCs by RT-qPCR after 4 and 7 days of coculture in OIM (Figure 4a-d). Genes of interest included runt-related transcription factor 2 (*Runx2*), also known as core-binding factor subunit alpha-1 (Cbfa1),

specificity protein transcription factor 7 (*Sp7*, encoding osterix), collagen type I alpha 1 chain (*Col1a1*), and bone gamma-carboxyglutamate protein (*Bglap,* encoding osteocalcin). *Runx2/Cbfa1* and *Sp7* are two master regulatory genes required for osteoblast differentiation [21–24]*.* Runx2/Cbfa1 is the earliest and the most specific transcription factor of osteoblastogenesis, guiding the immature bone development. This protein can regulate the expression of important osteoblastic genes, regulate *Runx2* itself, and also interacts with other proteins expressed in osteoblasts, including osterix, to modulate the osteoblast genetic program [25–27]. *Col1a1* is considered an early marker for osteoblast differentiation associated to bone ECM formation [28,29]. On the other hand, *Bglap* is characterized as a highly specific late osteoblastic marker related to bone ECM mineralization [30]. In our research, we found a significant upregulation of *Runx2/Cbfa1* (2.5-fold change), *Sp7* (2.8-fold change), *Col1a1* (2-fold change), and *Bglap* (3.4-fold change) in MSCs cocultured with DRG neurons for 4 days, when compared with MSCs in monoculture (Figure 4a-d). Similarly, an increase of *Bglap* expression was detected on day 7 in MSCs in coculture (3.4-fold change compared with monoculture at the same timepoint) (Figure 4d). Interestingly, there were no differences in the transcription of osteoblast-related genes between mono and cocultured MSCs under standard culture conditions without osteogenic stimulation (Supplementary Figure S2A-E). These findings reveal that coculture with DRG neurons leads to an increase in the transcriptional expression of osteoblast-specific genes in MSCs during osteoblastogenesis.

Alkaline phosphatase (Alp) is another early marker for osteoblast lineage development participating in the bone ECM deposition. Intracellular Alp quantification assay and cytochemical staining were conducted to further understand the effect of coculture with DRG neurons on osteoblast differentiation capacity of MSCs (Figure 4e and f). Accordingly, MSCs cocultured with DRG neurons for 4 days exhibited more intense purple staining for Alp than monocultured MSCs (Figure 4e). On the other hand, there were no differences between MSCs in mono and coculture after 7 days, showing both for cell conditions a weak Alp-staining (Figure 4e). Identical results were achieved with Alp activity quantification assay (Figure 4f). Additionally, no differences were found in the Alp activity between mono and cocultured MSCs under standard culture conditions (Supplementary Figure S2F). These results suggest that coculture with DRGs neurons promotes the osteogenic activity in MSCs during osteoblast differentiation. Taken together, these results strongly suggest a direct involvement of SNS in the regulation of osteoblastogenesis in MSCs.

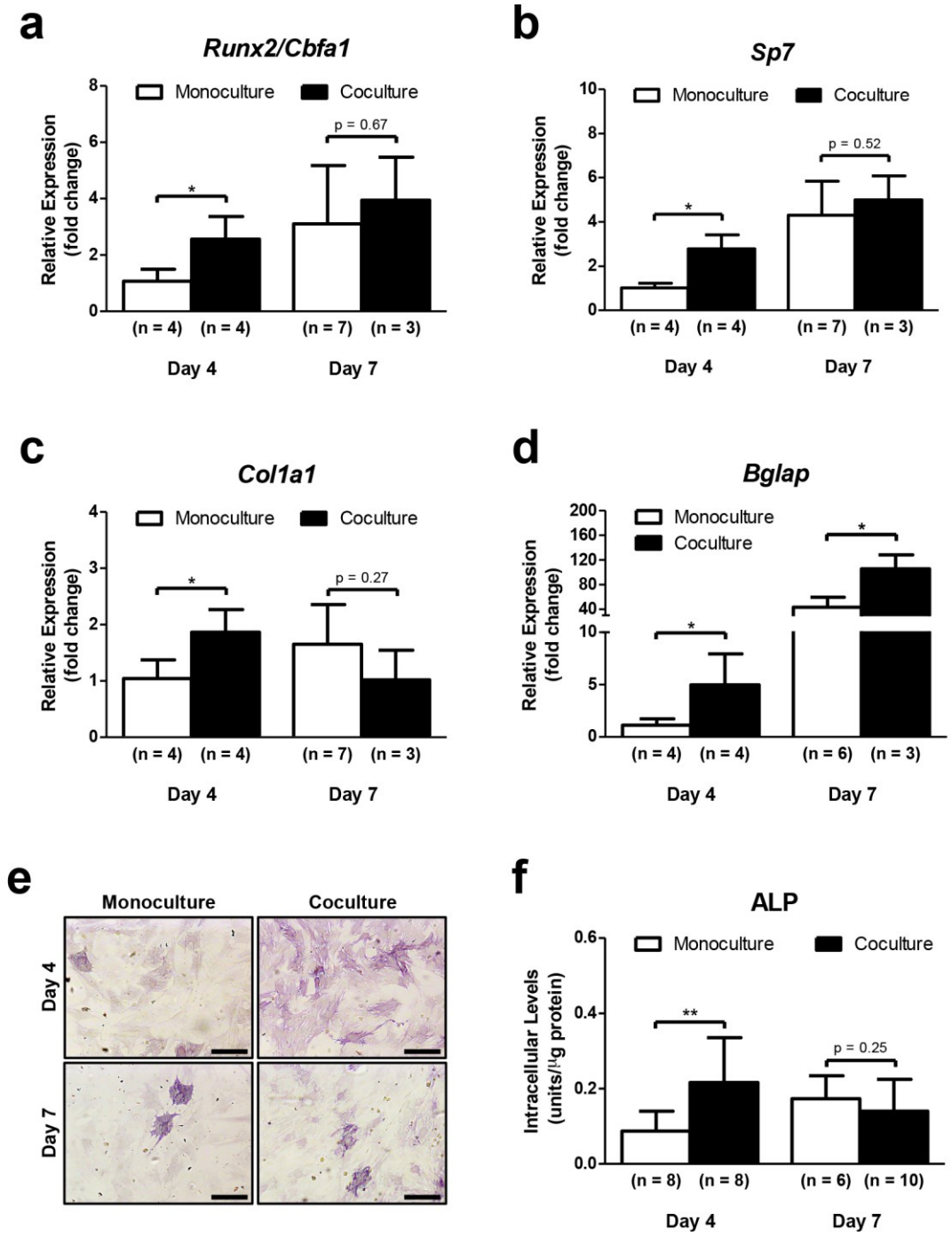

Figure 4. DRG neurons enhance the osteoblast differentiation ability of MSCs. Sensory neurons derived from rat DRG (5 x 10^4 cells/cm^2) and rat bone marrow MSCs (10^4 cells/cm^2) were cocultured in microfluidic devices for 7 days. DRG neurons were maintained in DMEM supplemented with 2 % (v/v) B-27 and 1 μM AraC; MSCs were incubated in OIM composed of DMEM-low glucose with 10 % (v/v) FBS, 1x10^{-9} M dexamethasone, 10 mM β-glycerophosphate, and 50 μg/mL ascorbic acid. (a-d) Expression profile of *Runx2*, *Sp7*, *Col1a1* and *Bglap* in MSCs was assessed at 4 and 7 days of coculture by RT-qPCR and depicted as a relative ratio to the housekeeping gene *Hprt1* normalized to the monoculture levels on day 4. (e and f) Alp activity in MSCs was analyzed at 4 and 7 days of coculture by Alp activity quantification assay and cytochemical staining. Scale bar = 300 μm. Data expressed as mean ± SD. (n) indicates the total number of samples for each group. *p < 0.05; **p < 0.01 statistically different from monoculture. The results represent three independent experiments.

3.3.3. DRG neurons modulate the expression of Cx43 and N-cadherin in MSCs during osteoblastogenesis

Direct cell-cell communication *via* gap junctions is an important mechanism by which bone cells coordinate their activities. Gap junction alpha-1 protein (GJA1), also known as connexin 43 (Cx43), is the most abundant connexin in all bone cells. Extensive research has established a crucial role for Cx43 and subsequent intercellular channels in differentiation, function, and survival of osteoblasts *in vitro* and *in vivo* [31,32]. Therefore, we evaluated the Cx43 localization and expression during the osteoblast differentiation of MSCs cocultured with DRG neurons in the microfluidic device. For this, we performed IF and Western blotting (WB) using an anti-Cx43 antibody (Figure 5a and b). We found an increase of Cx43 levels mainly in the cytosol and perinuclear area of MSCs after 4 and 7 days of coculture compared with control MSCs cultured for the same period of time (Figure 5a and b). Interestingly, the highest expression of Cx43 was detected on day 4 of coculture (Figure 5a and b). These observations show that DRG neurons have a positive impact on Cx43 levels in MSCs during osteoblastogenesis.

Several lines of evidence have indicated that N-cadherin, also known as Cadherin-2 or neural cadherin, regulates the osteoblastogenesis [33]. On the light of these findings, we conducted IF and WB against N-cadherin in order to investigate the impact of coculture with DRG neurons on N-cadherin localization and expression of MSCs maintained in OIM (Figure 5a and b). We observed that MSCs cocultured with DRG neurons for 4 days exhibited a sharp increase of N-cadherin levels compared with MSCs cultured alone mostly in the cytosol and perinuclear region (Figure 5a and b). Conversely, the levels of N-cadherin after 7 days of coculture were lower than MSCs in monoculture (Figure 5a and b). In both mono and cocultured MSCs, the staining of N-cadherin was diffuse, with a nonjunctional as well as junctional localization (Figure 5a). These findings demonstrate that coculture with DRG neurons mediates N-cadherin expression changes in MSCs during osteoblast differentiation.

Taken together, these findings suggest that SNS modulates the Cx43 and N-cadherin expression in MSCs during osteoblastogenesis.

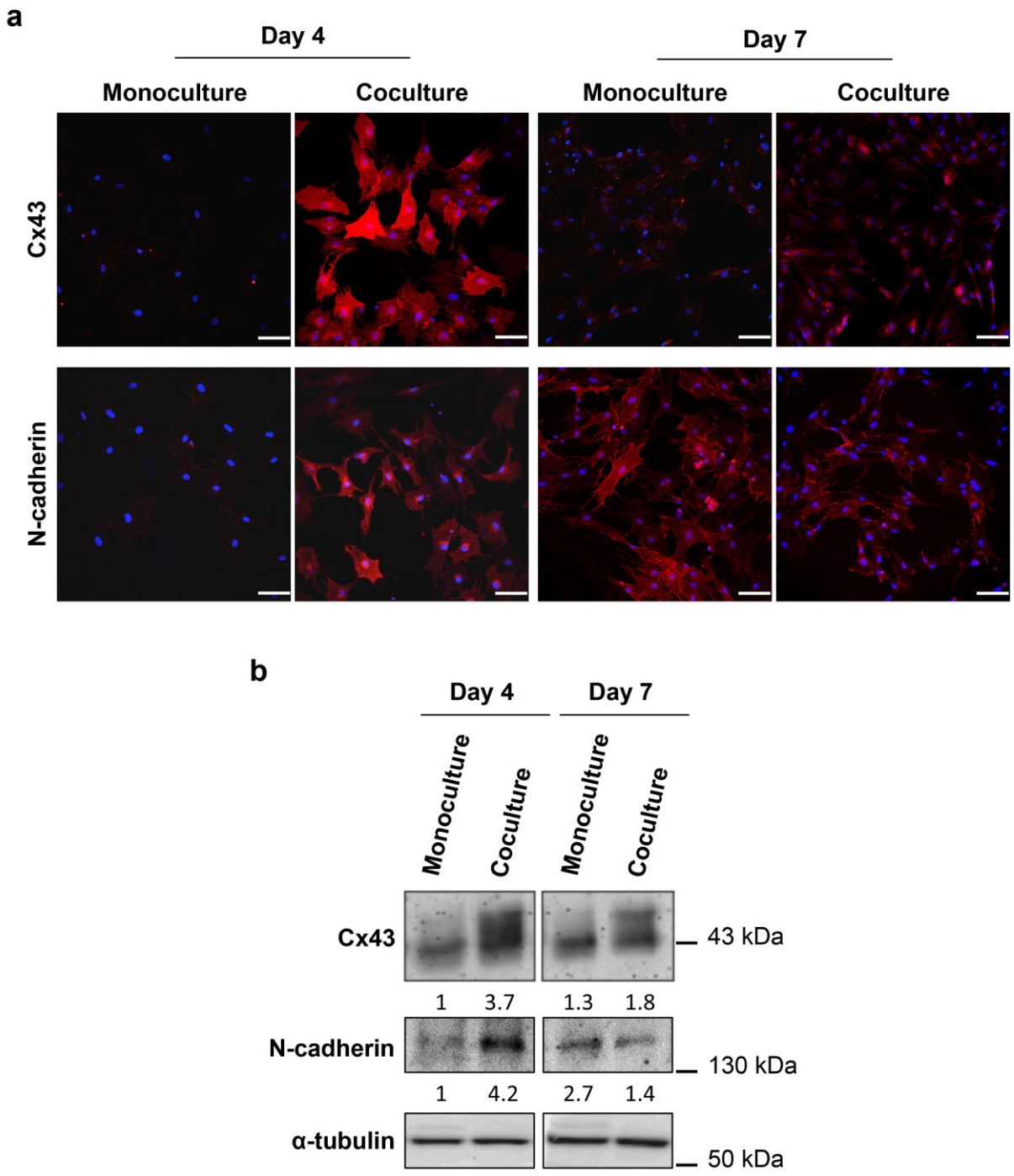

Figure 5. DRG neurons have an impact on Cx43 and N-cadherin expression in MSCs during osteoblast differentiation. Sensory neurons derived from rat DRG (5 x 10^4 cells/cm^2) and rat bone marrow MSCs (10^4 cells/cm^2) were cocultured in microfluidic devices for 7 days. DRG neurons were maintained in DMEM supplemented with 2 % (v/v) B-27 and 1 µM AraC; MSCs were incubated in OIM composed of DMEM-low glucose with 10 % (v/v) FBS, 1x10^{-9} M dexamethasone, 10 mM β-glycerophosphate, and 50 µg/mL ascorbic acid. (a) Subcellular distribution of Cx43 and N-cadherin in MSCs was evaluated at 4 and 7 days of coculture by IF using antibodies directed against Cx43 and N-cadherin coupled to Alexa Fluor® 594 (red), and DAPI (nuclei; blue) under a confocal microscope. Scale bar = 100 µm. (b) Cx43 and N-cadherin expression in MSCs was analyzed at 4 and 7 days of coculture by WB and depicted as a relative ratio to the respective loading control α-tubulin normalized to the monoculture value on day 4. The results represent three independent experiments.

3.3.4. DRG neurons promotes the activation of the Canonical/β-catenin Wnt signaling pathway in MSCs

It has been widely demonstrated that the canonical Wnt signaling pathway is a key regulator of osteogenesis by determining the cell fate decision of MSCs. β-catenin is the molecular node of this pathway and its stability and localization are crucial for intracellular signal transduction [34]. To elucidate whether this mechanism is implicated in osteoblast differentiation of MSCs cocultured with DRG neurons in the microdevice, we evaluated the subcellular distribution of β-catenin in MSCs by IF (Figure 6). In our study, we observed a significant increase of cytoplasmic β-catenin expression in cocultured MSCs for 4 and 7 days compared with the respective control MSCs (Figure 6a and b). We also found that the nuclei of MSCs in coculture for 4 days exhibited greater β-catenin levels than those in monoculture, indicating more β-catenin translocated from the cytoplasm to the nucleus (Figure 6a, c, and d). Interestingly, the addition of DRG neurons to the MSCs culture resulted in a 3.4-fold increase of nuclear β-catenin in MSCs on day 7 of coculture, although not associated with a significant transfer of β-catenin into the nucleus (Figure 6a, c, and d). Furthermore, a significant 1.6-fold increase of β-catenin gene (*Ctnnb1*) was detected in cocultured MSCs for 4 days compared with MSCs in monoculture (Figure 6e). In contrast, no differences were observed in *Ctnnb1* expression between MSCs in mono and coculture after 7 days (Figure 6e). These results show that coculture with DRG neurons promotes the cytosolic accumulation and nuclear translocation of β-catenin in MSCs.

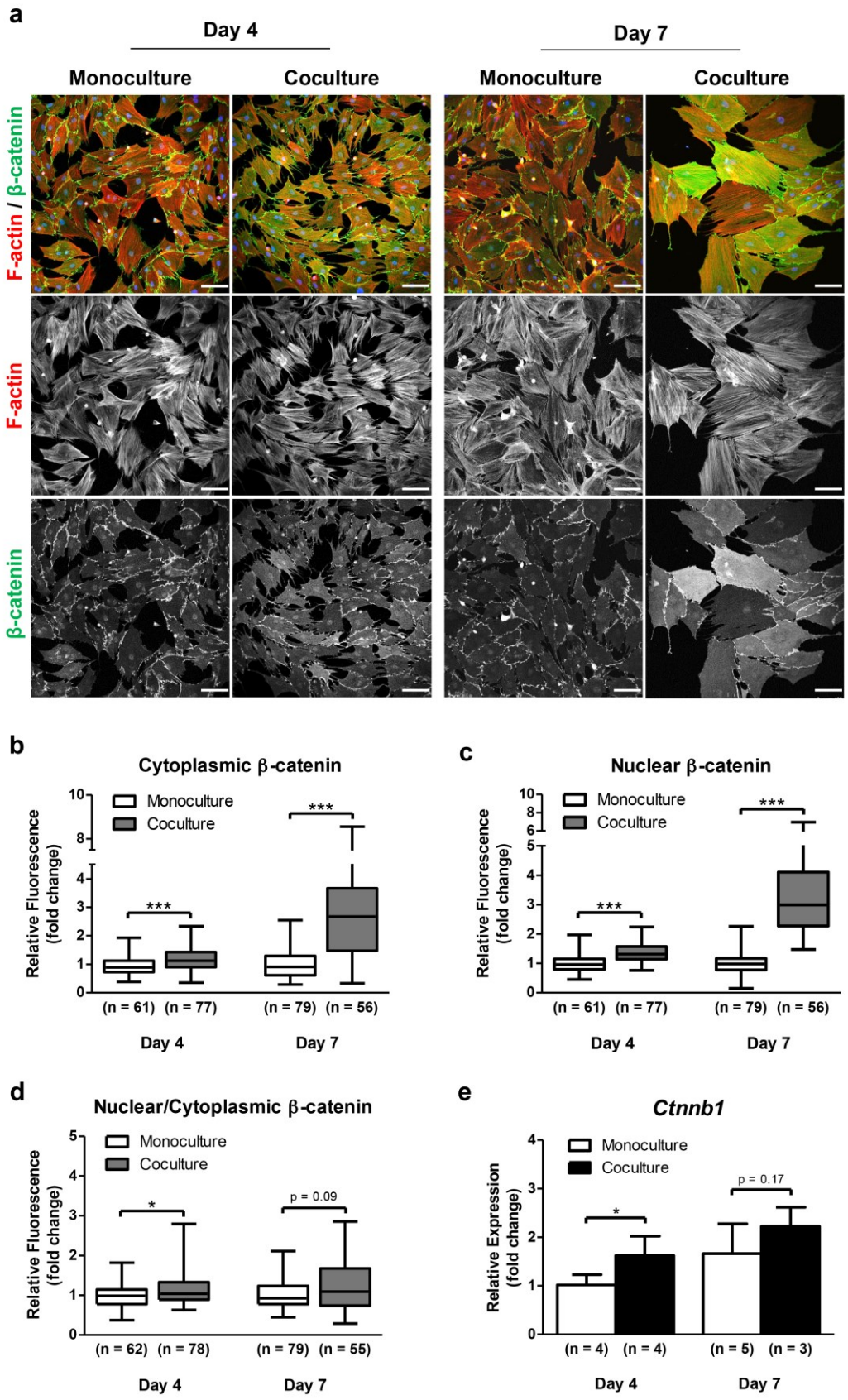

Figure 6. DRG neurons induce cytoplasmic accumulation of β-catenin and its translocation into the nucleus in MSCs. Sensory neurons derived from rat DRG (5 x 10^4 cells/cm^2) and rat bone marrow MSCs (10^4 cells/cm^2) were cocultured in microfluidic devices for 7 days. DRG neurons were maintained in DMEM supplemented with 2 % (v/v) B-27 and 1 µM AraC; MSCs were incubated in OIM composed of DMEM-low glucose with 10 % (v/v) FBS, 1x10^{-9} M dexamethasone, 10 mM β-glycerophosphate, and 50 µg/mL ascorbic acid.

It is well documented that β-catenin exerts its effect on gene transcription by functioning as a transcriptional co-activator. The best-characterized binding partners for β-catenin in the nucleus are the members of the T-cell factor (Tcf)/lymphoid enhancer factor (Lef) DNA-binding family. In osteoblast progenitor cells, this interaction leads to transcriptional activation of Wnt target genes, particularly *Runx2/Cbfa1*, *Sp7*, TNF receptor superfamily member 11b (*Tnfrsf11b*), and CCN family member 1 (*Ccn1*), also known as cysteine-rich angiogenic inducer 61 (*Cyr61*), which regulate the osteoblastogenesis [35–37]. Based on this, we first examined the nuclear colocalization between active-β-catenin and Lef1 in MSCs committed to osteoblast lineage and cocultured with DRG neurons in the microfluidic platform. To achieve this, we performed IF using double labeling against these proteins (Figure 7a). The yellow fluorescence resulting of the β-catenin and Lef1 channels overlap showed a strong colocalization between these two proteins in nuclei of cocultured MSCs for 7 days (Figure 7a, arrows). On the other hand, there seemed to be no differences between MSCs in mono and coculture after 4 days (Figure 7a). Then, we analyzed the expression of *Tnfrsf11b* and *Ccn1/Cyr61* Wnt-responsive genes in MSCs by RT-qPCR after 4 and 7 days of the coculture. We found a significant upregulation of *Tnfrsf11b* (1.5-fold change) and *Ccn1/Cyr61* (1.8-fold change) in MSCs cocultured with DRG neurons for 4 days, when compared with monocultured MSCs (Figure 7b and c). The same results were not verified for day 7 (Figure 7b and c). These findings demonstrate that coculture with DRG neurons controls the Lef1-responsive transcriptional activation of *Tnfrsf11b* and *Ccn1/Cyr61* in MSCs during osteoblast differentiation.

Together, these results suggest that SNS regulates the activation of the canonical/β-catenin Wnt signaling pathway in MSCs during osteoblastogenesis.

Figure 6. (continuation) (a) Subcellular distribution of β-catenin in MSCs was evaluated at 4 and 7 days of coculture by IF using antibodies directed against β-catenin coupled to Alexa Fluor® 488 (green), and DAPI (nuclei; blue) under a confocal microscope. Scale bar = 100 μm. (b-d) The level of fluorescence for β-catenin was measured at 4 and 7 days of coculture by using the ImageJ software in each MSC and normalized to the monoculture value on day 4. Data expressed as median, 25 and 75 percentiles, min/max. (n) indicates the total number of cells counted for each group. (e) Expression profile of *Ctnnb1* in MSCs was assessed at 4 and 7 days of coculture by RT-qPCR and depicted as a relative ratio to the housekeeping gene *Hprt1* normalized to the monoculture value on day 4. Data expressed as mean ± SD. (n) indicates the total number of samples for each group. *p < 0.05; ***p < 0.001 statistically different from monoculture. The results represent three independent experiments.

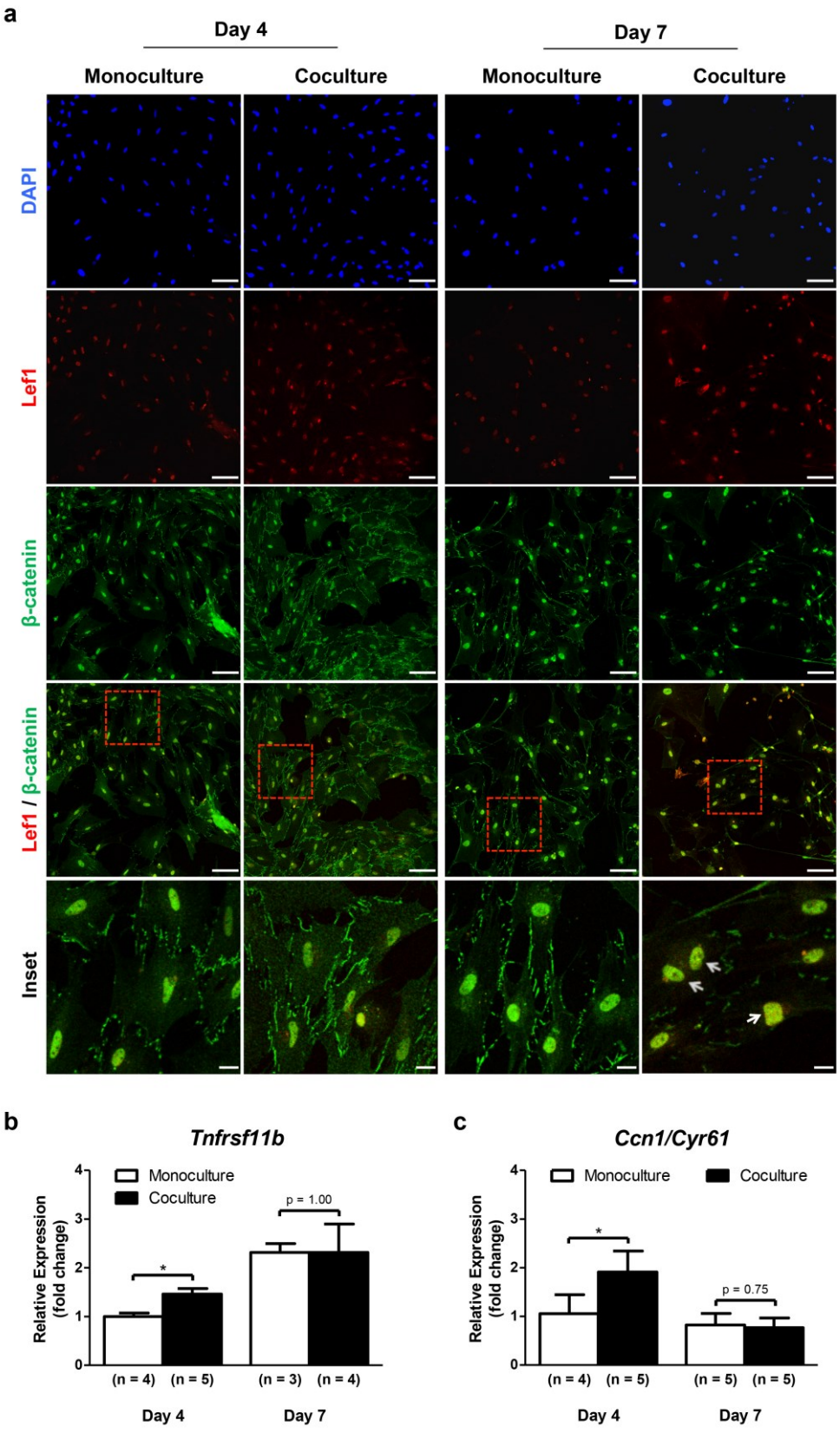

Figure 7. DRG neurons lead to colocalization between β-catenin and Lef1 into the nucleus, where together regulate the expression of Wnt-responsive genes in MSCs. Sensory neurons derived from rat DRG (5 x 10^4 cells/cm^2) and rat bone marrow MSCs (10^4 cells/cm^2) were cocultured in microfluidic devices for 4 and 7 days. DRG neurons were maintained in DMEM supplemented with 2 % (v/v) B-27 and 1 μM AraC; MSCs were incubated in OIM composed of DMEM-low glucose with 10 % (v/v) FBS, 1x10^{-9} M dexamethasone, 10 mM β-glycerophosphate, and 50 μg/mL ascorbic acid.

The majority of the existent *in vitro* studies focusing on the communication between the SNS and bone tissue were performed with coculture models using direct cell-cell contact [14–16]. However, these models have been widely criticized for not mimicking the *in vivo* scenario of bone sensory innervation. To circumvent this drawback, we developed microfluidic devices in order to establish a controlled and isolated coculture system between DRG neurons and MSCs, where only the neurites reach the MSCs as it happens in the *in vivo* situation. Despite embryonic DRG neuron cultures have the advantage of higher cell density and greater neurite outgrowth they are dependent on neurotrophins to survive. Most neurotrophins, especially nerve growth factor (NGF or beta-NGF), are pleiotropic causing multiple biological effects [38]. For this reason we focused on the use of adult DRG neurons.

Osteoblast differentiation of MSCs *in vitro* can be achieved by the presence of dexamethasone, ascorbic acid and β-glycerol phosphate in the culture medium [39,40]. Under these culture conditions, the commitment/maturation of MSCs towards osteoblast lineage have been divided into three hallmark stages. The first stage is marked by the increase in the number of cells as result of MSCs proliferation. This is followed by cell cycle arrest and early osteoblastic differentiation of MSCs associated with ECM deposition/maturation. The final stage is characterized by the late osteoblastic differentiation related to ECM mineralization [41]. The temporal pattern of expression of genes/proteins characterizing the different stages of osteoblast lineage development varies according to the cell culture models [42].

The formation of bone ECM during the second stage of osteoblastogenesis is associated with the maximal expression of Alp and transcriptional activation of early osteoblastic genes, particularly *Col1a1*. In the later stages of osteoblast

---

Figure 7. (continuation) (a) Nuclear colocalization of active-β-catenin and Lef1 in MSCs was evaluated at 4 and 7 days of coculture by IF with antibodies directed against active-β-catenin coupled to Alexa Fluor® 488 (green), Lef1 coupled to Alexa Fluor® 594 (red), and DAPI (nuclei; blue) under a confocal microscope. Arrows point to nuclear colocalization. Scale bar = 100 μm and 20 μm inset images. (b and c) Expression profile of *Tnfrsf11b* and *Ccn1/Cyr61* in MSCs was assessed at 4 and 7 days of coculture by RT-qPCR, and depicted as a relative ratio to the housekeeping gene *Hprt1* normalized to the monoculture value on day 4. Data expressed as mean ± SD. (n) indicates the total number of samples for each group. *p < 0.05 statistically different from monoculture. The results represent three independent experiments.

differentiation while the Alp levels are decreased, the expression of genes related to mineralization, such as *Bglap* and *Spp1* (encoding osteopontin), are increased at the transcriptional level [41,43]. Accordingly, in our research, we found a significant upregulation of early osteoblast-specific genes, especially *Runx2*, *Sp7*, and *Col1a1* in MSCs cocultured with DRG neurons for 4 days in the presence of OIM. We also observed a peak on day 4 of Alp levels in cocultured MSCs under the same culture conditions. Moreover, after 7 days of coculture under osteogenic stimulation, the mRNA expression of *Bglap* in MSCs was significantly increased, and the levels of Alp tended to decline. These results indicate that on day 4 of coculture with DRG neurons, MSCs were in the second stage of osteoblastogenesis. We can also presume that on day 7 of coculture, the now preosteoblasts had progressed to the final stage to become mature osteoblasts. The effect of DRG neurons on transcriptional regulation of osteoblast-marker genes in MSCs after 14 days of coculture in the presence of OIM was also evaluated, but no differences were detected between mono and cocultured MSCs (data not shown). Interestingly, there were no differences in the transcription of osteoblast-related genes and also in the activity of Alp between MSCs in mono and coculture without OIM (Supplementary Figure S2). Together, these results provide a strong evidence for a role of DRG neurons in enhancing the osteoblast differentiation from MSCs. However, its effect *per se* is not sufficient to induce the osteoblastogenesis *in vitro*.

Multiple studies have provided insights into the importance of Cx43 in osteoblast and bone formation [31,32]. Specifically, it was shown that mutations in *GJA1* impair the osteoblast lineage development and cause skeletal anomalies associated with oculodentodigital dysplasia [44]. The impact of the SNS on Cx43-mediated osteoblastogenesis is unknown, although few reports indicate a role of neuropeptides in this process. Specifically, was demonstrated that CGRP and Substance P are implicated on the promotion of osteoblast proliferation and activity through an increase of gap junctional intercellular communication (GJIC) and Cx43 expression [45,46]. Recently, an *in vitro* study showed that Cx43 expression and GJIC are increased during the osteoblast formation, both at transcriptional and translational levels. The authors also demonstrated that Cx43 and subsequent GJIC play a central role in early osteoblast differentiation by mediating the expression of Runx2 [47]. These reports may explain the sharp increase of Cx43 expression in MSCs cocultured with DRG neurons for 4 days in the presence of the OIM. Despite a significant decrease on day 7, the Cx43 levels in cocultured MSCs were significantly higher than in MSCs

cultured alone for the same period. Interestingly, we observed a mainly cytosolic and perinuclear distribution of Cx43. Some studies have proposed that the subcellular localization of Cx43 is related to different signaling activities, which contribute differently to the regulation of cell proliferation and differentiation [48]. These results show for the first time that DRG neurons have a positive effect on MSCs Cx43 expression and maybe on GJIC during osteoblast differentiation, especially at an early stage.

N-cadherin is another functional protein involved in osteogenesis [33]. However, its impact on osteoblast lineage development is not consensual among experts. Many reports have shown that N-cadherin hinders the osteoblast formation and function [49,50]. On the other hand, we and others have demonstrated that N-cadherin is required for early stages of osteoblastogenesis [51,52]. A recent *in vivo* study described a dual action of this protein on osteolineage cells depending upon their differentiation level. The authors demonstrated that N-cadherin maintains the pool of osteoprogenitor and stem cells and prevents the osteoblast differentiation of lineage-committed cells and function of mature osteoblasts [53]. In our research, we detected an increase of N-cadherin expression in MSCs cocultured with DRG neurons for 4 days, followed by a decrease three days later. These findings indicate that DRG neurons differentially modulate the expression of N-cadherin in MSCs according to their osteoblast developmental stage.

Different mechanisms have been proposed for regulation of osteoblast differentiation by N-cadherin. One of them is the increase of N-cadherin-mediated cell-cell adhesion, resulting in activation of signaling events that promote osteoblast gene expression. Interestingly, was suggested that the increase of cell-cell adhesion leads to an increase of Cx43-mediated GJIC and subsequent activation of osteoblast-marker genes, both at transcriptional and translational levels. It has also been reported that the interaction of N-cadherin with molecular players of the Wnt signaling pathway triggers intracellular signal transduction. In particular, the interaction of N-cadherin with β-catenin at the plasma membrane results in β-catenin sequestration, reduction of the cytosolic β-catenin pool and inhibition of the canonical Wnt signaling. Finally, N-cadherin can interact with the Wnt-co-receptors LRP5 or LRP6, promoting the β-catenin degradation, reduction of Wnt/β-catenin signaling, and decrease of osteoblastogenesis [54].

In this study, we detected a sharp increase in cytoplasmic accumulation of β-catenin and its translocation into the nucleus of MSCs cocultured with DRG neurons. In

addition, the IF staining showed that β-catenin largely colocalized with Lef1 in the nucleus of MSCs cocultured for 7 days. More importantly, we found an upregulation of Wnt target genes implicated in the osteoblast lineage development in MSCs cocultured with DRG neurons for 4 days. These results reveal for the first time that DRG neurons promote the activation of the canonical Wnt signaling pathway in MSCs. Interestingly, recent reports have indicated that this pathway directly increases the metabolism of osteoblast-lineage cells by stimulating the aerobic glycolysis, glutamine catabolism as well as fatty acid oxidation [55]. Consistently, we observed an increase in the metabolic activity of MSCs cocultured with DRG neurons. However, we cannot exclude that the sensory neurons may also be acting through other signaling pathways. Indeed, a recent study showed that NGF-TrkA signaling by sensory nerves coordinates the osteoprogenitor lineage progression and bone formation *in vivo* [56].

The present study provides several lines of evidence that DRG neurons play an incremental role for osteoblastogenesis by acting directly on MSCs and activating the Wnt/β-catenin signaling pathway. Furthermore, we were able to define the temporal pattern of expression of genes/proteins involved in the ability of MSCs to undergo osteogenic differentiation in response to DRG neurons communication (Figure 8).

Overall, these findings provide new insights into how SNS enhances bone formation and can inform the development of future therapeutic strategies for bone regeneration/repair that takes into account the SNS.

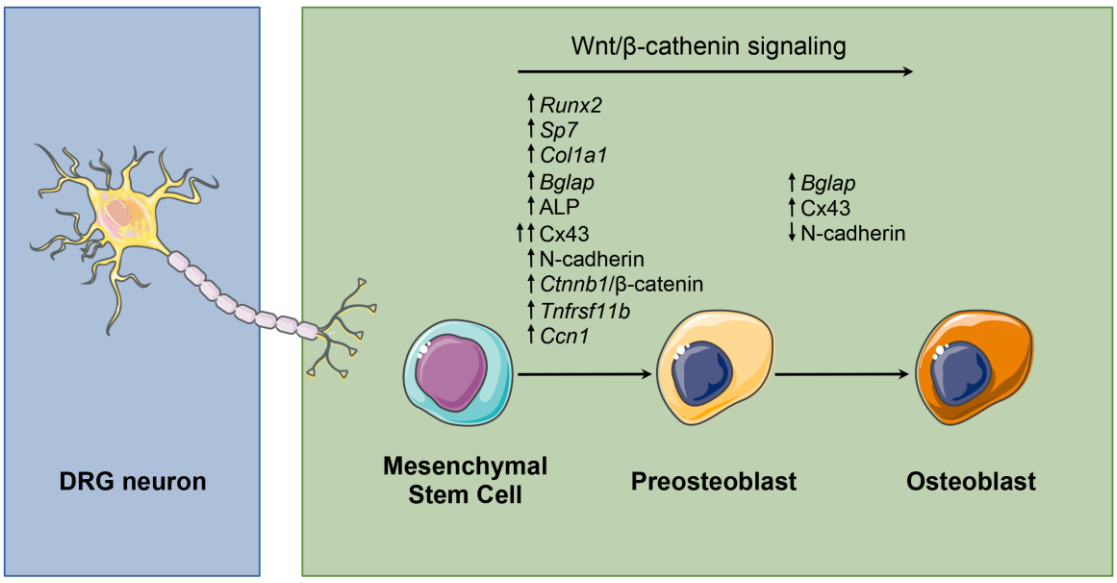

Figure 8. Role of DRG neurons in different phases of osteoblast differentiation from MSCs. DRG neurons promote the osteogenic differentiation potential of MSCs by regulating the canonical/β-catenin Wnt signaling pathway and expression of osteoblast-related genes/proteins in MSCs.

3.5.1. Microfluidic devices fabrication

Microfluidic devices were obtained using standard photolithography and soft lithography procedures [17].

3.5.2. Coculture of DRG neurons and MSCs in the microfluidic devices

Microfluidic devices were electrostatically attached over glass coverslips, previously coated with 0.1 mg/mL Poly-D-lysine (PDL, Sigma-Aldrich®, St. Louis, MI, USA) and 20 µg/mL laminin (Sigma-Aldrich®). After attained the confluence, MSCs were seeded in the axonal side of a microfluidic device at a density of 10^4 cells/cm^2 while freshly harvested and dissociated DRG neurons were plated in the somal side at a density of 5 x 10^4 cells/cm^2 and left undisturbed in a humidified incubator to allow adhesion. DRG neurons were cultured in growing medium composed of Dulbecco's modified eagle's medium (DMEM, Life Technologies™, Gibco®, Carlsbad, CA, USA), with 2 % (v/v) B-27 Serum-Free Supplement® (B-27, Gibco®) and 1 % (v/v) penicillin/streptomycin (Pen/Strep, Gibco®). MSCs were incubated in OIM, which consisted of DMEM - low glucose supplemented with 10 % (v/v) fetal bovine serum (FBS, P30-3305, PAN™ - Biotech, Aidenbach, Germany), 1 % (v/v) Pen/Strep, $1x10^{-9}$ M dexamethasone (Sigma-Aldrich®), 10 mM β-glycerophosphate (Sigma-Aldrich®) and 50 µg/mL ascorbic acid (Sigma-Aldrich®). Non-neuronal cells were eliminated using 1 µM cytosine arabinofuranoside (AraC, also known as cytarabine, Sigma-Aldrich®). Cocultures were maintained for 7 days in a humidified atmosphere, and the media were renewed on day 4 of coculture.

3.5.3. Immunofluorescence staining

DRG neurons and MSCs were washed with Phosphate-Buffered Saline (PBS; 0.1 M, pH 7.4) and fixed in 1 % (v/v) paraformaldehyde (PFA, MM France, Brignais, France) for 10 min at room temperature (RT). After a wash with PBS, cells were permeabilized for 5 min with 0.1 % (v/v) triton® X-100 (EDM Millipore, Billerica, MA,

USA) and washed once more. Then, cells were blocked with 1 % (w/v) bovine serum albumin (BSA, GE Healthcare, Chicago, IL, USA) for 30 min at RT to minimize the non-specific binding. Cells were further incubated with the primary antibody solution for 1 h at RT. After a wash with PBS, cells were incubated for 45 min in the dark with a solution containing the appropriated conjugated secondary antibody. Nuclei were counterstained for 5 min with 4',6-diamidino-2-phenylindole (DAPI, 1:5000; Life Technologies™, Molecular Probes®). All dilutions were made in PBS. Images were acquired in a Leica TCS SPE Confocal Laser Scanning Microscope (Leica, Wetzlar, Germany).

3.5.4. *Cell metabolic activity and proliferation assays*

DNA content of MSCs was determined using CyQUANT™ Cell Proliferation Assay Kit (Life technologies™, Molecular Probes®), according to manufacturer's instructions.

The resazurin-based assay was performed for detection of metabolic activity of MSCs. Briefly, 400 µL of fresh culture medium supplemented with 0.01 mg/mL (w/v) resazurin (Sigma-Aldrich®) was added directly to each microfluidic device. MSCs were incubated at 37 ºC for 4 h, and then 100 µL from each device was transferred to a 96-well microplate. Fluorescence (λem = 530 nm, λex = 590 nm) was measured on a VICTOR™ X3 Multilabel Plate Reader (PerkinElmer, Waltham, MA, USA). DNA content of MSCs was determined using CyQUANT™ Cell Proliferation Assay kit (Life technologies™, Molecular Probes®), according to manufacturer's instructions.

3.5.5. *RNA extraction, cDNA synthesis, and RT-qPCR analysis*

Total RNA was extracted from MSCs by using the RNeasy® Plus Micro Kit (Qiagen, Hilden, Germany) according to the manufacturer's protocol. RNA final concentration and purity ($OD_{260/280}$) was determined using a NanoPhotometer® P 330 (Implen GmbH, Munich, Germany). 50 ng of total RNA was reverse transcribed into cDNA using the Maxima Reverse Transcriptase kit (Thermo Scientific™, Thermo Fisher Scientific, Waltham, MA, USA), according to the manufacturer's protocol. RT-qPCR experiments were run using a CFX Connect™ Real-Time PCR Detection System (Bio-Rad Laboratories, Hercules, CA, USA) and analyzed with the CFX Manager™

software, version 3.0 (Bio-Rad Laboratories). Target gene expression was quantified using the cycle threshold (Ct) values and relative mRNA expression levels were calculated as follows: 2^ (Ct reference gene - Ct target gene). Rat ribosomal protein lateral stalk subunit P0 (*Rplp*0), glyceraldehyde 3-phosphate dehydrogenase (*Gapdh*), and hypoxanthine phosphoribosyl transferase 1 (*Hprt1*) were used as reference genes.

3.5.6. *Alkaline phosphatase activity detection*

Quantitative determinations of Alp were performed in MSCs lysates by using the LabAssay™ ALP kit (Wako Pure Chemical Industries, Ltd., Chūō-ku, Osaka, Japan) following manufacturer's instructions. Absorbance at 405 nm was measured on a VICTOR™ X3 Multilabel Plate Reader. Cell lysates were analyzed for protein content using the Pierce™ BCA Protein Assay Kit (Thermo Scientific™) according to the manufacturer's protocol, and intracellular Alp levels were normalized for total protein concentration.

For cytochemical staining, MCSs were washed with PBS and fixed in 4 % (v/v) PFA for 10 min at RT. After a wash with water, cells were incubated for 30 min in a solution with 0.01 % Naphtol AS-MX phosphate (Sigma-Aldrich®) and 0.03 % Fast Violet B salt (Sigma-Aldrich®), at RT in the dark. Finally, cells were washed with water and air-dried. Images were acquired in a Leica MZ10F stereomicroscope (Leica).

3.5.7. *Protein extraction, precipitation and Western blotting analysis*

Cells were lysed on ice for 15 min with lysis buffer containing 1 % (v/v) triton® X-100, and 1 % (v/v) Nonidet-P40 enriched with a protease and phosphatase inhibitor cocktail (Sigma-Aldrich®). To separate proteins from cellular debris, cells lysates were spun down and the supernatant (proteins) were quantified using the Pierce BCA Protein Assay Kit (Thermo Scientific™). 40 µg of total protein was precipitated with acetone, denatured in loading buffer, separated by sodium dodecyl sulphate-polyacrylamide gel electrophoresis (SDS-PAGE), on a 10 % polyacrylamide gel, and electroblotted to the Hybond™-C Extra nitrocellulose membrane (GE Healthcare Life Sciences, Chicago IL, USA). Membranes were blocked for 1 h with 5 % BSA and 0.5

% Tween-20 in PBS and immunoblotted overnight at 4 °C with primary antibodies. Horseradish peroxidase (HRP) - conjugated secondary antibodies were used accordingly. Immunodetection was carried out with the Clarity™ Western ECL detection kit reagents (Bio-Rad Laboratories). Membranes were visualized on ImageQuant™ LAS 4000 mini (GE Healthcare Life Sciences) and bands intensity was quantified using the ImageJ software.

3.5.8. Statistical analysis

GraphPad Prism® software, version 5.0 (GraphPad Software Inc, Sandiego, CA, USA) was used for statistical analysis. Results are presented as a bar with the mean ± standard deviation (mean ± SD) or box-plot with median and min to max whiskers. Significant differences between two independent groups were established using the Mann-Whitney *U* test. Values of $p < 0.05$ were considered statistically significant.

ACKNOWLEDGMENTS & AUTHOR CONTRIBUTIONS.3.6

This work was supported by grants from the Bordeaux Consortium for Regenerative Medicine (BxCRM). D.I.S is supported by Institut National de la Santé et de la Recherche Médicale (INSERM), University of Bordeaux, and Direction Générale de l'Armement (DGA). The authors thank Dr. Meriem Lamghari from i3S – Instituto de Investigação e Inovação em Saúde for helpful advice.

DIS performed the experiments, analysed the data, and wrote the manuscript; BPS performed the flow cytometric analysis; JL contributed with materials and expertise for the photolithography technique. DIS, HO and JA coordinated the work. All the authors discussed the results and revised the manuscript text.

1 Siddiqui JA, Partridge NC. Physiological Bone Remodeling: Systemic Regulation and Growth Factor Involvement. *Physiology (Bethesda)* 2016; **31**:233–45.

2 Alves CJ, Alencastre IS, Neto E, Ribas J, Ferreira S, Vasconcelos DM *et al.* Bone Injury and Repair Trigger Central and Peripheral NPY Neuronal Pathways. *PLoS One* 2016; **11**: e0165465.

3 Bjurholm A, Kreicbergs A, Brodin E, Schultzberg M. Substance P- and CGRP-immunoreactive nerves in bone. *Peptides* 1988; **9**: 165–71.

4 Bjurholm A, Kreicbergs A, Terenius L, Goldstein M, Schultzberg M. Neuropeptide Y-, tyrosine hydroxylase- and vasoactive intestinal polypeptide-immunoreactive nerves in bone and surrounding tissues. *J Auton Nerv Syst* 1988; **25**: 119–25.

5 Castañeda-Corral G, Jimenez-Andrade JM, Bloom AP, Taylor RN, Mantyh WG, Kaczmarska MJ *et al.* The majority of myelinated and unmyelinated sensory nerve fibers that innervate bone express the tropomyosin receptor kinase A. *Neuroscience* 2011; **178**: 196–207.

6 Hill EL, Elde R. Distribution of CGRP-, VIP-, D beta H-, SP-, and NPY-immunoreactive nerves in the periosteum of the rat. *Cell Tissue Res* 1991; **264**: 469–80.

7 Hara-Irie F, Amizuka N, Ozawa H. Immunohistochemical and ultrastructural localization of CGRP-positive nerve fibers at the epiphyseal trabecules facing the growth plate of rat femurs. *Bone* 1996; **18**: 29–39.

8 Serre CM, Farlay D, Delmas PD, Chenu C. Evidence for a dense and intimate innervation of the bone tissue, including glutamate-containing fibers. *Bone* 1999; **25**: 623–629.

9 Su Y-W, Zhou X-F, Foster BK, Grills BL, Xu J, Xian CJ. Roles of neurotrophins in skeletal tissue formation and healing. *J Cell Physiol* 2017. doi:10.1002/jcp.25936.

10 Edoff K, Hellman J, Persliden J, Hildebrand C. The developmental skeletal growth in the rat foot is reduced after denervation. *Anat Embryol (Berl)* 1997; **195**: 531–8.

11 Song D, Jiang X, Zhu S, Li W, Khadka A, Hu J. Denervation impairs bone regeneration during distraction osteogenesis in rabbit tibia lengthening. *Acta Orthop* 2012; **83**: 406–410.

12 Fukuda T, Takeda S, Xu R, Ochi H, Sunamura S, Sato T *et al.* Sema3A regulates bone-mass accrual through sensory innervations. *Nature* 2013; **497**: 490–3.

13 Hayashi M, Nakashima T, Taniguchi M, Kodama T, Kumanogoh A, Takayanagi H. Osteoprotection by semaphorin 3A. *Nature* 2012; **485**: 69–74.

14 Kodama D, Hirai T, Kondo H, Hamamura K, Togari A. Bidirectional communication between sensory neurons and osteoblasts in an *in vitro* coculture system. *FEBS Lett* 2017; **591**: 527–539.

15 Obata K, Furuno T, Nakanishi M, Togari A. Direct neurite-osteoblastic cell communication, as demonstrated by use of an in vitro co-culture system. *FEBS Lett* 2007; **581**: 5917–5922.

16 Zhang P-X, Jiang X-R, Wang L, Chen F-M, Xu L, Huang F. Dorsal root ganglion neurons promote proliferation and osteogenic differentiation of bone marrow mesenchymal stem cells. *Neural Regen Res* 2015; **10**: 119–23.

17 Park JW, Vahidi B, Taylor AM, Rhee SW, Jeon NL. Microfluidic culture platform for neuroscience research. *Nat Protoc* 2006; **1**: 2128–36.

18 Neto E, Alves CJ, Sousa DM, Alencastre IS, Lourenço AH, Leitão L *et al.* Sensory neurons and osteoblasts: close partners in a microfluidic platform. *Integr Biol* 2014; **6**: 586–95.

19 Neto E, Leitão L, Sousa DM, Alves CJ, Alencastre IS, Aguiar P *et al.* Compartmentalized Microfluidic Platforms: The Unrivaled Breakthrough of *In Vitro* Tools for Neurobiological Research. *J Neurosci* 2016; **36**: 11573–11584.

20 Long F. Building strong bones: molecular regulation of the osteoblast lineage. *Nat Rev Mol Cell Biol* 2011; **13**: 27–38.

21 Baek W-Y, Lee M-A, Jung JW, Kim S-Y, Akiyama H, de Crombrugghe B *et al.* Positive Regulation of Adult Bone Formation by Osteoblast-Specific Transcription Factor Osterix. *J Bone Miner Res* 2009; **24**: 1055–1065.

22 Komori T, Yagi H, Nomura S, Yamaguchi A, Sasaki K, Deguchi K *et al.* Targeted disruption of Cbfa1 results in a complete lack of bone formation owing to maturational arrest of osteoblasts. *Cell* 1997; **89**: 755–64.

23 Nakashima K, Zhou X, Kunkel G, Zhang Z, Deng JM, Behringer RR *et al.* The novel zinc finger-containing transcription factor osterix is required for osteoblast

differentiation and bone formation. *Cell* 2002; **108**: 17–29.

24 Otto F, Thornell AP, Crompton T, Denzel A, Gilmour KC, Rosewell IR *et al.* Cbfa1, a candidate gene for cleidocranial dysplasia syndrome, is essential for osteoblast differentiation and bone development. *Cell* 1997; **89**: 765–71.

25 Ducy P, Zhang R, Geoffroy V, Ridall AL, Karsenty G. Osf2/Cbfa1: a transcriptional activator of osteoblast differentiation. *Cell* 1997; **89**: 747–54.

26 Kern B, Shen J, Starbuck M, Karsenty G. Cbfa1 Contributes to the Osteoblast-specific Expression of type I collagen Genes. *J Biol Chem* 2001; **276**: 7101–7107.

27 Li Y, Ge C, Long JP, Begun DL, Rodriguez JA, Goldstein SA *et al.* Biomechanical stimulation of osteoblast gene expression requires phosphorylation of the RUNX2 transcription factor. *J Bone Miner Res* 2012; **27**: 1263–74.

28 Jikko A, Harris SE, Chen D, Mendrick DL, Damsky CH. Collagen integrin receptors regulate early osteoblast differentiation induced by BMP-2. *J Bone Miner Res* 1999; **14**: 1075–83.

29 Dacic S, Kalajzic I, Visnjic D, Lichtler AC, Rowe DW. Col1a1-Driven Transgenic Markers of Osteoblast Lineage Progression. *J Bone Miner Res* 2001; **16**: 1228–1236.

30 Aubin JE. Bone stem cells. *J Cell Biochem Suppl* 1998; **30**–**31**: 73–82.

31 Moorer MC, Stains JP. Connexin43 and the Intercellular Signaling Network Regulating Skeletal Remodeling. *Curr Osteoporos Rep* 2017; **15**: 24–31.

32 Plotkin LI, Laird DW, Amedee J. Role of connexins and pannexins during ontogeny, regeneration, and pathologies of bone. *BMC Cell Biol* 2016; **17**: S19.

33 Marie PJ, Haÿ E, Saidak Z. Integrin and cadherin signaling in bone: role and potential therapeutic targets. *Trends Endocrinol Metab* 2014; **25**: 567–575.

34 Zhong Z, Ethen NJ, Williams BO. WNT signaling in bone development and homeostasis. *Wiley Interdiscip Rev Dev Biol* 2014; **3**: 489–500.

35 Huber O, Korn R, McLaughlin J, Ohsugi M, Herrmann BG, Kemler R. Nuclear localization of beta-catenin by interaction with transcription factor LEF-1. *Mech Dev* 1996; **59**: 3–10.

36 Kobayashi Y, Uehara S, Udagawa N, Takahashi N. Regulation of bone metabolism by Wnt signals. *J Biochem* 2016; **159**: 387–392.

37 Si W, Kang Q, Luu HH, Park JK, Luo Q, Song W-X *et al.* CCN1/Cyr61 is regulated by the canonical Wnt signal and plays an important role in Wnt3A-

induced osteoblast differentiation of mesenchymal stem cells. *Mol Cell Biol* 2006; **26**: 2955–64.

38 Melli G, Höke A. Dorsal Root Ganglia Sensory Neuronal Cultures: a tool for drug discovery for peripheral neuropathies. *Expert Opin Drug Discov* 2009; **4**: 1035–1045.

39 Grigoriadis AE, Heersche JN, Aubin JE. Differentiation of muscle, fat, cartilage, and bone from progenitor cells present in a bone-derived clonal cell population: effect of dexamethasone. *J Cell Biol* 1988; **106**: 2139–51.

40 McCulloch CA, Strugurescu M, Hughes F, Melcher AH, Aubin JE. Osteogenic progenitor cells in rat bone marrow stromal populations exhibit self-renewal in culture. *Blood* 1991; **77**: 1906–11.

41 Lian JB, Stein GS. The developmental stages of osteoblast growth and differentiation exhibit selective responses of genes to growth factors (TGF beta 1) and hormones (vitamin D and glucocorticoids). *J Oral Implantol* 1993; **19**: 95-105–7.

42 Khurana JS, Safadi FF. Bone Structure, Development and Bone Biology. In: *Essentials in Bone and Soft-Tissue Pathology*. Springer US: Boston, MA, 2010, pp 1–15.

43 Choi M-H, Noh W-C, Park J-W, Lee J-M, Suh J-Y. Gene expression pattern during osteogenic differentiation of human periodontal ligament cells in vitro. *J Periodontal Implant Sci* 2011; **41**: 167–75.

44 Laird DW. Syndromic and non-syndromic disease-linked Cx43 mutations. *FEBS Lett* 2014; **588**: 1339–1348.

45 Xu G, Jiang D. The Role and Mechanism of Exogenous Calcitonin Gene-Related Peptide on Mesenchymal Stem Cell Proliferation and Osteogenetic Formation. *Cell Biochem Biophys* 2014; **69**: 369–378.

46 Ma WH, Liu YJ, Wang W, Zhang YZ. Neuropeptide Y, substance P, and human bone morphogenetic protein 2 stimulate human osteoblast osteogenic activity by enhancing gap junction intercellular communication. *Brazilian J Med Biol Res = Rev Bras Pesqui medicas e Biol* 2015; **48**: 299–307.

47 Talbot J, Brion R, Lamora A, Mullard M, Morice S, Heymann D *et al.* Connexin43 intercellular communication drives the early differentiation of human bone marrow stromal cells into osteoblasts. *J Cell Physiol* 2017. doi:10.1002/jcp.25938.

48 Krutovskikh VA, Troyanovsky SM, Piccoli C, Tsuda H, Asamoto M, Yamasaki

H. Differential effect of subcellular localization of communication impairing gap junction protein connexin43 on tumor cell growth in vivo. *Oncogene* 2000; **19**: 505–513.

49 Haÿ E, Laplantine E, Geoffroy V, Frain M, Kohler T, Muller R *et al.* N-Cadherin Interacts with Axin and LRP5 To Negatively Regulate Wnt/Beta-Catenin Signaling, Osteoblast Function, and Bone Formation. *Mol Cell Biol* 2009; **29**: 953–964.

50 Di Benedetto A, Watkins M, Grimston S, Salazar V, Donsante C, Mbalaviele G *et al.* N-cadherin and cadherin 11 modulate postnatal bone growth and osteoblast differentiation by distinct mechanisms. *J Cell Sci* 2010; **123**: 2640–8.

51 Haÿ E, Lemonnier J, Modrowski D, Lomri A, Lasmoles F, Marie PJ. N- and E-cadherin mediate early human calvaria osteoblast differentiation promoted by bone morphogenetic protein-2. *J Cell Physiol* 2000; **183**: 117–28.

52 Li H, Daculsi R, Grellier M, Bareille R, Bourget C, Amedee J. Role of neural-cadherin in early osteoblastic differentiation of human bone marrow stromal cells cocultured with human umbilical vein endothelial cells. *AJP Cell Physiol* 2010; **299**: C422–C430.

53 Fontana F, Hickman-Brecks CL, Salazar VS, Revollo L, Abou-Ezzi G, Grimston SK *et al.* N-cadherin Regulation of Bone Growth and Homeostasis Is Osteolineage Stage-Specific. *J Bone Miner Res* 2017; **32**: 1332–1342.

54 Marie PJ. N-Cadherin-Wnt connections and the control of bone formation. *IBMS Bonekey* 2009; **6**: 150–156.

55 Karner CM, Long F. Wnt signaling and cellular metabolism in osteoblasts. *Cell Mol Life Sci* 2017; **74**: 1649–1657.

56 Tomlinson R, Li Z, Zhang Q, Goh B, Li Z, Thorek DJ *et al.* NGF-TrkA Signaling by Sensory Nerves Coordinates the Vascularization and Ossification of Developing Endochondral Bone. *Cell Rep* 2016; **16**: 2723–2735.

3.8.1. *Supplementary Figures*

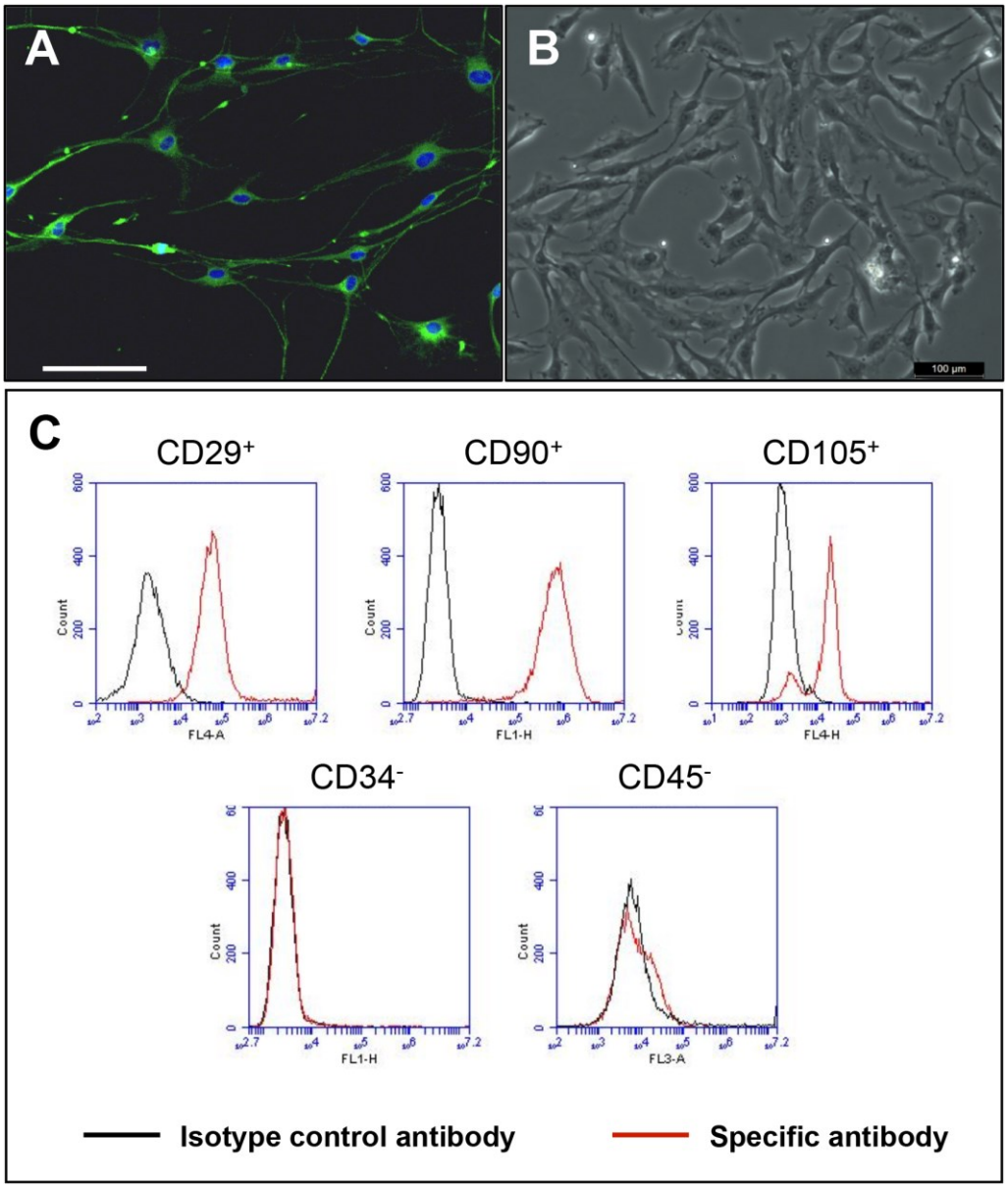

Supplementary Figure S1. DRG neurons and MSCs rat primary cultures characterization. (A) Sensory neurons, isolated from rat DRG and dissociated using a prolonged collagenase treatment followed by mechanical trituration, were cultured in DMEM containing 2 % (v/v) B-27 supplement and 1 % Pen/Strep. Cell morphology was evaluated by IF 7 days after isolation, using an antibody directed against calcitonin gene-related peptide (CGRP) coupled to Alexa Fluor® 488 (green), and DAPI (nuclei; blue) under a confocal microscope. Scale bar = 100 µm. (B and C) Rat bone marrow MSCs were selected by plastic adherence in the presence of DMEM - low glucose supplemented with 10 % (v/v) FBS and 1 % (v/v) Pen/Strep. (B) 5 days after isolation, cell morphology was observed under an inverted phase contrast microscope and (C) immunophenotypic analysis was performed by flow cytometry (CD29, CD90 and CD105 as MSCs specific markers and CD34 and CD45 as hematopoietic markers).

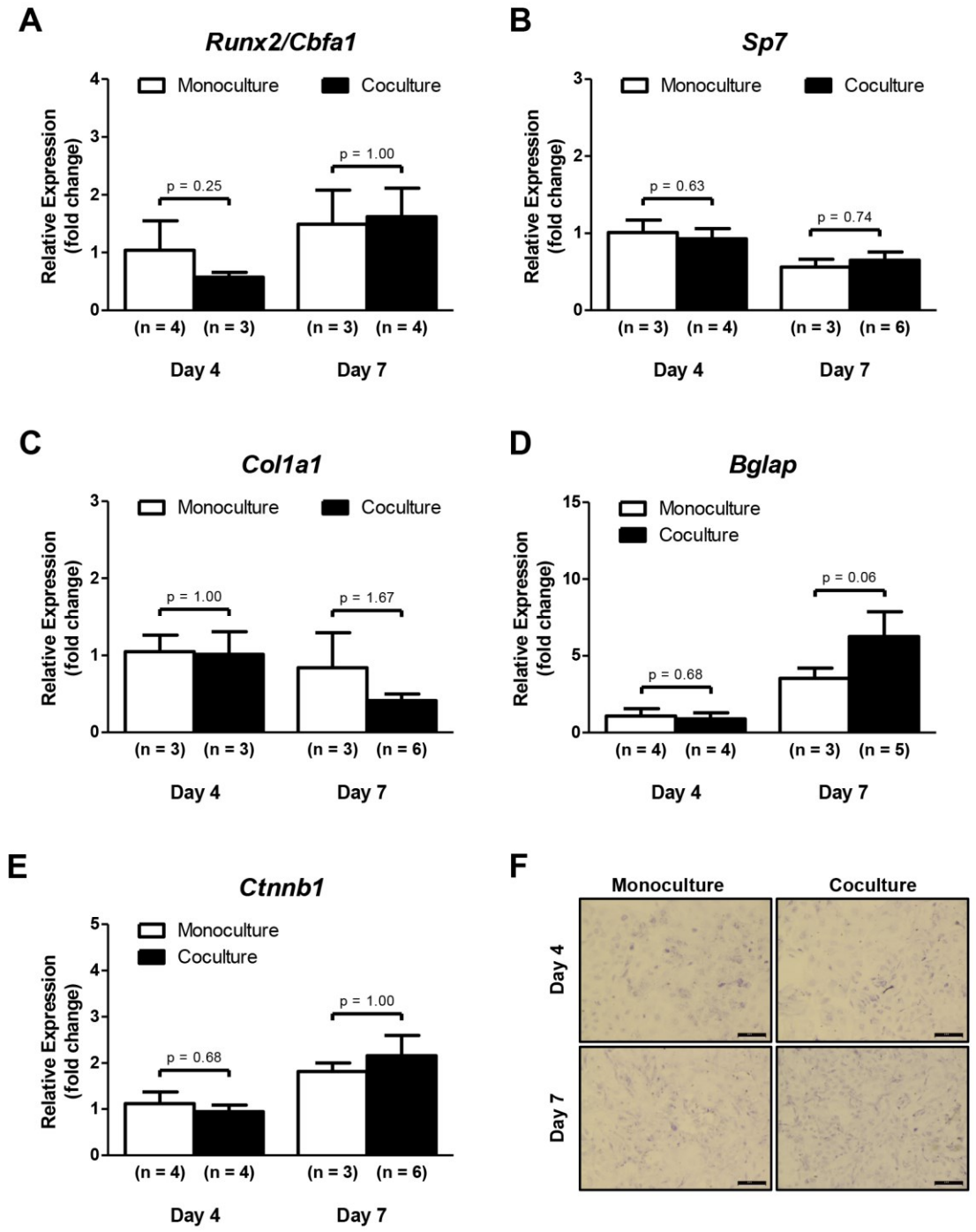

Supplementary Figure S2. DRG neurons do not have the capacity to induce osteoblast differentiation of MSCs in the absence of an osteogenic stimulus. Sensory neurons derived from rat DRG (5 x 10^4 cells/cm^2) and rat bone marrow MSCs (10^4 cells/cm^2) were cocultured in microfluidic devices for 7 days. DRG neurons were maintained in DMEM supplemented with 2 % (v/v) B-27 and 1 µM AraC; MSCs were incubated in standard culture medium composed of DMEM-low glucose with 10 % (v/v) FBS. (A-E) Expression profile of *Runx2*, *Sp7*, *Col1a1*, *Bglap,* and *Ctnnb1* in MSCs was assessed at 4 and 7 days of coculture by RT-qPCR and normalized to the monoculture levels on day 4. Gene expression levels were calculated as a relative ratio to the average value of housekeeping gene *Rplp0*. Data expressed as mean ± SD. (n) indicates the total number of samples for each group. (F) Alp activity in MSCs was analyzed at 4 and 7 days of coculture by Alp cytochemical staining. The results represent four independent experiments.

3.8.2. *Supplementary Experimental Procedures*

3.8.2.1. Microfluidic devices fabrication

Microfluidic devices were obtained using standard photolithography and soft lithography procedures. The first step comprised the fabrication of a master mold, which consists of two layers of photoresist structures on a flat silicon wafer substrate. Afterward, poly (dimethylsiloxane) (PDMS, Sylgard 184, Dow Corning, Midland, MI, USA) was mixed with a curing agent at a w/w of 10:1 and poured onto the silicon wafer. Master mold with PDMS was then placed in a vacuum desiccator for 15 min to remove air bubbles from the PDMS. Subsequently, PDMS was cured at 60 ºC for 2 h, and microfluidic chambers were cut and separated from the master mold. Reservoirs were punched out using an 8 mm tissue biopsy punch. Finally, the microfluidic devices were sterilized in 70 % (v/v) ethanol and allowed to dry in a laminar flow hood.

Before use, microfluidic devices were irradiated with UV light for 20 min to create reactive species on the surface, which when placed together with glass coverslips to form an electrostatic bond. UV irradiation also makes the surface hydrophilic helping the addition of liquids.

3.8.2.2. Rat bone marrow mesenchymal stem cells isolation

Primary bone marrow MSCs were obtained from a healthy 6-10 week-old male Wistar rat. Briefly, after sacrificing the rat by CO_2, back limbs were harvested and soft tissue attached to the skeleton was removed. Femora and tibia were washed with ice-cold hank's balanced salt solution (HBSS, Gibco®), supplemented with 10 % (v/v) Pen/Strep, and the extremities were clipped to expose the marrow. Bones were then transferred to a 1.5 mL microcentrifuge tube, which was subsequently inserted into a 15 mL centrifuge tube and centrifuged for 1 minute at 3000 rpm to collect the marrow. The obtained pellet was resuspended in standard culture medium, which consisted of DMEM - low glucose with 10 % (v/v) FBS and 1 % (v/v) Pen/Strep. Cells were dispersed using a 21G needle for 4-6 times and filtered through a 100 µm cell strainer to remove bone fragments and cell clumps. The cell suspension was then centrifuged at 1200 rpm for 5 min, resuspended in standard culture medium, and maintained in a humidified incubator (37 °C and 5 % CO_2). The medium was changed after 3 days to remove non-adherent cells, and subsequently, the adherent

cells were cultured to confluence (the medium was renewed every 3/4 days). Cells from the first passage were used in all studies.

3.8.2.3. Rat dorsal root ganglion neurons isolation

Primary DRG neurons were obtained from healthy 6-10 week-old male Wistar rats. Briefly, after sacrificing the rats by CO_2, spinal columns were removed and placed in HBSS with 10 % (v/v) Pen/Strep. Columns were opened from the caudal to the rostral end with scissors to reveal the DRG. Then, DRG were individually recovered, placed in DMEM and the nerve trunks removed with a scalpel blade. Subsequently, DRG were digested with 10 mg/mL Collagenase, Type IV (Gibco®) for 2 h at 37 ºC. After centrifugation at 1200 rpm for 5 min, the pellet was resuspended in DMEM. Afterward, DRG were mechanically dissociated using fire-polished glass Pasteur pipettes (full diameter and ½ diameter). The cell suspension was then centrifuged at 1200 rpm for 5 min 3 times and resuspended in growing medium composed of DMEM with 2 % (v/v) B-27, 1 µM cytosine arabinofuranoside (AraC, also known as cytarabine), and 1 % (v/v) Pen/Strep.

3.8.2.4. Flow cytometric analysis

Trypsinized MSCs (5 x 10^4 cells) were fixed in 1 % (v/v) PFA for 10 min at 4 °C. Cells were then washed with PBS and incubated in the dark with antibodies anti-CD29-Cy5, anti-CD34-FITC, anti-CD105-Cy5 (20 µg/mL; Bioss Antibodies Inc., Woburn, MA, USA), anti-CD45-PE-CY5, and anti-CD90-FITC (20 µg/mL; Becton Dickinson, East Rutherford, NJ, USA) for 60 min at 4 °C. Matched isotype control antibodies were used as negative controls. Cells were then washed twice with PBS and resuspended in PBS. For immunophenotyping analysis, a typical forward and side scatter gate was set to exclude dead cells and aggregates. A total of 7000 events in the gate were collected and fluorescence was analyzed with a BD Accuri™ C6 Flow Cytometer (Becton Dickinson, Franklin Lakes, NJ, USA) using the CFlow® Plus software.

IN BRIEF.3.9

Data presented in this first part show an enhancement of osteoblast differentiation potential of MSCs in a direct response to the DRG neurons interaction and communication. The osteogenic effect of DRG neurons on MSCs is mediated through the activation of the canonical Wnt signaling pathway. This “efferent” function of DRG neurons raises a question about the specific identity of its subpopulation. Indeed, the capsaicin-sensitive sensory neurons represent a peculiar type of sensory neurons able to communicate peripherally with target cells *via* release of the stored neurotransmitters [60]. Based on this, in the second part of this dissertation, we aimed at better characterizing the subset of DRG neurons involved in osteoblast differentiation of MSCs, by investigating the effect of capsaicin-activated sensory neurons on this process and identifying the key neurotransmitters.

ARTICLE 2.04

Activation of capsaicin-sensitive dorsal root ganglion neurons induces the osteoblast differentiation of mesenchymal stem cells *in vitro*

Diana Isabel Silva[1]*, Bruno Paiva dos Santos[1], Hugo Oliveira[1], Joëlle Amédée[1]

[1] Univ. Bordeaux, Tissue Bioengineering, U1026, F-33076 Bordeaux, France; INSERM, Tissue Bioengineering, U1026, F-33076 Bordeaux, France.

*Correspondence: diana.da-silva@inserm.fr

Manuscript under preparation

ABSTRACT.4.1

Bone formation, remodeling, and regeneration processes are under the control of the sensory nervous system. Recently, we identified the mesenchymal stem cells (MSCs) as a direct target of the sensory neurons. However, little knowledge concerning the subpopulation of these neurons that is involved in osteoblast differentiation of MSCs has been accumulated. In this study, we focused on the effect of capsaicin-sensitive sensory neurons activation on osteoblastogenesis *in vitro*.

Bone marrow MSCs were cultured with conditioned medium (CM) originated from the culture medium of dorsal root ganglion (DRG) neurons treated with capsaicin. The transcriptional and translational expressions of genes known as markers of osteoblast differentiation were analysed in MSCs by RT-qPCR and alkaline phosphatase (ALP) activity assay.

The activation of capsaicin-sensitive DRG neurons was confirmed by an increase in the levels of two important sensory neuropeptides, calcitonin gene-related peptide and Substance P, in the culture medium. We report that MSCs cultured for 4 days with CM obtained from culture medium of capsaicin-activated DRG neurons showed a transcriptional upregulation of osteoblast-related genes. Moreover, we observed a significant increase of ALP intracellular levels in MSCs maintained under these culture conditions for 7 days. Our study suggests that the activation of capsaicin-sensitive DRG neurons induces the osteoblast differentiation of MSCs.

Keywords: DRG neurons, mesenchymal stem cells, osteoblast differentiation, capsaicin, Substance P, CGRP

Accumulated evidence supports the concept that innervation is involved in the regulation of bone development, maintenance and healing [1–3]. Moreover, evidence for an important role of the sensory innervation has emerged in the regulation of osteoblast and bone formation [4–7]. A study of Fukuda and colleagues revealed that Semaphorin 3A produced by sensory nerves plays a key role in bone homeostasis through the modulation of the local nerve ingrowth [6]. The role of the sensory nervous system on osteogenesis was further explored in a recent work published by our group. In this study, we demonstrated that sensory neurons play a direct and positive role on transcriptional and translational programs of osteoblast differentiation of MSCs *in vitro.* However, the specific subset of sensory neurons and the main neuropeptides directly implicated in this process remain unclear.

Extensive research has described that the activation of transient receptor potential vanilloid subfamily member 1 (TRPV1) in sensory neurons by capsaicin, the pungent compound in hot chili pepper, promotes the release of neuropeptides, particularly calcitonin gene-related peptide (CGRP) and Substance P [8–12]. Interestingly, it was shown that the amount of sensory neuropeptides is markedly increased at the sites of bone formation due to the increase of TRPV1 expression in the local sensory neurons [13]. TRPV1 is commonly found in small diameter (Aδ) myelinated and peptidergic C-sensory nerve fibers [14–16]. However, some studies have suggested that TRPV1 is also expressed at very low levels in a substantial portion of nonpeptidergic C-sensory nerve fibers [17–20]. Activation of TRPV1 by noxious mechanical, chemical, or thermal stimuli, leads to the influx of calcium and sodium cations into the sensory neurons triggering its depolarization and consequent neurotransmitter release [8,21,22].

In the present study, we used conditioned medium (CM) originated from the culture medium of capsaicin-stimulated dorsal root ganglion (DRG) neurons to culture MSCs.

The objective was to explore the role of activated capsaicin-sensitive DRG neurons, on the ability of MSCs to undergo osteoblast differentiation. Our results suggest that capsaicin-induced activation of sensory neurons induces the osteoblastogenesis *in vitro* possibly by mediating the release of neuropeptides.

4.3.1. CM obtained from the culture medium of activated capsaicin-sensitive DRG neurons triggers the osteoblast differentiation process in MSCs

Sensory neurons are an important target for capsaicin, and its activation elicite the release of CGRP and Substance P [8–12]. In this sense, after 4 days of culture, DRG neurons were treated with 100 nM capsaicin for 1h. Subsequently, ELISA was conducted to measure the levels of CGRP and Substance P levels in culture medium (Figure 1). As expected, DRG neurons exposure to capsaicin significantly increased the release of CGRP (Figure 1A) and Substance P (Figure 1B), when compared with unexposed DRG neurons, suggesting an activation of capsaicin-sensitive sensory neurons.

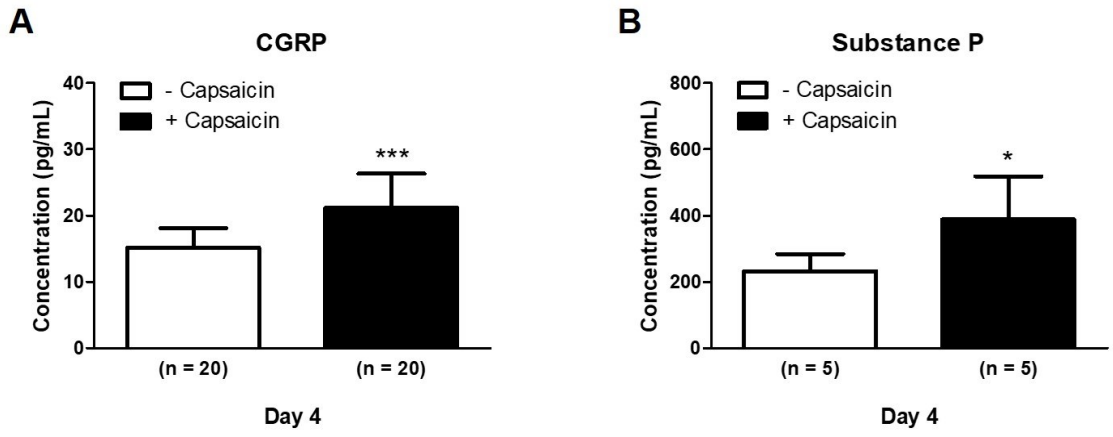

Figure 1. Capsaicin evokes a marked release of CGRP and Substance P in primary cultures of DRG neurons. Sensory neurons isolated from rat DRG (5 x 10^4 cells/cm^2) were treated on day 4 of culture with capsaicin (100 nM, for 1h). ELISA determined (A) CGRP and (B) Substance P levels in the cell culture medium. Data express mean ± SD. (n) indicates the total number of samples for each group. *p < 0.05, ***p < 0.001, statistical difference from the control without capsaicin.

Osteoblastogenesis is characterized by transcriptional and translational regulation of bone phenotyping genes [23]. To investigate whether the culture with CM derived from the culture medium of capsaicin-activated DRG neurons had an influence on the

osteoblast differentiation capacity of MSCs, we analysed the expression of osteoblast-related genes in MSCs by RT-qPCR after 4 and 7 days of culture (Figure 2). The studied genes included runt-related transcription factor 2 (*Runx2*), specificity protein transcription factor 7 (*Sp7*, encoding osterix), collagen type I alpha 1 chain

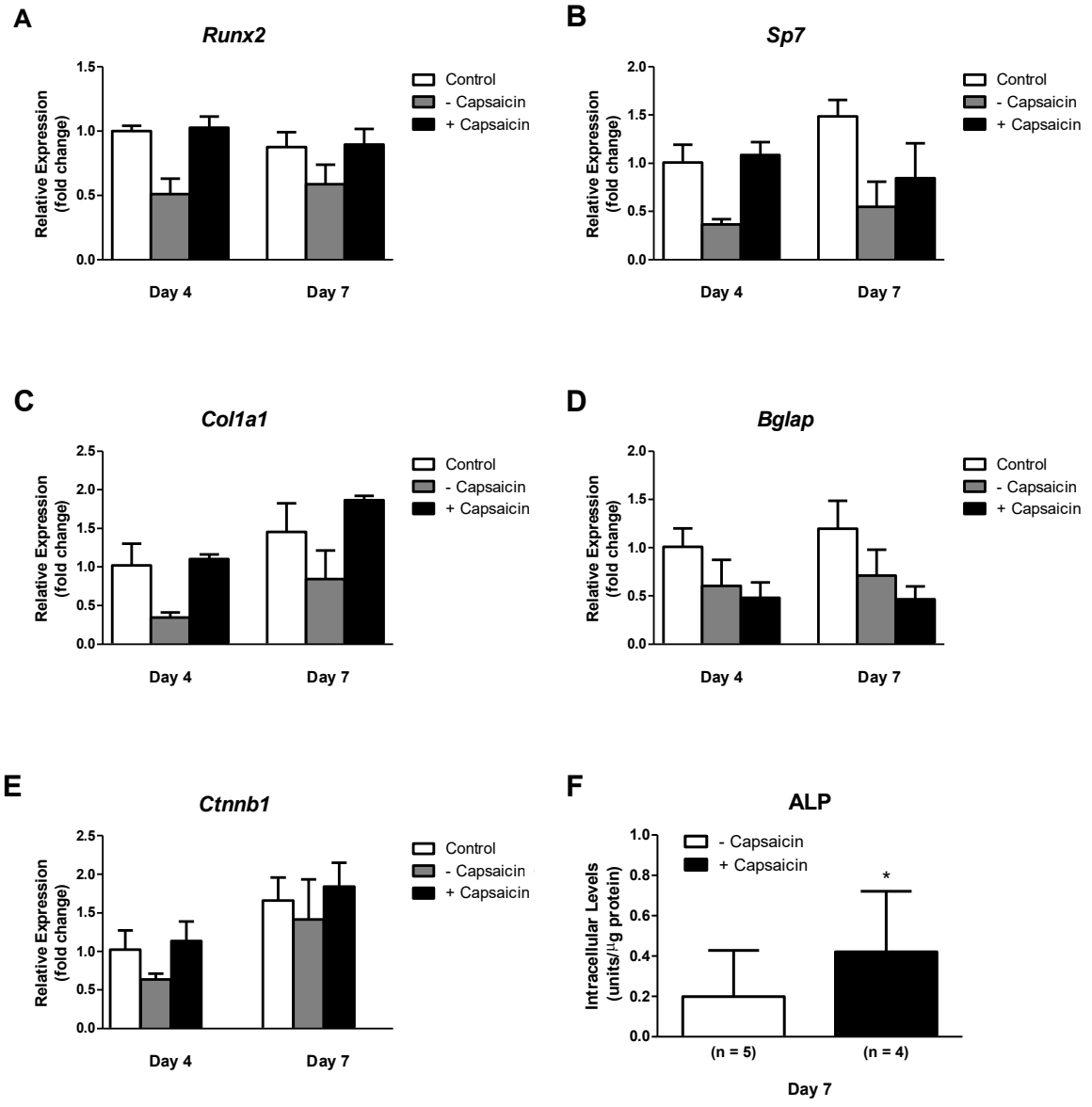

Figure 2. CM originated from capsaicin-sensitive DRG neurons leads to osteoblast lineage development from MSCs. Rat bone marrow MSCs (10^4 cells/cm^2) were cultured in a six-well plate for 7 days with CM from DRG neurons treated with capsaicin (100 nM, for 1h). (A-E) Expression profile of *Runx2*, *Sp7*, *Col1a1, Bglap* and *Ctnnb1* in MSCs was assessed at 4 and 7 days of culture by RT-qPCR and depicted as a relative ratio to the housekeeping gene *Gapdh,* normalized to the levels of positive control (MSCs cultured under osteogenic conditions) on day 4. (F) ALP activity in MSCs was analyzed on day 7 of culture by ALP activity quantification assay. Data expressed as mean ± SD. (n) indicates the total number of samples for each group. *$p < 0.05$ statistically different from control without capsaicin.

(*Col1a1*), bone gamma-carboxyglutamate protein (*Bglap,* encoding osteocalcin), and catenin beta 1 (*Ctnnb1*, encoding β-catenin). *Runx2*, *Sp7*, *Col1a1*, and *Ctnnb1* were considered markers of early osteoblastogenesis, and *Bglap* was used as a late marker. We found an upregulation of the early osteoblastic genes in MSCs maintained for 4 days in CM originated from the culture medium of capsaicin-treated DRG neurons when compared with MSCs incubated with nontreated DRG neurons-CM (Figure 2A-E). In addition, the alkaline phosphatase (ALP) activity quantification assay revealed a significant increase of intracellular levels of this protein in MSCs cultured with CM obtained from the culture medium of stimulated DRG neurons (Figure 2F). These findings suggest that the activation of capsaicin-sensitive sensory neurons induces the osteoblast differentiation and activity in MSCs.

It has been demonstrated a pivotal participation of sympathetic and sensory nervous systems in both local and systemic bone metabolism [23–26]. Electrophysiological and histological studies have enabled to identify the nature and distribution of bone nerve fibers [19,23–25,27–30]. Furthermore, several studies have identified the expression of receptors for numerous neurotransmitters in bone cells [31]. Small diameter myelinated fibers, particularly Aδ, and unmyelinated peptide-rich C-fibers are the main sensory nerve fibers found on bone tissue [19,20,32,33]. Sensory neuropeptides, especially CGRP and Substance P, are expressed in these type of fibers [34]. In addition, both Aδ- and C-fibers are characterized by expression of TRPV1 [14–16,20]. It is well documented that the TRPV1 activation in sensory neurons by a noxious stimulus (*e.g.* capsaicin) promotes the release of neurotransmitters from both central and peripheral terminals [10–12]. Accordingly, we found that capsaicin-induced activation of DRG neurons elicited a pronounced release of CGRP and Substance P [8,10–12]. Multiple studies have provided insights into the importance of sensory neuropeptides in bone integrity [13]. It was shown that some hereditary sensory neuropathies, such as familial dysautonomia, are related to skeletal disorders due to decrease of unmyelinated sensory nerve fibers and consequent decrease of local neuropeptides [35–37]. Specifically, CGRP and Substance P have been identified to contribute to osteoblastogenesis *in vitro* [38–41]. Some studies have demonstrated that the addition of CGRP to MSCs osteogenic culture medium results in an increase of osteoblast marker genes expression, particularly, *Runx2*, *Alp*, *Col1a1*, and *Bglap*, in these cells [42]. Likewise, the addition of Substance P to the cell culture medium has been reported to increase the transcriptional expression of *Runx2*, *Col1a1* and *Bglap* in osteoblastic cells at a late stage of osteoblast differentiation [41,43]. Moreover, it was described that Substance P stimulates the early osteoblastogenesis by upregulating the *Sp7* in MSCs and activating the Wnt-β-catenin signaling pathway in MC3T3-E1 cells [41,44,45]. Interestingly, this neuropeptide was also described to stimulate the osteoblast activity by enhancing gap junction intercellular communication [46]. In our research, we observed an upregulation of early osteoblastic genes (*i.e. Runx2*, *Sp7*, *Col1a1*, and *Ctnnb1*) in MSCs cultured for 4 days with CM obtained from the culture medium of capsaicin-activated sensory neurons. Furthermore, under the same

culture conditions, we found on day 7 a significant increase of osteogenic activity in MSCs.

Together, these findings suggest an involvement of stimulated myelinated Aδ and unmyelinated peptide-rich C-fibers in the positive regulation of early osteoblastic differentiation of MSCs *in vitro*, possibly by mediating the release of neuropeptides like CGRP and Substance P.

Understanding the neuro-skeletal interplay can inform the development of new therapeutic approaches for bone regeneration/repair based on the targeting of receptors activated by neuropeptides released from a specific type of sensory nerve fibers.

4.5.1. Rat primary cells isolation and culture

Primary DRG neurons and bone marrow MSCs were obtained from healthy male 6-10 week-old male Wistar rats, as described previously.

DRG neurons (10^4 cells/cm^2) were seeded on glass coverslips, previously coated with 0.1 mg/mL Poly-D-lysine (PDL, Sigma-Aldrich®, St. Louis, MI, USA) and 20 µg/mL laminin (Sigma-Aldrich®). Cells were maintained for 4 days in Dulbecco's modified eagle's medium (DMEM, Life Technologies™, Gibco®, Carlsbad, CA, USA), with 2 % (v/v) B-27 Serum-Free Supplement® (B-27, Gibco®), and 1 % (v/v) penicillin/streptomycin (Pen/Strep, Gibco®). On day 4 of culture, DRG neurons were treated for 1h with 100 nM capsaicin (Sigma-Aldrich®). Then, samples of collected medium were centrifuged at 3,000 rpm for 10 min at 4 ºC to remove cell debris, filtered through a 0.22 µm filter, and stored at -80°C until use.

Conditioned medium (CM) was originated from cultured medium of DRG neurons untreated or treated with capsaicin.

MSCs (10^4 cells/cm^2) were plated in a six-well plate and preincubated for 3 days with standard culture medium, consisting of DMEM - low glucose supplemented with 10 % (v/v) fetal bovine serum (FBS, P30-3305, PAN™ - Biotech, Aidenbach, Germany), 1 % (v/v) Pen/Strep. Then, cells were cultured for 7 days with 50% standard culture medium plus 50% untreated or capsaicin-treated DRG neurons-CM in a humidified incubator (the CM was renewed on day 4 of culture). MSCs incubated for the same period with osteogenic medium (standard culture medium containing $1x10^{-9}$ M dexamethasone, 10 mM β-glycerophosphate, and 50 µg/mL ascorbic acid) were used as a positive control of osteoblast differentiation.

4.5.2. CGRP and Substance P levels quantification

Measurements of the CGRP and Substance P levels in cell culture medium of capsaicin-stimulated DRG neurons were performed using CGRP (rat) EIA Kit (SPI-Bio®, Bertin Pharma, Montigny-le-Bretonneux, France) and ELISA Kit for Substance P (SP) (Cloud-clone Corp, Katy TX, USA), respectively, according to the manufacturer's instruction.

4.5.3. *RNA extraction, cDNA synthesis, and RT-qPCR analysis*

Total RNA was extracted from MSCs by using the RNeasy® Micro Kit (Qiagen, Hilden, Germany) according to the manufacturer's protocol. RNA final concentration and purity ($OD_{260/280}$) was determined using a NanoPhotometer® P 330 (Implen GmbH, Munich, Germany). 100 ng of total RNA was reverse transcribed into cDNA using the Maxima Reverse Transcriptase kit (Thermo Scientific™, Thermo Fisher Scientific, Waltham, MA, USA), according to the manufacturer's protocol. RT-qPCR experiments were run using a CFX Connect™ Real-Time PCR Detection System (Bio-Rad Laboratories, Hercules, CA, USA) and analyzed with the CFX Manager™ software, version 3.0 (Bio-Rad Laboratories). Target gene expression was quantified using the cycle threshold (Ct) values and relative mRNA expression levels were calculated as follows: 2^ (Ct reference gene - Ct target gene). Rat ribosomal protein lateral stalk subunit P0 (*Rplp*0), glyceraldehyde 3-phosphate dehydrogenase (*Gapdh*) and hypoxanthine phosphoribosyl transferase 1 (*Hprt1*) were used as reference genes.

4.5.4. *Alkaline phosphatase activity assay*

Quantitative determinations of ALP were performed in MSCs lysates by using the LabAssay™ ALP kit (Wako Pure Chemical Industries, Ltd., Chūō-ku, Osaka, Japan) following manufacturer's instructions. Absorbance at 405 nm was measured on a VICTOR™ X3 Multilabel Plate Reader. Cell lysates were analyzed for protein content using the Pierce™ BCA Protein Assay Kit (Thermo Scientific™) according to the manufacturer's protocol, and intracellular ALP levels were normalized by the total protein concentration.

4.5.5. *Statistical analysis*

GraphPad Prism® software, version 5.0 (GraphPad Software Inc, Sandiego, CA, USA) was used for statistical analysis. Results are presented as a bar with the mean ± standard deviation (mean ± SD). Significant differences between two independent groups were established using the Mann-Whitney *U* test. Values of $p < 0.05$ were considered statistically significant.

ACKNOWLEDGMENTS AUTHOR CONTRIBUTIONS.4.6

This work was supported by grants from the Bordeaux Consortium for Regenerative Medicine (BxCRM). D.I.S is supported by Institut National de la Santé et de la Recherche Médicale (INSERM), University of Bordeaux, and Direction Générale de l'Armement (DGA).

DIS performed the experiments, analysed the data, and wrote the manuscript; DIS, HO and JA coordinated the work. All the authors discussed the results and revised the manuscript text.

1 Vadivel A, Alphonse RS, Collins JJP, van Haaften T, O?Reilly M, Eaton F *et al.* The Axonal Guidance Cue Semaphorin 3C Contributes to Alveolar Growth and Repair. *PLoS One* 2013; **8**: e67225.

2 Medina A, Yamada S, Hara A, Hamamoto K, Kojima I. Involvement of the parasympathetic nervous system in the initiation of regeneration of pancreatic β-cells. *Endocr J* 2013; **60**: 687–96.

3 Mahmoud AI, O'Meara CC, Gemberling M, Zhao L, Bryant DM, Zheng R *et al.* Nerves Regulate Cardiomyocyte Proliferation and Heart Regeneration. *Dev Cell* 2015; **34**: 387–399.

4 Ding Y, Arai M, Kondo H, Togari A. Effects of capsaicin-induced sensory denervation on bone metabolism in adult rats. *Bone* 2010; **46**: 1591–6.

5 Hayashi M, Nakashima T, Taniguchi M, Kodama T, Kumanogoh A, Takayanagi H. Osteoprotection by semaphorin 3A. *Nature* 2012; **485**: 69–74.

6 Fukuda T, Takeda S, Xu R, Ochi H, Sunamura S, Sato T *et al.* Sema3A regulates bone-mass accrual through sensory innervations. *Nature* 2013; **497**: 490–3.

7 Zhang P-X, Jiang X-R, Wang L, Chen F-M, Xu L, Huang F. Dorsal root ganglion neurons promote proliferation and osteogenic differentiation of bone marrow mesenchymal stem cells. *Neural Regen Res* 2015; **10**: 119–23.

8 Julius D, Caterina MJ, Schumacher MA, Tominaga M, Rosen TA, Levine JD. The capsaicin receptor: a heat-activated ion channel in the pain pathway. *Nature* 1997; **389**: 816–824.

9 Aikawa F, Iwai Y. Capsaicin Activates Transient Receptor Potential Vanilloid Subtype 1 (TRPV1) of Rat Bone Marrow-derived Stromal Cells (BMSCs) in vitro. *J Oral Tissue Engin* 2008; **6**: 41–55.

10 Zaidi M, Bevis PJ, Girgis SI, Lynch C, Stevenson JC, MacIntyre I. Circulating CGRP comes from the perivascular nerves. *Eur J Pharmacol* 1985; **117**: 283–4.

11 Lundberg JM, Franco-Cereceda A, Hua X, Hökfelt T, Fischer JA. Co-existence of substance P and calcitonin gene-related peptide-like immunoreactivities in sensory nerves in relation to cardiovascular and bronchoconstrictor effects of capsaicin. *Eur J Pharmacol* 1985; **108**: 315–9.

12 Gibbins IL, Furness JB, Costa M, MacIntyre I, Hillyard CJ, Girgis S. Co-localization of calcitonin gene-related peptide-like immunoreactivity with substance P in cutaneous, vascular and visceral sensory neurons of guinea pigs. *Neurosci Lett* 1985; **57**: 125–30.

13 Offley SC, Guo T-Z, Wei T, Clark JD, Vogel H, Lindsey DP *et al.* Capsaicin-Sensitive Sensory Neurons Contribute to the Maintenance of Trabecular Bone Integrity. *J Bone Miner Res* 2004; **20**: 257–267.

14 Helliwell RJ, McLatchie LM, Clarke M, Winter J, Bevan S, McIntyre P. Capsaicin sensitivity is associated with the expression of the vanilloid (capsaicin) receptor (VR1) mRNA in adult rat sensory ganglia. *Neurosci Lett* 1998; **250**: 177–80.

15 Michael GJ, Priestley J V. Differential expression of the mRNA for the vanilloid receptor subtype 1 in cells of the adult rat dorsal root and nodose ganglia and its downregulation by axotomy. *J Neurosci* 1999; **19**: 1844–54.

16 Tominaga M, Caterina MJ, Malmberg AB, Rosen TA, Gilbert H, Skinner K *et al.* The cloned capsaicin receptor integrates multiple pain-producing stimuli. *Neuron* 1998; **21**: 531–43.

17 Hjerling-Leffler J, Alqatari M, Ernfors P, Koltzenburg M. Emergence of functional sensory subtypes as defined by transient receptor potential channel expression. *J Neurosci* 2007; **27**: 2435–43.

18 Breese NM, George AC, Pauers LE, Stucky CL. Peripheral inflammation selectively increases TRPV1 function in IB4-positive sensory neurons from adult mouse. *Pain* 2005; **115**: 37–49.

19 Ivanusic JJ. Size, neurochemistry, and segmental distribution of sensory neurons innervating the rat tibia. *J Comp Neurol* 2009; **517**: 276–83.

20 Castañeda-Corral G, Jimenez-Andrade JM, Bloom AP, Taylor RN, Mantyh WG, Kaczmarska MJ *et al.* The majority of myelinated and unmyelinated sensory nerve fibers that innervate bone express the tropomyosin receptor kinase A. *Neuroscience* 2011; **178**: 196–207.

21 Basbaum AI, Bautista DM, Scherrer G, Julius D. Cellular and Molecular Mechanisms of Pain. *Cell* 2009; **139**: 267–284.

22 Snider WD, McMahon SB. Tackling pain at the source: new ideas about nociceptors. *Neuron* 1998; **20**: 629–32.

23 Long F. Building strong bones: molecular regulation of the osteoblast lineage. *Nat Rev Mol Cell Biol* 2011; **13**: 27–38.

24 Bjurholm A, Kreicbergs A, Brodin E, Schultzberg M. Substance P- and CGRP-immunoreactive nerves in bone. *Peptides* 1988; **9**: 165–71.

25 Bjurholm A, Kreicbergs A, Terenius L, Goldstein M, Schultzberg M. Neuropeptide Y-, tyrosine hydroxylase- and vasoactive intestinal polypeptide-immunoreactive nerves in bone and surrounding tissues. *J Auton Nerv Syst* 1988; **25**: 119–25.

26 Tabarowski Z, Gibson-Berry K, Felten SY. Noradrenergic and peptidergic innervation of the mouse femur bone marrow. *Acta Histochem* 1996; **98**: 453–7.

27 Serre CM, Farlay D, Delmas PD, Chenu C. Evidence for a dense and intimate innervation of the bone tissue, including glutamate-containing fibers. *Bone* 1999; **25**: 623–629.

28 Hara-Irie F, Amizuka N, Ozawa H. Immunohistochemical and ultrastructural localization of CGRP-positive nerve fibers at the epiphyseal trabecules facing the growth plate of rat femurs. *Bone* 1996; **18**: 29–39.

29 Hill EL, Elde R. Distribution of CGRP-, VIP-, D beta H-, SP-, and NPY-immunoreactive nerves in the periosteum of the rat. *Cell Tissue Res* 1991; **264**: 469–80.

30 Hukkanen M, Konttinen YT, Rees RG, Gibson SJ, Santavirta S, Polak JM. Innervation of bone from healthy and arthritic rats by substance P and calcitonin gene related peptide containing sensory fibers. *J Rheumatol* 1992; **19**: 1252–9.

31 Su Y-W, Zhou X-F, Foster BK, Grills BL, Xu J, Xian CJ. Roles of neurotrophins in skeletal tissue formation and healing. *J Cell Physiol* 2017. doi:10.1002/jcp.25936.

32 Mahns DA, Ivanusic JJ, Sahai V, Rowe MJ. An intact peripheral nerve preparation for monitoring the activity of single, periosteal afferent nerve fibres. *J Neurosci Methods* 2006; **156**: 140–144.

33 Mach DB, Rogers SD, Sabino MC, Luger NM, Schwei MJ, Pomonis JD *et al.* Origins of skeletal pain: sensory and sympathetic innervation of the mouse femur. *Neuroscience* 2002; **113**: 155–66.

34 Bernardini N, Neuhuber W, Reeh P., Sauer S. Morphological evidence for functional capsaicin receptor expression and calcitonin gene-related peptide exocytosis in isolated peripheral nerve axons of the mouse. *Neuroscience* 2004; **126**: 585–590.

35 Maayan C, Bar-On E, Foldes AJ, Gesundheit B, Dresner Pollak R. Bone Mineral Density and Metabolism in Familial Dysautonomia. *Osteoporos Int* 2002; **13**: 429–433.

36 Pearson J, Dancis J, Axelrod F, Grover N. The sural nerve in familial dysautonomia. *J Neuropathol Exp Neurol* 1975; **34**: 413–24.

37 Maayan C, Becker Y, Gesundheit B, Girgis SI. Calcitonin gene related peptide in familial dysautonomia. *Neuropeptides* 2001; **35**: 189–195.

38 Bernard GW, Shih C. The osteogenic stimulating effect of neuroactive calcitonin gene-related peptide. *Peptides*; **11**: 625–32.

39 Adamus MA, Dabrowski ZJ. Effect of the neuropeptide substance P on the rat bone marrow-derived osteogenic cells in vitro. *J Cell Biochem* 2001; **81**: 499–506.

40 Shih C, Bernard GW. Neurogenic substance P stimulates osteogenesis in vitro. *Peptides* 1997; **18**: 323–6.

41 Fu S, Mei G, Wang Z, Zou Z-L, Liu S, Pei G-X *et al.* Neuropeptide substance P improves osteoblastic and angiogenic differentiation capacity of bone marrow stem cells in vitro. *Biomed Res Int* 2014; **2014**: 596023.

42 Wang L, Shi X, Zhao R, Halloran BP, Clark DJ, Jacobs CR *et al.* Calcitonin-gene-related peptide stimulates stromal cell osteogenic differentiation and inhibits RANKL induced NF-κB activation, osteoclastogenesis and bone resorption. *Bone* 2010; **46**: 1369–1379.

43 Goto T, Nakao K, Gunjigake KK, Kido MA, Kobayashi S, Tanaka T. Substance P stimulates late-stage rat osteoblastic bone formation through neurokinin-1 receptors. *Neuropeptides* 2007; **41**: 25–31.

44 Mei G, Zou Z, Fu S, Xia L, Zhou J, Zhang Y *et al.* Substance P Activates the Wnt Signal Transduction Pathway and Enhances the Differentiation of Mouse Preosteoblastic MC3T3-E1 Cells. *Int J Mol Sci* 2014; **15**: 6224–6240.

45 Sun H, Chen J, Liu Q, Guo M, Zhang H. Substance P stimulates differentiation of mice osteoblast through up-regulating Osterix expression. *Chinese J Traumatol = Zhonghua chuang shang za zhi* 2010; **13**: 46–50.

46 Ma WH, Liu YJ, Wang W, Zhang YZ. Neuropeptide Y, substance P, and human bone morphogenetic protein 2 stimulate human osteoblast osteogenic activity by enhancing gap junction intercellular communication. *Brazilian J Med Biol Res* 2015; **48**: 299–307.

IN BRIEF.4.8

Data presented in this second part suggest an inducement of osteoblast differentiation of MSCs in response to the culture with CM obtained from culture medium of capsaicin-activated DRG neurons. We also suggest that this osteogenic effect could be mediated through the increased release of sensory neuropeptides, especially CGRP and SP. However, further studies are required to confirm these hypotheses.

GENERAL DISCUSSION.05

An increasing number of bone sensory innervation studies have been contributing to the understanding of bone physiology and pathophysiology. Notably, independent data indicate that the sensory nervous system has a positive role in the regulation of bone development, metabolism, and repair [61–64]. Despite being an area of intensive research, the direct or indirect link between sensory neurons and bone cells is not clear. Indeed, there is still much to be uncovered about the cellular and molecular mechanisms involved in this link. The main purpose of this work was to explore the role of the sensory neurons on the successive steps of osteoblast differentiation from MSCs.

In article 1, we were interested in clarifying whether DRG neurons would be able to induce osteoblastogenesis by acting directly on MSCs. To address this question, we employed a microfluidic platform to coculture DRG neurons and MSCs in separate compartments. Despite the spatial and fluidic isolation, this platform allowed the interaction of DRG neurons with MSCs *via* neurites extended along well-defined microchannels, as it happens in the *in vivo* scenario of bone sensory innervation. We started by optimizing the culture conditions of each cell population in order to preserve their physiological properties (see section 8.1). Then, we focused on the expression analysis of key osteoblastic genes in MSCs cocultured with DRG neurons. We showed for the first time that although sensory neurons are not able to induce the osteoblast differentiation of MSCs *in vitro*, they significantly enhance this process, by increasing the mRNA levels of early and late markers of osteoblogenesis and promoting the ALP activity in lineage-committed MSCs after 4 and 7 days of coculture. Interestingly, this effect was abolished for longer coculture times. Afterwards, we investigated a possible involvement of Cx43 and N-cadherin during DRG neurons-enhanced osteoblastogenesis. A number of studies have been evidentiating a modulatory effect of these proteins in bone formation and remodeling [65–67]. In our study, we revealed that sensory neurons modulate the Cx43 and N-cadherin levels during osteoblast differentiation of MSCs. Finaly, we attempted to understand whether the canonical Wnt signaling pathway could be implicated in the osteoblastogenesis enhanced by DRG neurons. Several studies have indicated that this pathway plays a central role in bone development and homeostasis [68,69]. Accordingly, we demonstrated that sensory neurons regulate the Wnt/β-catenin

signaling activation during osteoblast differentiation of MSCs. However, we cannot reject an eventual contribution of other signaling pathways in this process. On the light of these findings, it would be interesting to analyse the effect of MSCs on the "classic" afferent function of sensory neurons. Recently, it was reported a bidirectional communication between osteoblast-like cells and sensory neurons. Kodama and colleagues demonstrated that the release of ATP from osteoblast-like cells, induced by an inflammatory stimulus like bradykinin, activates the P2X7 receptor expressed in sensory neurons. This finding suggests that osteoblast-like cells might serve as sensors of environmental stimuli, which are then transmitted to the CNS *via* sensory neurons [70]. In addition, it would also be interesting to investigate the role of sensory neurons in differentiation and activity of other bone cells, particularly in osteoclasts.

In article 2, we aimed at better characterizing the subset of DRG neurons involved in the regulation of osteoblast differentiation from MSCs. For this, we maintained MSCs with culture medium obtained from CM of capsaicin-activated DRG neurons and searched for genes and proteins that are known markers of osteoblastogenesis. We suggest that the activation of capsaicin-sensitive sensory neurons induce the osteoblast lineage development from MSCs *in vitro*, by increasing the ALP intracellular levels and transcriptional expression of early osteoblastic genes in MSCs after 4 and 7 days of culture. In this regard, it would be important to analyse the expression of late osteoblastic genes and proteins at longer culture times. We also suggest that the osteogenic effect of sensory neurons on MSCs could be mediated by the increased release of sensory neuropeptides, especially CGRP and SP. Indeed these sensory neuropeptides were already described to contribute to osteoblastogenesis *in vitro* [71–74]*.* In order to clarify whether the CGRP and/or SP are directly involved in osteoblast differentiation, we intend to test the inhibitory effect of antagonists for CGRP (*e.g*. BIBN4096BS) and SP (*e.g.* SR140333) receptors expressed in MSCs. Based on the remarkable specificity of capsaicin for Aδ- and peptidergic C- fibers [37], we assume a particular involvement of these fiber types in osteoblastogenesis. Because it was shown that capsaicin receptor TRPV1 is expressed in osteoblast-like cells and regulates the osteoblast differentiation [75] one of the main concerns regarding this second work is whether the capsaicin, present in the CM, may be acting directly on MSCs, thus influencing its differentiation.

Taken together, these findings establish that sensory neurons have an important role in osteoblastogenesis. However, we can presume that these neurons can have a

differentiated role in two distinct *in vivo* processes. In the absence of an environmental stimulus sensory neurons are not able to induce osteoblast and bone formation. However, they seem to contribute to bone metabolism and homeostasis by improving osteoblast and bone formation (Article 1). On the other hand, in the presence of a noxious stimulus similar to the capsaicin, such as bradykinin (produced at the sites of tissue injury), they should have an essential role for bone repair/regeneration by inducing osteoblastogenesis and bone formation (Article 2).

Altogether, this work offers new comprehensive data regarding how bone tissue is regulated at the cellular and molecular levels by the sensory nervous system. It further supports the idea that the role of sensory innervation is particularly important at early stages of the osteoblast differentiation process.

PERSPECTIVES.06

6.1. Angiogenesis and sensory innervation: impact on osteogenesis

Unequivocal evidence has been provided on the pivotal role of angiogenesis in skeletal development and bone repair [76,77]. Moreover, it has been recognized an important role of the sensory nervous system on angiogenesis [31,76–79]. However, the interplay between the endothelial cells, sensory neurons, and bone cells remains obscure.

A number of molecular partners have been identified in angiogenesis and neural development. For instance, although PDGF and VEGF are recognized for their role in angiogenesis, they also enhance the proliferation, migration, and survival of glial cells and stimulate the axonal outgrowth [78–80]. Furthermore, it has been demonstrated that endothelial cells respond to neural guidance molecules, including netrins, slits, semaphorins and ephrins, suggesting interplay between endothelial and neuronal cells. Indeed, it was shown that Sema3A suppress VEGF-mediated angiogenesis, by binding to the neuropilin 1 (NRP1) expressed in endothelial cells. NRP1 is a receptor for both Sema3A and VEGF and it has been proposed to integrate the co-patterning between the nervous and vascular systems [81]. In addition, it was reported that peripheral nerves, associated with Schwann cells, are able to secrete VEGF and thereby promote blood vessels development [81]. Notably, it was recently demonstrated that the activation of the tyrosine kinase receptor type 1 (TrkA) by nerve growth factor (NGF) coordinates the angiogenesis and ossification of developing endochondral bone [82,83].

Based on these events and in our new discoveries, we perspective to understand whether the sensory nervous system may promote the osteogenic effect of endothelial cells. For this, we intend to explore the interaction/communication between endothelial precursor cells, sensory neurons, and MSCs in a microfluidic platform in order to identify main regulators of both osteoblastic and endothelial precursor cells differentiation.

6.2. Angiogenesis and neurotisation in bone tissue engineering

The knowledge obtained from this work allowed us to start to develop a new composite material to favor neurotisation, angiogenesis, and osteogenesis in a bone regeneration context. This material consists on a biphasic composite formed by a polymeric phase, elastin-like polypeptides (ELPs) cross-linked through polyethylene glycol (PEG) to form a gel, and a mineral phase composed of nano-hydroxyapatite (nHA). ELPs are formed by multiple repeats of Val-Pro-Gly-*Xaa*-Gly pentapeptides, where *Xaa* can be any amino acid except proline. As ELPs are derived from elastin, which is an extracellular matrix protein, they can offer biologically relevant functional cues to cells and tissues. Furthermore, ELPs are genetically encoded biopolymers and thus bioactive peptide moieties, particularly the pentapeptide Ile-Lys-Val-Ala-Val (IKVAV), can be included in its backbone [84,85]. IKVAV is a motif derived from laminin, which has shown to promote neuron attachment and growth, endothelial cell mobilization, capillary branching, and revascularization [86–89]. This peptide is our candidate to include in the ELP backbone in order to provide a composite material with fundamental cues for both neurotisation and angiogenesis.

PEG is currently FDA-approved for multiple medical applications. When combined with biodegradable polymers, such as ELPs, PEG presents a great potential for the design of tailor made extracellular matrices for tissue repair. Although PEG is not biodegradable, it has been shown that PEG with a molar mass below 20kDa is easily secreted in urine, reducing the risk of its *in vivo* accumulation and associated toxicity [90].

Finally, the use of nHA particles will allow mimicking the nano/microstructure of bone tissue. Previous studies in our group have shown that the inclusion of nHA at low mass ratios (2.8% w/w) within a pullulan/dextran matrix is sufficient to support new bone formation [91,92].

In conclusion, ELPs will provide the polymeric phase with cellular adhesion sequences to promote both neurotisation and angiogenesis; PEG phase will enable to modulate degradation and the rigidity profile of the composite and; nHA combined with the developed composite gel will offer osteoconductive cues to favor osteogenesis without compromising the composite rigidity and degradability.

The different components will be obtained by chemical synthesis (PEG and nHA) and protein engineering (ELPs), allowing to precisely control of the system composition.

This new composite will be first evaluated in cultures of endothelial cells, sensory

neurons and MSCs, and then in small animal models.

This approach, focusing on a holistic approach for bone tissue, represents a novelty in the field of bone tissue engineering and has the potential to rupture with current bone regeneration approaches.

REFERENCES.07

1 Florencio-Silva R, Sasso GR da S, Sasso-Cerri E, Simões MJ, Cerri PS. Biology of Bone Tissue: Structure, Function, and Factors That Influence Bone Cells. *Biomed Res Int* 2015; **2015**: 1–17.

2 Tzelepi V, Tsamandas AC, Zolota V, Scopa CD. Bone Anatomy, Physiology and Function. Springer, Dordrecht, 2009, pp 3–30.

3 Clarke B. Normal bone anatomy and physiology. *Clin J Am Soc Nephrol* 2008; **3 Suppl 3**: S131-9.

4 Babaji P, Devanna R, Jagtap K, Chaurasia V, Jerry J, Choudhury B *et al.* The cell biology and role of resorptive cells in diseases: A review. *Ann Afr Med* 2017; **16**: 39.

5 Marenzana M, Arnett TR. The Key Role of the Blood Supply to Bone. *Bone Res* 2013; **1**: 203–15.

6 Ramasamy SK. Structure and Functions of Blood Vessels and Vascular Niches in Bone. *Stem Cells Int* 2017; **2017**: 1–10.

7 García-Castellano JM, Díaz-Herrera P, Morcuende JA. Is bone a target-tissue for the nervous system? New advances on the understanding of their interactions. *Iowa Orthop J* 2000; **20**: 49–58.

8 Mach DB, Rogers SD, Sabino MC, Luger NM, Schwei MJ, Pomonis JD *et al.* Origins of skeletal pain: sensory and sympathetic innervation of the mouse femur. *Neuroscience* 2002; **113**: 155–66.

9 Nencini S, Ivanusic JJ. The Physiology of Bone Pain. How Much Do We Really Know? *Front Physiol* 2016; **7**: 157.

10 Hinton RJ, Jing Y, Jing J, Feng JQ. Roles of Chondrocytes in Endochondral Bone Formation and Fracture Repair. *J Dent Res* 2017; **96**: 23–30.

11 Berendsen AD, Olsen BR. Bone development. *Bone* 2015; **80**: 14–18.

12 Filipowska J, Tomaszewski KA, Niedźwiedzki Ł, Walocha JA, Niedźwiedzki T. The role of vasculature in bone development, regeneration and proper systemic functioning. *Angiogenesis* 2017; **20**: 291–302.

13 Katsimbri P. The biology of normal bone remodelling. *Eur J Cancer Care (Engl)* 2017; **26**: e12740.

14 Raggatt LJ, Partridge NC. Cellular and molecular mechanisms of bone remodeling. *J Biol Chem* 2010; **285**: 25103–8.

15 Crockett JC, Rogers MJ, Coxon FP, Hocking LJ, Helfrich MH. Bone remodelling at a glance. *J Cell Sci* 2011; **124**: 991–8.

16 Delaisse J-M. The reversal phase of the bone-remodeling cycle: cellular prerequisites for coupling resorption and formation. *Bonekey Rep* 2014; **3**. doi:10.1038/bonekey.2014.56.

17 Sims NA, Martin TJ. Coupling the activities of bone formation and resorption: a multitude of signals within the basic multicellular unit. *Bonekey Rep* 2014; **3**. doi:10.1038/bonekey.2013.215.

18 Zuo C, Huang Y, Bajis R, Sahih M, Li Y-P, Dai K *et al.* Osteoblastogenesis regulation signals in bone remodeling. *Osteoporos Int* 2012; **23**: 1653–1663.

19 Siddiqui JA, Partridge NC. Physiological Bone Remodeling: Systemic Regulation and Growth Factor Involvement. *Physiology* 2016; **31**: 233–245.

20 Rahman MS, Akhtar N, Jamil HM, Banik RS, Asaduzzaman SM. TGF-β/BMP signaling and other molecular events: regulation of osteoblastogenesis and bone formation. *Bone Res* 2015; **3**: 15005.

21 Wu M, Chen G, Li Y-P. TGF-β and BMP signaling in osteoblast, skeletal development, and bone formation, homeostasis and disease. *Bone Res* 2016; **4**: 16009.

22 Negishi-Koga T, Shinohara M, Komatsu N, Bito H, Kodama T, Friedel RH *et al.* Suppression of bone formation by osteoclastic expression of semaphorin 4D. *Nat Med* 2011; **17**: 1473–1480.

23 Fukuda T, Takeda S, Xu R, Ochi H, Sunamura S, Sato T *et al.* Sema3A regulates bone-mass accrual through sensory innervations. *Nature* 2013; **497**: 490–493.

24 Alečković M, Kang Y. Bone marrow stroma-derived miRNAs as regulators, biomarkers and therapeutic targets of bone metastasis. *Bonekey Rep* 2015; **4**: 671.

25 Wang Y, Li Y-P, Paulson C, Shao J-Z, Zhang X, Wu M *et al.* Wnt and the Wnt signaling pathway in bone development and disease. *Front Biosci (Landmark Ed* 2012; **19**: 379–407.

26 Baron R, Kneissel M. WNT signaling in bone homeostasis and disease: from human mutations to treatments. *Nat Med* 2012; **19**: 179–192.

27 Zhong Z, Ethen NJ, Williams BO. WNT signaling in bone development and homeostasis. *Wiley Interdiscip Rev Dev Biol* 2012; **3**: 489–500.

28 Karner CM, Long F. Wnt signaling and cellular metabolism in osteoblasts. *Cell*

Mol Life Sci 2012; **74**: 1649–1657.

29 Fukumoto S, Martin TJ. Bone as an endocrine organ. *Trends Endocrinol Metab* 2009; **20**: 230–6.

30 Lafage-Proust M-H, Roche B, Langer M, Cleret D, Vanden Bossche A, Olivier T *et al.* Assessment of bone vascularization and its role in bone remodeling. *Bonekey Rep* 2015; **4**. doi:10.1038/bonekey.2015.29.

31 Carmeliet P, Tessier-Lavigne M. Common mechanisms of nerve and blood vessel wiring. *Nature* 2005; **436**: 193–200.

32 Li B, Wang H, Qiu G, Su X, Wu Z. Synergistic Effects of Vascular Endothelial Growth Factor on Bone Morphogenetic Proteins Induced Bone Formation In Vivo: Influencing Factors and Future Research Directions. *Biomed Res Int* 2016; **2016**: 1–11.

33 The emerging role of endothelin-1 in the pathogenesis of subchondral bone disturbance and osteoarthritis. *Osteoarthr Cartil* 2015; **23**: 516–524.

34 Izu Y, Mizoguchi F, Kawamata A, Hayata T, Nakamoto T, Nakashima K *et al.* Angiotensin II Type 2 Receptor Blockade Increases Bone Mass. *J Biol Chem* 2009; **284**: 4857–4864.

35 Nakagami H, Osako MK, Morishita R. Potential effect of angiotensin II receptor blockade in adipose tissue and bone. *Curr Pharm Des* 2013; **19**: 3049–53.

36 Lee S-W, Moskowitz MA, Sims JR. Sonic hedgehog inversely regulates the expression of angiopoietin-1 and angiopoietin-2 in fibroblasts. *Int J Mol Med* 2007; **19**: 445–51.

37 Squire LR. *Encyclopedia of Neuroscience: Volume One*. Academic Press: London, 2009.

38 Purves D, Augustine GJ, Fitzpatrick D, Hall WC, LaMantia A-S, McNamara JO *et al. Neuroscience*. 3rd Edition. Sinauer Associates, Inc.: Sunderland (MA), 2004.

39 Society for Neuroscience. *Brain Facts: A primer on the brain and nervous system*. 7th Editio. Society for Neuroscience: Washington (DC), 2012.

40 Morell P, Quarles RH. The Myelin Sheath. In: *Basic Neurochemistry: Molecular, Cellular and Medical Aspects.* Lippincott-Raven: Philadelphia (PA), 1999https://www.ncbi.nlm.nih.gov/books/NBK27954/ (accessed 9 Nov2017).

41 Roatta S, Passatore M, Roatta S, Passatore M. Muscle Sensory Receptors. In: *Wiley Encyclopedia of Biomedical Engineering*. John Wiley & Sons, Inc.: Hoboken, NJ, USA, 2006 doi:10.1002/9780471740360.ebs0809.

42 Whitwam JG. Classification of peripheral nerve fibres. An historical perspective. *Anaesthesia* 1976; **31**: 494–503.

43 Holzer P, Maggi CA. Dissociation of dorsal root ganglion neurons into afferent and efferent-like neurons. *Neuroscience* 1998; **86**: 389–98.

44 Hara-Irie F, Amizuka N, Ozawa H. Immunohistochemical and ultrastructural localization of CGRP-positive nerve fibers at the epiphyseal trabecules facing the growth plate of rat femurs. *Bone* 1996; **18**: 29–39.

45 Hill EL, Elde R. Distribution of CGRP-, VIP-, D beta H-, SP-, and NPY-immunoreactive nerves in the periosteum of the rat. *Cell Tissue Res* 1991; **264**: 469–80.

46 Castañeda-Corral G, Jimenez-Andrade JM, Bloom AP, Taylor RN, Mantyh WG, Kaczmarska MJ *et al.* The majority of myelinated and unmyelinated sensory nerve fibers that innervate bone express the tropomyosin receptor kinase A. *Neuroscience* 2011; **178**: 196–207.

47 Bjurholm A, Kreicbergs A, Brodin E, Schultzberg M. Substance P- and CGRP-immunoreactive nerves in bone. *Peptides*; **9**: 165–71.

48 Bjurholm A, Kreicbergs A, Terenius L, Goldstein M, Schultzberg M. Neuropeptide Y-, tyrosine hydroxylase- and vasoactive intestinal polypeptide-immunoreactive nerves in bone and surrounding tissues. *J Auton Nerv Syst* 1988; **25**: 119–25.

49 Offley SC, Guo T-Z, Wei T, Clark JD, Vogel H, Lindsey DP *et al.* Capsaicin-Sensitive Sensory Neurons Contribute to the Maintenance of Trabecular Bone Integrity. *J Bone Miner Res* 2004; **20**: 257–267.

50 Heffner MA, Anderson MJ, Yeh GC, Genetos DC, Christiansen BA. Altered bone development in a mouse model of peripheral sensory nerve inactivation. *J Musculoskelet Neuronal Interact* 2014; **14**: 1–9.

51 Mahns DA, Ivanusic JJ, Sahai V, Rowe MJ. An intact peripheral nerve preparation for monitoring the activity of single, periosteal afferent nerve fibres. *J Neurosci Methods* 2006; **156**: 140–4.

52 Ivanusic JJ. Size, neurochemistry, and segmental distribution of sensory neurons innervating the rat tibia. *J Comp Neurol* 2009; **517**: 276–83.

53 Mach DB, Rogers SD, Sabino MC, Luger NM, Schwei MJ, Pomonis JD *et al.* Origins of skeletal pain: sensory and sympathetic innervation of the mouse femur. *Neuroscience* 2002; **113**: 155–66.

54 Zylka MJ, Rice FL, Anderson DJ. Topographically distinct epidermal

nociceptive circuits revealed by axonal tracers targeted to Mrgprd. *Neuron* 2005; **45**: 17–25.

55 Jimenez-Andrade JM, Mantyh WG, Bloom AP, Xu H, Ferng AS, Dussor G *et al.* A phenotypically restricted set of primary afferent nerve fibers innervate the bone versus skin: therapeutic opportunity for treating skeletal pain. *Bone* 2010; **46**: 306–13.

56 Su Y-W, Zhou X-F, Foster BK, Grills BL, Xu J, Xian CJ. Roles of neurotrophins in skeletal tissue formation and healing. *J Cell Physiol* 2017. doi:10.1002/jcp.25936.

57 Wang L, Zhao R, Shi X, Wei T, Halloran BP, Clark DJ *et al.* Substance P stimulates bone marrow stromal cell osteogenic activity, osteoclast differentiation, and resorption activity in vitro. *Bone* 2009; **45**: 309–20.

58 He H, Chai J, Zhang S, Ding L, Yan P, Du W *et al.* CGRP may regulate bone metabolism through stimulating osteoblast differentiation and inhibiting osteoclast formation. *Mol Med Rep* 2016; **13**: 3977–84.

59 Wang L, Shi X, Zhao R, Halloran BP, Clark DJ, Jacobs CR *et al.* Calcitonin-gene-related peptide stimulates stromal cell osteogenic differentiation and inhibits RANKL induced NF-kappaB activation, osteoclastogenesis and bone resorption. *Bone* 2010; **46**: 1369–79.

60 Maggi CA, Meli A. The sensory-efferent function of capsaicin-sensitive sensory neurons. *Gen Pharmacol* 1988; **19**: 1–43.

61 Ding Y, Arai M, Kondo H, Togari A. Effects of capsaicin-induced sensory denervation on bone metabolism in adult rats. *Bone* 2010; **46**: 1591–1596.

62 Li Z, Hao J, Duan X, Wu N, Zhou Z, Yang F *et al.* The Role of Semaphorin 3A in Bone Remodeling. *Front Cell Neurosci* 2017; **11**: 40.

63 Fukuda T, Takeda S, Xu R, Ochi H, Sunamura S, Sato T *et al.* Sema3A regulates bone-mass accrual through sensory innervations. *Nature* 2013; **497**: 490–3.

64 Zhang P-X, Jiang X-R, Wang L, Chen F-M, Xu L, Huang F. Dorsal root ganglion neurons promote proliferation and osteogenic differentiation of bone marrow mesenchymal stem cells. *Neural Regen Res* 2015; **10**: 119–23.

65 Marie PJ, Haÿ E, Saidak Z. Integrin and cadherin signaling in bone: role and potential therapeutic targets. *Trends Endocrinol Metab* 2014; **25**: 567–75.

66 Plotkin LI, Laird DW, Amedee J. Role of connexins and pannexins during ontogeny, regeneration, and pathologies of bone. *BMC Cell Biol* 2016; **17**

Suppl 1: 19.

67 Moorer MC, Stains JP. Connexin43 and the Intercellular Signaling Network Regulating Skeletal Remodeling. *Curr Osteoporos Rep* 2017; **15**: 24–31.

68 Wang Y, Li Y-P, Paulson C, Shao J-Z, Zhang X, Wu M *et al.* Wnt and the Wnt signaling pathway in bone development and disease. *Front Biosci (Landmark Ed* 2014; **19**: 379–407.

69 Zhong Z, Ethen NJ, Williams BO. WNT signaling in bone development and homeostasis. *Wiley Interdiscip Rev Dev Biol* 2014; **3**: 489–500.

70 Kodama D, Hirai T, Kondo H, Hamamura K, Togari A. Bidirectional communication between sensory neurons and osteoblasts in an *in vitro* coculture system. *FEBS Lett* 2017; **591**: 527–539.

71 Bernard GW, Shih C. The osteogenic stimulating effect of neuroactive calcitonin gene-related peptide. *Peptides* 1990; **11**: 625–32.

72 Fu S, Mei G, Wang Z, Zou Z-L, Liu S, Pei G-X *et al.* Neuropeptide substance P improves osteoblastic and angiogenic differentiation capacity of bone marrow stem cells in vitro. *Biomed Res Int* 2014; **2014**: 596023.

73 Shih C, Bernard GW. Neurogenic substance P stimulates osteogenesis in vitro. *Peptides* 1997; **18**: 323–6.

74 Adamus MA, Dabrowski ZJ. Effect of the neuropeptide substance P on the rat bone marrow-derived osteogenic cells in vitro. *J Cell Biochem* 2001; **81**: 499–506.

75 Abed E, Labelle D, Martineau C, Loghin A, Moreau R. Expression of transient receptor potential (TRP) channels in human and murine osteoblast-like cells. *Mol Membr Biol* 2009; **26**: 146–158.

76 Guerrero J, Catros S, Derkaoui S-M, Lalande C, Siadous R, Bareille R *et al.* Cell interactions between human progenitor-derived endothelial cells and human mesenchymal stem cells in a three-dimensional macroporous polysaccharide-based scaffold promote osteogenesis. *Acta Biomater* 2013; **9**: 8200–13.

77 Grellier M, Bordenave L, Amédée J. Cell-to-cell communication between osteogenic and endothelial lineages: implications for tissue engineering. *Trends Biotechnol* 2009; **27**: 562–571.

78 Chauvet S, Burk K, Mann F. Navigation rules for vessels and neurons: cooperative signaling between VEGF and neural guidance cues. *Cell Mol Life Sci* 2013; **70**: 1685–703.

79 Jin K, Zhu Y, Sun Y, Mao XO, Xie L, Greenberg DA. Vascular endothelial growth factor (VEGF) stimulates neurogenesis in vitro and in vivo. *Proc Natl Acad Sci* 2002; **99**: 11946–11950.

80 Lee C, Zhang F, Tang Z, Liu Y, Li X. PDGF-C: a new performer in the neurovascular interplay. *Trends Mol Med* 2013; **19**: 474–86.

81 Raimondi C, Ruhrberg C. Neuropilin signalling in vessels, neurons and tumours. *Semin Cell Dev Biol* 2013; **24**: 172–8.

82 Tomlinson RE, Li Z, Zhang Q, Goh BC, Li Z, Thorek DLJ *et al.* NGF-TrkA Signaling by Sensory Nerves Coordinates the Vascularization and Ossification of Developing Endochondral Bone. *Cell Rep* 2016; **16**: 2723–2735.

83 Tomlinson RE, Li Z, Li Z, Minichiello L, Riddle RC, Venkatesan A *et al.* NGF-TrkA signaling in sensory nerves is required for skeletal adaptation to mechanical loads in mice. *Proc Natl Acad Sci* 2017; **114**: E3632–E3641.

84 Urry DW, Trapane TL, Prasad KU. Phase-structure transitions of the elastin polypentapeptide-water system within the framework of composition-temperature studies. *Biopolymers* 1985; **24**: 2345–2356.

85 MacEwan SR, Chilkoti A. Elastin-like polypeptides: Biomedical applications of tunable biopolymers. *Biopolymers* 2010; **94**: 60–77.

86 Structure-activity study of a laminin α1 chain active peptide segment Ile-Lys-Val-Ala-Val (IKVAV). *FEBS Lett* 1995; **365**: 227–231.

87 Silva GA, Czeisler C, Niece KL, Beniash E, Harrington DA, Kessler JA *et al.* Selective Differentiation of Neural Progenitor Cells by High-Epitope Density Nanofibers. *Science (80-)* 2004; **303**: 1352–1355.

88 Grant DS, Kinsella JL, Fridman R, Auerbach R, Piasecki BA, Yamada Y *et al.* Interaction of endothelial cells with a laminin A chain peptide (SIKVAV) in vitro and induction of angiogenic behavior in vivo. *J Cell Physiol* 1992; **153**: 614–625.

89 Nakamura M, Mie M, Mihara H, Nakamura M, Kobatake E. Construction of multi-functional extracellular matrix proteins that promote tube formation of endothelial cells. *Biomaterials* 2008; **29**: 2977–86.

90 Pasut G, Veronese FM. Polymer–drug conjugation, recent achievements and general strategies. *Prog Polym Sci* 2007; **32**: 933–961.

91 Catros S, Fricain J-C, Guillotin B, Pippenger B, Bareille R, Remy M *et al.* Laser-assisted bioprinting for creating on-demand patterns of human osteoprogenitor cells and nano-hydroxyapatite. *Biofabrication* 2011; **3**: 25001.

92 Fricain JC, Schlaubitz S, Le Visage C, Arnault I, Derkaoui SM, Siadous R *et al.* A nano-hydroxyapatite – Pullulan/dextran polysaccharide composite macroporous material for bone tissue engineering. *Biomaterials* 2013; **34**: 2947–2959.

ANNEXES.08

The effect of four different sera on morphology, viability, and osteogenic activity of MSCs was tested in order to define which one was the most appropriate to our studies (Table 1 and Figure 1). We found that MSCs cultured with sera 1, 3 and 4 for 5 days exhibited a characteristic long and fusiform shape, while MSCs incubated with serum 5 showed heterogeneous size and morphology (Figure 1A). A resazurin-based assay revealed that MSCs cultured with serum 4 for 4 and 7 days displayed more viability than MSCs incubated with sera 1, 3 and 5 (Figure 1B). Importantly, there were no differences between MSCs maintained in standard culture medium and osteogenic medium with serum 4 (Figure 1B). Contrariwise, sera 1, 3 and 5 seem to have a detrimental effect on viability of MSCs commited to osteoblast lineage (Figure 1B). The ALP activity assay showed an increase of ALP intracellular levels in MSCs cultured with serum 5, when compared with MSCs incubated with other sera (Figure 1C). However, only MSCs maintained with serum 4 seem to positively respond to the osteogenic induction (Figure 1C). These findings indicate that the serum 4 is the most appropriate to analyse the role of DRG neurons on osteoblast lineage development from MSCs.

Table 1. Tested sera specifications.

Serum	Catalog	Lote	Manufacturer
1	S1810	S13903S1810	Biowest
3	S1810	S13604S1810	Dominique Dutscher
4	P30-3301A	P150508	PAN-Biotech
5	500101KK	P160308	PAN-Biotech

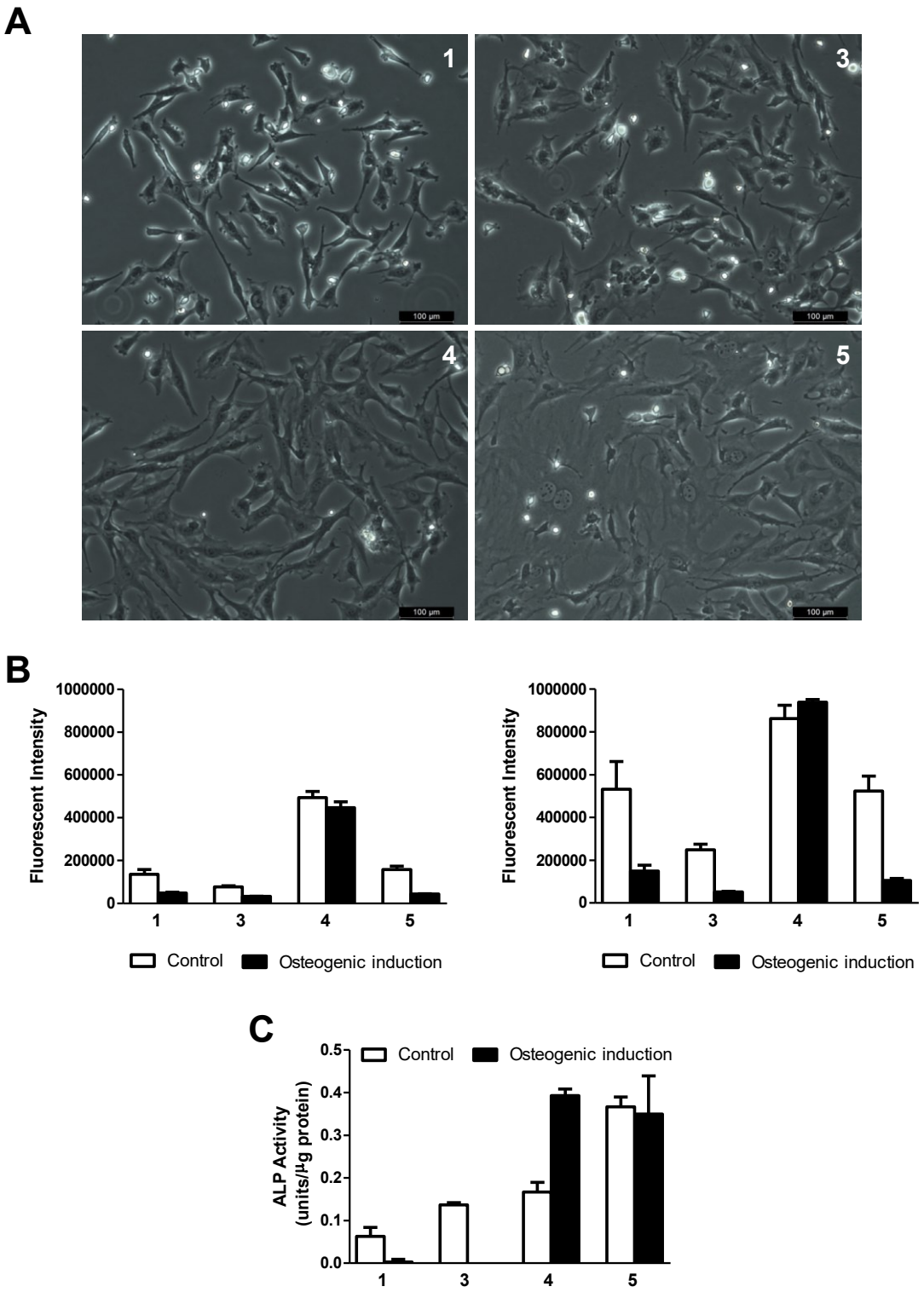

Figure 1. The effect of four different sera on morphology, viability and osteogenic activity of MSC. Rat bone marrow MSCs (10^4 cells/cm^2) were cultured with different sera (1, 3, 4 and 5) in a six-well plate for 7 days. (A) 5 days after isolation, the cell morphology was observed under an inverted phase contrast microscope. (B) The viability of MSCs maintained with or without osteogenic induction was measured at 4 and 7 days of culture by resazurin-based assay, and (C) the intracellular levels of ALP were determined on day 7 by using ALP activity quantification assay.

To assess the effect of mitotic inhibition on DRG neurons culture heterogeneity and neurite formation within the microfluidic platform, we cocultured MSCs with DRG neurons maintained in the presence or absence of the AraC mitotic inhibitor (also known as Cytosine β-D-arabinofuranoside, (β-D-Arabinofuranosyl)cytosine, Arabinocytidine, Arabinosylcytosine, Cytarabine, or Cy tosine arabinoside).

The population of DRG neurons within the microdevice was evaluated on day 7 of coculture by phase contrast microcopy (Figure 2A and B) and IF against β-III Tubulin (Figure 2C and D). We found the formation of extended DRG neurons projections towards the axonal side of the microfluidic device in both cell culture conditions

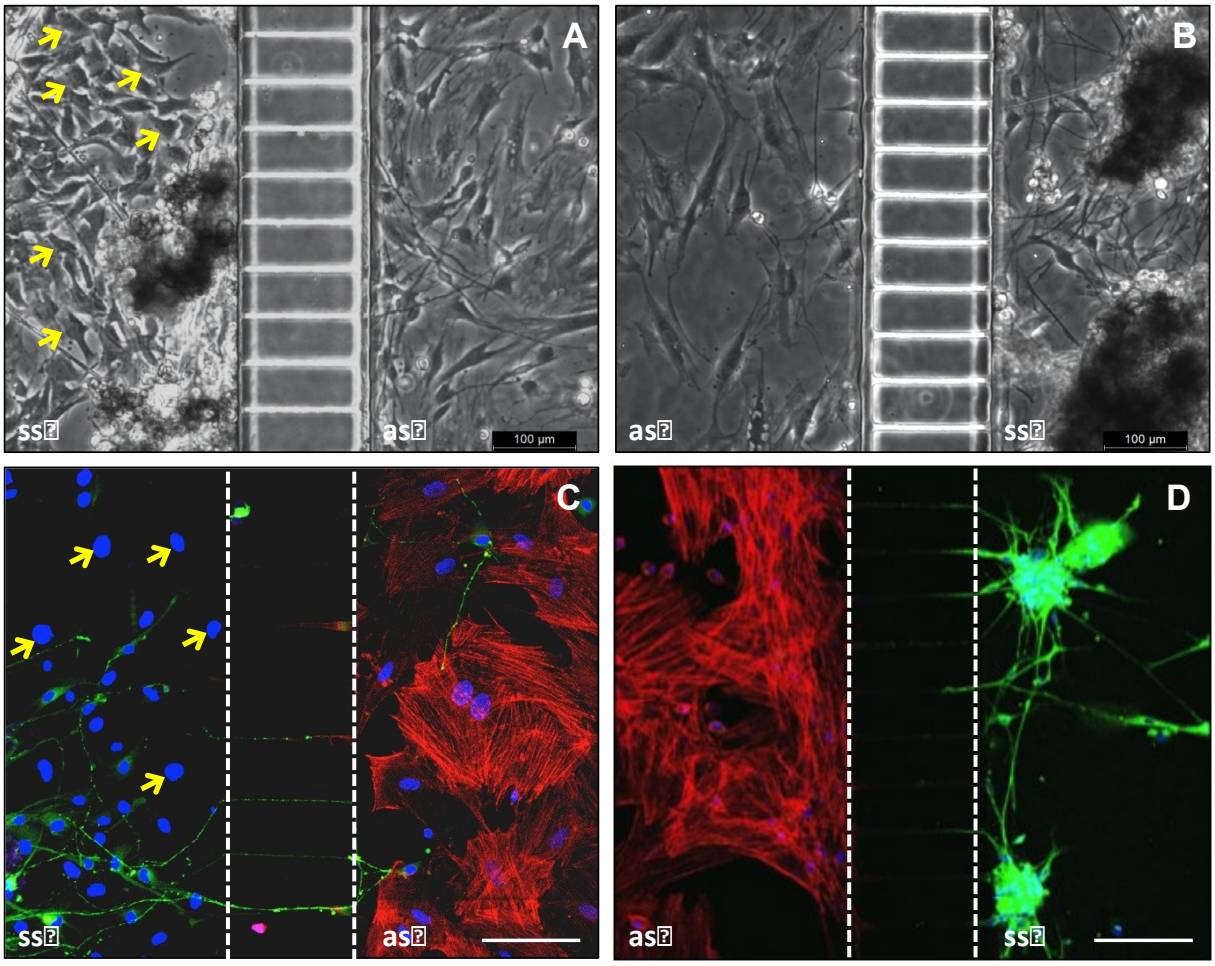

Figure 2. The effect of mitotic inhibition on DRG neurons culture heterogeneity and neurite formation within the microfluidic platform. Sensory neurons derived from rat DRG (5 x 10^4 cells/cm^2) and rat bone marrow MSCs (10^4 cells/cm^2) were cultured in the microfluidic devices for 7 days. MSCs were maintained in standard culture medium and DRG neurons were incubated in growing medium (A and C) nonsupplemented or (B and E) supplemented with 1 µM AraC mitotic inhibitor. DRG neurons culture heterogeneity and neurite formation were evaluated on day 7 of coculture under (A and B) inverted phase contrast microscopy, and (C and D) IF confocal microscopy using an antibody directed against β-III Tubulin coupled to Alexa Fluor® 488 (green), and DAPI (nuclei; blue). Actin filaments of MSCs were stained using Alexa Fluor® 568 (red)-conjugated phalloidin.
(as) axonal side; (ss) somal side; arrows point to non-neuronal cells; Scale bar = 100 µm.

(Figure 2C and D). However, the culture of DRG neurons without mitotic inhibition exhibited a heterogeneous population of DRG neurons and non-neuronal cells (Figure 2A and C, arrows). A homogeneous population of pure DRG neurons was achieved by using the AraC during the culture time (Figure 4B and D). These results show that use of a mitotic inhibitor is required to establish a coculture of pure DRG neurons and MSCs in the microfluidic platform.

8.2.1. Oral Communications

Silva DI, Paiva dos Santos B, Leng J, Amédée J, Oliveira H. "Sensory neurons enhance osteoblastogenesis in a microfluidic device", ESB, Athens, Greece, 4-8 September, 2017.

Silva DI, Paiva dos Santos B, Leng J, Amédée J, Oliveira H. "Sensory neurons contribute to osteoblast differentiation of mesenchymal stem cells in a microfluidic coculture system", JFBTM, Lyon, France, 18-20 May, 2017.

Silva DI, Paiva dos Santos B, Leng J, Garbay B, Garanger E, Amédée J, Oliveira H. "Sensory neurons and mesenchymal stem cells in a microfluidic device for exploring osteogenesis and bone regeneration", BxCRM, Bordeaux. France, 24-26 October, 2016.

Silva DI, Paiva dos Santos B, Leng J, Garbay B, Garanger E, Amédée J, Oliveira H. "Exploring the role of sensory innervation on bone regeneration: coculture of sensory neurons and mesenchymal stem cells in a microfluidic system", EORS, Bologne, Italy, 14-16 September, 2016.

8.2.2. Poster Communications

Silva DI, Paiva dos Santos B, Leng J, Amédée J, Oliveira H. "Studying the role of sensory innervation on osteogenesis in a microfluidic coculture system comprising sensory neurons and mesenchymal stem cells", TERMIS, Davos, Switzerland, 26-30 June, 2017.

Silva DI, Paiva dos Santos B, Leng J, Garbay B, Garanger E, Amédée J, Oliveira H. "Sensory innervation and osteoblast differentiation – understanding the interplay between sensory neurons and mesenchymal stem cells in a microfluidic coculture system", Journée scientifique de la FrTecSan, Bordeaux, France, 14 June, 2016.

Silva DI, Paiva dos Santos B, Leng J, Garbay B, Garanger E, Amédée J, Oliveira H. "The role of sensory nervous system on bone regeneration", JFBTM, Nancy, France, 1-3 June, 2016.

Silva DI, Paiva dos Santos B, Leng J, Garbay B, Garanger E, Amédée J, Oliveira H. "Exploring the role of sensory neurons in the differentiation of mesenchymal stem cells into the osteoblast lineage in a microfluidic platform", YSS, European Institute for Chemistry and Biology, Pessac, France, 26-27 May, 2016.